HABILITATION THESIS

Contributions to continuous and discrete dynamical systems theory

Specialization: Mathematics

Conf. dr. Gheorghe TIGAN

Contents

Chapter 1

Summary

The **first part** of this thesis describes the evolution of the academic career of the candidate Gheorghe TIGAN and contains brief details about: education, employment history, teaching activities (seminars and courses taught, respectively, published books for students), scientific activities such as participation in conferences, workshops, seminars and research stages, coordination of research projects and research teams, and participation in the reviewing process of research articles from various international journals.

The **second part** of the thesis contains a brief description of the main scientific achievements of the candidate for the period following his Ph. D. award to present. The results are grouped into four sections as follows.
a) The **section one** describes the results we obtained on periodic, homoclinic and heteroclinic orbits in several three-dimensional differential systems, namely in Chen, Lü, T and Shimizu-Morioka systems. For the first three systems we used a method based on Lyapunov-like functions and showed that the systems under some constraints of their parameters have neither homoclinic orbits nor closed orbits but they have heteroclinic orbits. Moreover, for the Chen system we obtained results on the existence of homoclinic orbits as well, by transforming the system to a new form and using some known results obtained by a method of systems comparison. We showed that the Chen system has two symmetrical homoclinic orbits to the equilibrium point O. For the T system we studied also periodic orbits arising from Bautin bifurcation. For the Shimizu-Morioka system we used a different method, namely a method based on detecting the traces left by the separatrices of a saddle point on certain surfaces. With this method we could prove the existence of homoclinic orbits in the Shimizu-Morioka system.

The methods we developed for these systems are fully analytic and can be applied successfully to other systems provided that adequate conditions are fulfilled.
b) In the **second section** we give details about the results we obtained on non-smooth dynamical systems. We studied a two-dimensional discrete non-smooth system (map), which is continuous but non-differentiable with respect to one of the variables. The map generalizes in some sense the so-called Nordmark map which is related to one-dimensional impact oscillators near grazing points. Examples of impact oscillators range from simple to complex phenomena such as, a ball bouncing on a vibrating table and a charged particle moving in strong magnetic fields in tokamaks (experimental devices trying to produce clean energy similar to the energy released from the Sun). Billiard theory, which refers to a particle traveling with high speed in a bounded region undergoing recurrent impacts with the region's boundary, is another important class of impact oscillators. We pointed out in the map's dynamics new types of orbits, such as orbits with at least two points on the impacting side. A reversed infinite period-adding cascade of bifurcations when one of map's parameters decreases continuously between two values have been also obtained, together with a scenario of alternating chaos with windows of stability. We presented also a case-study model of impact oscillators with improper grazing orbits and obtained complete chattering orbits and incomplete impacting orbits.
c) The **third section** presents the results we obtained on perturbed Hamiltonian systems. We studied firstly a one-and-a-half degrees of freedom perturbed Hamiltonian system with a quartic unperturbed part and broad perturbation spectrum. An approximate interpolating Hamiltonian system was firstly studied. We pointed out results on the behaviour of the Poincaré–Birkhoff or dimerised chains in their routes to reconnection when the perturbation parameter varies. A discrete system associated to the full Hamiltonian system was constructed and studied. Pairs of homoclinic orbits to the same equilibrium point (sand-glasses) and triple reconnection were particularly revealed. Finally, we used the scenario of reconnections to explain the destruction of transport barriers in the non-autonomous system. Secondly, we studied a class of planar Hamiltonian systems perturbed with general quadratic polynomials in order to identify the number of limit cycles. In our study we used an approach based on Melnikov functions of any order and showed that the class of systems can have at most three limit cycles and the number is reached.
d) In the **fourth section** we present details on the results we obtained on degenerate fold-Hopf bifurcations. We studied degenerate with respect to parameters

fold–Hopf bifurcations in three-dimensional differential systems. Such degeneracies arise when the transformations between parameters leading to a normal form are not regular at some points in the parametric space. The fold-Hopf bifurcation (or zero-Hopf) occurs in smooth differential systems of minimum dimension three and having minimum two independent parameters. The hallmark of the bifurcation is that at certain values of the parameters the linearized system has an eigenvalue equals to zero and two purely complex eigenvalues. We obtained new generic results for the dynamics of the systems in such a degenerate framework. The bifurcation diagrams we obtained show that in a degenerate context the dynamics may be completely different than in a non-degenerate framework.

The **third part** of the thesis is about the future plans the candidate has to continue his professional career. He is eager to continue his teaching and research activities. Besides other activities related to teaching, he plans to support students by publishing teaching materials (text books, lecture notes, monographs) for their use. He aims to develop his scientific research and potential by studying new research themes and publishing research articles, especially in the field of dynamical systems theory and their applications. He is particularly interested in their applications in Engineering, Biology and Medicine. He plans to write research projects and participate in national and international competitions to obtain funds for the projects and coordinate research groups. He wants to extend his present scientific collaborations with new worldwide others.

Chapter 2

Academic, scientific and professional career development

2.1 General presentation

2.1.1 Studies and employment

I graduated in Mathematics in 1996 from the Faculty of Mathematics, West University of Timisoara, Romania. My general mean for the five years of study was 9.40 (maximum is 10), respectively, 9.84 for the final licence exams, being ranked in the first 6% students of the class. One year later in 1997 I obtained a Master degree in Mathematics. In 2006 I defended my doctoral thesis in Mathematics, West University of Timisoara, in Dynamical Systems Theory gaining a PhD in Mathematics.

Since 1998 I have been working at the **Department of Mathematics**, Politehnica University of Timisoara, Romania, occupying the academic positions corresponding to age and work experience, namely:
- **assistant professor** between 1998–2009,
- **lecturer** between 2009–2015,
- **associate professor** (conferentiar) from 2015 to present.

During this period I have conducted seminars at various courses in Mathematics (such as Differential and Integral Calculus, Algebra and Geometry, Probabilities and Statistics, Computer Assisted Mathematics and others). As a lecturer and associate professor (from 2009) I have been teaching regular courses for students, especially, Differential and Integral Calculus and Computer Assisted Mathematics, both in romanian and english.

2.1.2 Research stages

During my employment at the Politehnica University of Timisoara, I alternated periods of teaching with periods of **research stages** at several renowned institutions in other countries, which I will mention briefly below.
1. Research visitor, National Institute of Neuroscience, National Center for Neurology and Psychiatry (NCNP), Tokyo, Japan, 6 months, 2014. During this period I studied various mathematical models used in biology, especially in neuroscience. I participated also as an observer at several experimental works for measuring ionic currents in biological neurons. I noticed how action potentials are formed in real neurons.
2. Research visitor, Department of Mathematics, Shanghai Jiao Tong University, China, 3 months, 2013. Within this internship I made research on fold-Hopf bifurcations.
3. Research visitor, Department of Mathematics, Sao Paolo University at Sao Carlos, Brazil, 3 months, 2013. During this period I studied several topics in dynamical systems theory such as: mathematical modeling in biology, codimension 2 bifurcations and averaging theory for determining limit cycles.
4. Research visitor, Department of Mathematics, UNICAMP, Brazil, 1 month, 2011. This was a short research stage on topics such as heteroclinic, homoclinic and closed orbits.
5. Research Associate (Marie Curie fellow) in Dynamical Systems Theory, Department of Mathematics, Imperial College of London, United Kingdom, 2 years, 07/2009-06/2011. This two year-period of working in research at a prestigious European university (ranked in the first 10 universities in the world) had an important contribution to my career development since, firstly, I could dedicate myself to research activities in this time and, secondly, I had the opportunity to interact with other researchers.
6. Postdoc researcher in Dynamical Systems Theory at Ben-Gurion University, Israel, 2007-2008, 12 months. This was also a beneficial period for my future scientific career since it was my first research stage after I got the Ph.D. degree.

I would also recall here three other research visits that contributed significantly toward my doctoral degree.
1. Research studentship offered by the Romanian Government through CNBSS

to Imperial College London, 2006, 3 months.
2. "Marie Curie" fellow at Imperial College London, 2004-2005, 12 months.
3. "Socrates" fellow in Mathematics at the University Claude Bernard, Lyon, France, 2000, 3 months.

2.1.3 Participation in conferences, workshops and seminars

A list with my **presentations** given in the last years is the following:
1. Periodic orbits in a non-smooth discrete map. The 15th International Conference on Applied Mathematics and Computer Science, 5-7 July, **2016**, Cluj.
2. Bifurcations in non-smooth impact oscillators. International Conference on Applied Mathematics and Numerical Methods, April 14-16, **2016**, Craiova, Romania.
3. Bautin bifurcations in the T system. The 14th International Conference on Mathematics and its Applications, Timisoara, November 5-7, **2015**, Romania.
4. Applications of dynamical systems in neuronal models. Workshop on Quantum Field Theory and Nonlinear Dynamics, 24-28 September **2014**, Sinaia, Romania.
5. A case-study model for impact oscillators. The 13th International Conference on Mathematics and its Applications, Timisoara, November 1-3, **2012**, Romania.
6. Analysis of the dynamics near a degenerate grazing point for rigid impact oscillators. SIAM International Conference, Applications of Dynamical Systems, Snowbird, May, **2011**, USA.
7. Analysis of a class of fold-Hopf bifurcations (seminar), Shanghai Jiao Tong Univ, July **2013**, China.
8. Mathematical models in Neuroscience (seminar), UPT, Timisoara, June **2013**, Romania.
9. Dynamical systems in Neuroscience (seminar), University of Sao Paolo, May **2013**, Brazil.
10. Homoclinic bifurcations in dynamical systems (seminar), UNICAMP, **2011**, Brazil.

2.1.4 Participation in research projects

- I was the **coordinator** of the research project DynSysApll, **FP7-PEOPLE-2012-IRSES-316338**, 48 months, october 2012-september 2016. The project aimed to bring new knowledge in dynamical systems theory. About 50 researchers from 18 worldwide universities participated in the project.

- In 2008 I proposed a research project in dynamical systems theory and submitted it to one of the Marie Curie actions within the European Framework Program 7 (FP7). The proposal was successful in a strong competition with the success rate of about 15%. Its identification details are **FP7-PEOPLE-IEF-2008-235415**. I carried out the project at the Department of Mathematics, Imperial College of London, for a period of 2 years, 2009–2011.

- I was the **unique researcher** on the project 3329/2006 funded by the Romanian Ministry of Education and Research. I carried out the project at Imperial College London in 2006 for a period of three months.

- I was a research team member on the FP6 project, **HPMT-CT-2001-00278**, for 12 months, 2004-2005, at Imperial College London.

2.2 Coordination of research teams

I have coordinated several research teams made up of 2 to 50 members. I took the initiative for the scientific research presented in my published papers in most of these works. For each paper we have formed a team and worked on the those scientific topics. I supervised the research activity related to these papers. Our activity led to the following main joint papers:
1. G. Tigan, D. Constantinescu, Bifurcations in a family of Hamiltonian systems and associated nontwist cubic maps, Chaos, Solitons and Fractals 91, 128–135, 2016.
2. G. Tigan, J. Llibre, Heteroclinic, homoclinic and closed orbits in the Chen system, International Journal of Bifurcation and Chaos, 26(4), 1–6, 2016.
3. G. Tigan, D. Constantinescu, Heteroclinic orbits in the T and the Lu systems, Chaos, Solitons and Fractals, 42(1), 20–23, 2009.
4. G. Tigan, D. Opris, Analysis of a 3D dynamical system, Chaos, Solitons and Fractals, 36(5), 1315–1319, 2008.

I was the **general manager** of the project **FP7-PEOPLE-IEF-2008-235415** for a period of 4 years, 01/10/2012–30/09/2016 with a budget of 500 000 euros. I was with this project from the beginning to the end. I initiated its creation in 2012 and supervised all activities during its implementation. The scope of the project was to bring new knowledge in the field of dynamical systems theory. A consortium of **18 worlwide universities** contributed to the project implementation and about **50 researchers** took part in its activities. I coordinated management and scientific activities within the project. I prepared 5 large scientific reports for the funding Agency from Brussels and several other financial reports on behalf of the all consortium partners. In the scientific reports I summarized the results obtained by all researchers involved in the project.

During the 4 years of project implementation, 7 Workshops have been organized in the framework of the project where about 100 talks have been presented by internal and external researchers. Other 100 seminar talks have been delivered by project participants during this time. A number of about 160 research papers have been published within the project and about 50 presentations were given in international conferences.

In the last ten years I have been activating as a scientific referent for about ten international Journals related to dynamical systems theory such as: International Journal of Bifurcation and Chaos, Nonlinear Dynamics, Nonlinear Analysis Series B: Real World Applications, Computers and Mathematics with Applications, Ecological Modelling, Discrete Dynamics in Nature and Society and others.

I am also a regular reviewer for a) American Mathematical Society, and b) Zentralblatt/MATH, with a reviewing rate of 10-15 articles per year.

Chapter 3

Description of the achieved scientific results

3.1 Bounded orbits in 3D smooth dynamical systems

Detecting periodic, homoclinic and heteroclinic orbits in dynamical systems generated by differential or difference equations represents a challenge for this field of research. It does not exist general methods for detecting analytically orbits of these types. Such orbits are bounded and their presence in a dynamical system contributes highly to the understanding of its dynamics. It is known that homoclinic and heteroclinic orbits are structurally unstable, that is, small perturbations applied to a system having such orbits destroy the bounded orbits and may bring chaos in the system. We have approached this subject in several published papers. A first method we used is based on *Lyapunov-like functions*. Using adequate functions of this type we could study the existence of closed, homoclinic and heteroclinic orbits in several known dynamical systems, such as the Chen, Lü and T systems. We have obtained large regions of the parameters where the systems have or not such bounded orbits. In [120] we reported results on the Lü and T systems while in [121] on the Chen system. A second method we used is based on *tracking the separatrices* of a saddle point. This method was useful for proving analytically the existence of homoclinic orbits in the Shimizu-Morioka three-dimensional (3D) system [122]-[123]. The methods we developed in these works can also be applied to other systems provided that adequate conditions are fulfilled.

The authors in [64] present an analysis about similarities and differences between the Lorenz system, respectively, the Chen, Lü and T systems. They conclude that studying Lorenz-like systems is important at least because this *stimulates the development of new methods for the analysis of chaotic systems.* It is explained in the paper that important properties of the Lorenz system have been discovered after studying Lorenz-like systems. The authors ask: *what was known about repulsor (or repellor) in the Lorenz system and the dynamics of time-reversal Lorenz system before the works [23]-[77] were published ?*

The Lü system is considered in [65] a transition system from the Lorenz system to the Chen system. Based on the concept of nonresonant parametric perturbations, new details about the forming mechanism and its compound structure for the chaotic Lü attractor are obtained. It is proven that the chaos follows novel routs in the Lü system: the compression and pull forming mechanism. By this novel mechanism, the transition from the canonical Lorenz attractor to the Chen attractor through the Lü attractor is pointed out. The authors conclude: *the scheme herein goes beyond the traditional framework for studying the Lorenz-like systems, which can be very helpful in generating and analyzing of all similar and closely related chaotic systems.* In a recent paper [143], the authors studied an open problem related to the global boundedness of the Lü system. It is proven in the work that the Lü system is globally bounded according to dynamical systems theory and the bounds are also determined.

The T system [118, 119] received increasing attention in the last ten years. The authors in [89] propose an image encryption scheme based on our system. The method uses binary sequences obtained from our chaotic system to construct a desired cipher stream to encrypt the original image. *The results show that the suggested scheme has some excellent properties and can be used to construct cryptosystem with high practical security to meet the requirements of Internet on security*, as written in [89]. A detailed Hopf bifurcation analysis of the T system is presented in [57]. The bifurcation's direction and the stability of bifurcating periodic solutions are presented. The analytic results are exemplified by numerical examples. The work [83] studies a class of Lorenz-like chaotic systems which contains the T system and investigates the localization problem of compact invariant sets. The systems have potential applications in secure communications. A study of complete chaos synchronization is also performed in the work.

3.1.1 Bounded orbits in the Chen system

In this section we present the results we obtained in [121] on closed, homoclinic and heteroclinic orbits in the Chen system [22], [23]. Using a Lyapunov-like function, we proved that the system under some constraints of its parameters has no homoclinic orbits and no closed orbits but it has exactly two heteroclinic orbits symmetrically with respect to the z-axis. Using results from [13], we obtained new insights on cases not covered in [77] concerning homoclinic orbits. A similar approach we used in [120] for the Lü and T systems. A difficult task in these studies was to identify an adequate Lyapunov-like function. We omit the proofs in this presentation. They can be found in [120] and [121]. The Lyapunov-like functions are different for the three systems.

If x_1 and x_2 are two hyperbolic equilibrium points of a system such that the stable manifold $W^s(x_1)$ intersects the unstable manifold $W^u(x_2)$ then the orbits belonging to their non-empty intersection

$$W^s(x_1) \cap W^u(x_2) \neq \emptyset$$

is called a **heteroclinic** orbit. If $\varphi\,(t, x_0)$ denotes the heteroclinic orbit then

$$\lim_{t\to-\infty} \varphi\,(t, x_0) = x_2 \text{ and } \lim_{t\to\infty} \varphi\,(t, x_0) = x_1.$$

Equally, a heteroclinic orbit may be obtained by intersecting the unstable manifold of x_1 with the stable manifold of x_2, that is $W^u(x_1) \cap W^s(x_2) \neq \Phi$. On the other hand, a **homoclinic** orbit to a hyperbolic equilibrium x_1 is determined by

$$W^s(x_1) \cap W^u(x_1) \neq \emptyset.$$

For a homoclinic orbit $\psi\,(t, x_0)$ we have

$$\lim_{t\to-\infty} \psi\,(t, x_0) = \lim_{t\to\infty} \psi\,(t, x_0) = x_1.$$

The Chen system is given by:

$$\dot{x} = a(y - x),\ \ \dot{y} = (c - a)x - xz + cy,\ \ \dot{z} = xy - bz, \tag{3.1}$$

where $a > 0$, $b > 0$ and $c > 0$ are positive real parameters. The system (3.1) has the origin O as an equilibrium point for any $a, b, c > 0$ and it has two more equilibrium points $S_1 = (x^*, x^*, 2c - a)$ and $S_2 = (-x^*, -x^*, 2c - a)$, $x^* = \sqrt{b(2c - a)}$, for $2c > a$. Assume also further $a > c$.

A result reported in [94] brings insights on the boundedness of solutions of the Chen system. In this regard, the following theorem is reported.

Theorem 3.1.1. *All solutions of the Chen system* (3.1) *with* $a > c > 0$ *and* $b > 2c > 0$ *are globally bounded for* $t \in [0, +\infty)$. *In particular, if* $a > 2c > 0$ *and* $b > 2c > 0$, *then the system's solutions* $(x(t), y(t), z(t)) \to (0, 0, 0)$ *as* $t \to +\infty$.

The authors in [17] study the problem of forcing the Chen chaotic attractor to track a desired sinusoidal and chaotic signal when the system's parameter values are characterized by uncertainties. The tools combine the theory of robust regulation and the exact Takagi-Sugeno fuzzy model. As written in the paper, *on the basis of designing a robust controller for each linear subsystem, it is shown that the aggregated controller assures robust tracking in the presence of variations on the parameters of each linear subsystems and in the membership functions as well.*

Existence of heteroclinic orbits. The Jacobian matrix of the system (3.1) at the origin O has the eigenvalues and the corresponding eigenvectors given by:

$$\begin{aligned} d_1 &= \tfrac{1}{2}c - \tfrac{1}{2}a + \tfrac{1}{2}\sqrt{6ac - 3a^2 + c^2}, \\ u_1 &= \begin{pmatrix} \frac{1}{2a-2c}\left(a + c - \sqrt{6ac - 3a^2 + c^2}\right) & 1 & 0 \end{pmatrix}^T; \end{aligned}$$

$$\begin{aligned} d_2 &= \tfrac{1}{2}c - \tfrac{1}{2}a - \tfrac{1}{2}\sqrt{6ac - 3a^2 + c^2}, \\ u_2 &= \begin{pmatrix} \frac{1}{2a-2c}\left(a + c + \sqrt{6ac - 3a^2 + c^2}\right) & 1 & 0 \end{pmatrix}^T; \end{aligned}$$

$$\begin{aligned} d_3 &= -b, \\ u_3 &= \begin{pmatrix} 0 & 0 & 1 \end{pmatrix}^T. \end{aligned}$$

Considering $2c > a > c > 0$, it follows that $d_1 > 0$ and $d_{2,3} < 0$, that is, the origin is a saddle point having a one-dimensional unstable manifold W_0^u and a two-dimensional stable manifold W_0^s. The tangent unstable subspace TW_0^u is given by

$$TW_0^u = \left\{ 2(a - c)y = \left(a + c - \sqrt{6ac - 3a^2 + c^2}\right) x, z = 0 \right\}.$$

The unstable manifold W_0^u contains O and is tangent to TW_0^u at the origin. Using the method of undetermined coefficients in a small neighborhood of the origin we get

$$W_0^u = \left\{ (x, y, z) \in R^3 \,\middle|\, \begin{aligned} y &= a_1 x + O(x^2) \\ z &= \tfrac{a_1}{-2a+b+2aa_1} x^2 + O(x^3) \end{aligned} \right\},$$

where $|x| \ll 1$ and $a_1 = \frac{1}{2(a-c)}\left(a + c - \sqrt{6ac - 3a^2 + c^2}\right)$.

Note that W_0^u is indeed tangent to TW_0^u since $z'(0) = 0$, $y'(0) = a_1$ and the vector $(1, y'(0), z'(0))^T$ is collinear to the direction vector u_1 of the line TW_0^u. Note also that the z-axis is included in W_0^s.

Denote in the following by

$$\phi_t u_0 = (x(t,u_0), y(t,u_0), z(t,u_0))$$

a solution of the system (3.1) through the initial point $u_0 = (x_0, y_0, z_0)$ and by W_+^u $\left(W_-^u\right)$ the positive (negative) branch of the unstable manifold W_0^u corresponding to $x > 0$ $(x < 0)$.

Define a Lyapunov-like function of the form

$$U(x,y,z) = A\,(y-x)^2 + B\left(z - x^2/b\right)^2 + C\left(x^2 - b(2c-a)\right)^2.$$

Choosing $A = b - 2a \geq 0$, $B = b > 0$ and $C = \frac{1}{2ab}\,(b-2a) \geq 0$, it follows that

$$\frac{dU}{dt} = -2(b-2a)\,(a-c)\,(x-y)^2 - 2\left(bz - x^2\right)^2 \leq 0. \tag{3.2}$$

Remark 3.1.1. *Different from [77], the Lyapunov function U is defined both for $b > 2a$ and $b = 2a$.*

Proposition 3.1.1. *If $2c > a > c > 0$, $b \geq 2a$ the following assertions are true:*
a) If there exist t_1 and t_2 such that $t_1 < t_2$ and U satisfies

$$U(\phi_{t_1} u_0) = U(\phi_{t_2} u_0)$$

then either
- *u_0 is an equilibrium point of system (3.1), or*
- *$b = 2a$ and the orbit $\phi_t u_0$ is contained in the parabolic cylinder $bz = x^2$.*

b) Assume $b > 2a$. If

$$\phi_t u_0 \to O$$

as $t \to -\infty$ and $x(t,u_0) > 0$ for some t, then $U(O) > U(\phi_t u_0)$ and $x(t,u_0) > 0$, for all $t \in \mathbb{R}$. Consequently $u_0 \in W_+^u$.

Theorem 3.1.2. *Consider $2c > a > c > 0$, $b > 2a$ and the above function U. Then the following assertions are true:*
a) The ω-limit of any orbit of the system (3.1) is an equilibrium point. In particular, the system (3.1) has no closed orbits.
b) System (3.1) has no homoclinic orbits.
c) System (3.1) has exactly two heteroclinic orbits.

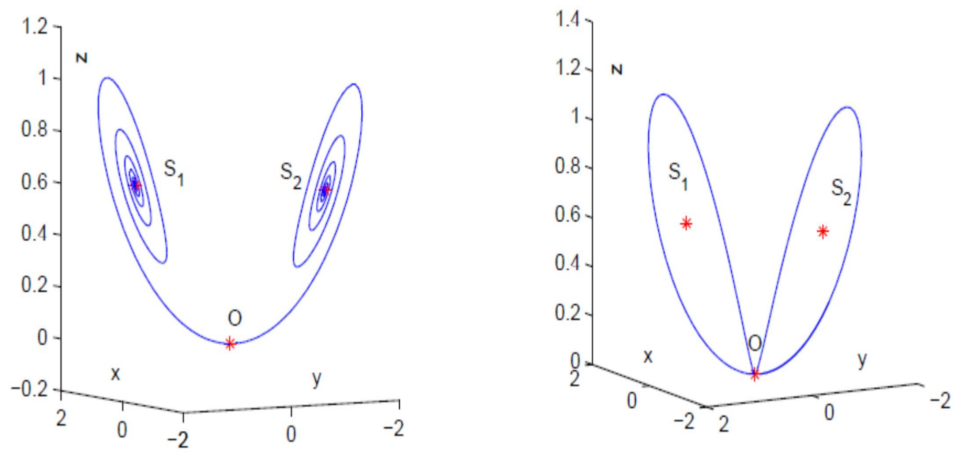

Figure 3.1: a) Two symmetrical heteroclinic orbits for $a = 1, b = 2.1, c = 0.8$. (left); b) Two symmetrical homoclinic orbits for $a = 1, b = 1.17, c = 0.8$ (right).

The proofs can be found in [121].

Existence of homoclinic orbits. Consider in the following the case $2c > a > c > 0$, $2a > b > 0$ and make the nonsingular transformation:

$$u = \alpha x, \;\; v = \beta(y - x), \;\; w = \gamma\left(z - \frac{x^2}{2a}\right),$$

and the rescaling $\tau = rt$. Then, for some values of α, β and γ (see [121]) the system (3.1) becomes

$$\begin{array}{rcl} \dot{u} & = & v, \\ \dot{v} & = & -\left(u^2 + w - 1\right)u - \lambda v, \\ \dot{w} & = & -\sigma w + \delta u^2, \end{array} \tag{3.3}$$

where $\lambda = \frac{a-c}{r}$, $\sigma = \frac{b}{\sqrt{a(2c-a)}}$, $\delta = (2a-b)\sqrt{\frac{1}{a(2c-a)}}$. Here $\beta = 2ar\alpha^3 = \frac{a}{r}\alpha$, $\gamma = 2a\alpha^2$ and $r^2 = \frac{1}{2\alpha^2}$. But the system (3.3) is treated in [13] and after a laborious study and using a method based on systems comparison, the following result is reported:

Theorem 3.1.3. *For each $\sigma > 0$, there is, in the region of positive parameters δ and λ, a bifurcation curve*

$$\{\rho(\sigma, \delta, \lambda) = 0\}$$

beginning at $(0,0)$ and going to infinity for $\delta \to \infty$, corresponding to a homoclinic orbit to the saddle point $O(0,0,0)$ of system (3.3).

It implies that for any a, b, c with $2c > a > c > 0$ and $2a > b > 0$, the Chen system (3.1) has two symmetrical homoclinic orbits to the equilibrium point O. A particular numerical case in this regard is presented in Fig.3.1 b) where the homoclinic orbits are depicted.

3.1.2 Bounded orbits in the Lü and the T systems

In [120] we obtained results on the the Lü and T systems. The Lü system, partially investigated in [77], is given by:

$$\dot{x} = a(y - x),\ \dot{y} = cy - xz,\ \dot{z} = -bz + xy, \tag{3.4}$$

where $a \neq 0$, $b \neq 0$ and $c \neq 0$ are real parameters. If $bc > 0$ the system has three equilibrium points $O(0,0,0)$, $S_1 = (\sqrt{bc}, \sqrt{bc}, c)$ and $S_2 = (-\sqrt{bc}, -\sqrt{bc}, c)$. Consider in the following $a, b, c > 0$. In this case, the Jacobian matrix of the system at the origin has the eigenvalues $d_1 = c > 0$, $d_2 = -a < 0$ and $d_3 = -b < 0$, that is, the origin is a saddle point with an 1-dimensional unstable manifold W_0^u and a 2-dimensional stable manifold W_0^s containing the z-axis. Define a Lyapunov-like function in the form

$$V(x, y, z) = A\left(y - x\right)^2 + B\left(bz - x^2\right)^2 + C\left(x^2 - bc\right)^2.$$

If one chooses $A = 2ab\left(b - 2a\right), B = 2a$ and $C = b - 2a$ with $b \geq 2a$, it follows that

$$\frac{dV}{dt}(\phi_t u_0) = -2A(a - c)\left(x(t, u_0) - y(t, u_0)\right)^2 - 2bB\left(bz(t, u_0) - x^2(t, u_0)\right)^2 \leq 0.$$

Based on the function V we obtained the following results. Their proofs can be found in [120].

Theorem 3.1.4. *Consider $a > c > 0$, $b \geq 2a$ and the above function V. Then the following assertions are true:*
a) The system (3.4) has no closed orbits;
b) The system (3.4) has no homoclinic orbits.

Theorem 3.1.5. *If $a > c > 0$ and $b \geq 2a$, the system (3.4) has exactly two heteroclinic orbits.*

The T system [118] - [120] is a 3D autonomous polynomial differential system given by:

$$\dot{x} = a(y-x),\ \dot{y} = (c-a)x - axz,\ \dot{z} = -bz + xy, \tag{3.5}$$

with a, b, c real parameters and $a \neq 0$. If $b(c-a)/a > 0$, the system has three equilibria:

$$O(0,0,0), \quad E_1(x_0, x_0, (c-a)/a) \text{ and } E_2(-x_0, -x_0, (c-a)/a)$$

with $x_0 = \sqrt{b(c-a)/a}$ and for $b \neq 0,\ b(c-a)/a \leq 0$ it has only one isolated equilibrium point, $O(0,0,0)$. One can check that, if $c > a > 0$ and $b > 0$, the Jacobian matrix of the system at the origin has the eigenvalues $d_1 > 0$ and $d_{2,3} < 0$, that is, the origin is a saddle point with an 1-dimensional unstable manifold W_0^u and a 2-dimensional stable manifold W_0^s. The unstable manifold W_0^u in a small neighborhood of the origin is given by

$$W_0^u:\ y = a_1 x + ...;\ z = \frac{a_1}{b - 2a + 2aa_1} x^2 + ... \tag{3.6}$$

with $|x| \ll 1$ and $a_1 = \frac{1}{2a}\left(a + \sqrt{4ac - 3a^2}\right)$. The stable manifold W_0^s contains the z-axis. Define a function in the form

$$V(x,y,z) = A\,(y-x)^2 + B\left(z - x^2/b\right)^2 + C\left(x^2 - b(c-a)/a\right)^2.$$

Choosing

$$A = 2b\,(b-2a)\,, B = 2ab^2, C = b - 2a$$

with $b \geq 2a$, it follows that

$$\frac{dV}{dt}(\phi_t u_0) = -2aA\,(x(t,u_0) - y(t,u_0))^2 - \frac{2B}{b}\left(bz(t,u_0) - x^2(t,u_0)\right)^2 \leq 0.$$

The following results are reported in [120].

Theorem 3.1.6. *Consider $c > a > 0$, $b \geq 2a$ and the above function V. Then the following assertions are true:*
a) The system (3.5) has no closed orbits;
b) The system (3.5) has no homoclinic orbits.

Theorem 3.1.7. *If $c > a > 0$ and $b \geq 2a$, the system (3.5) has exactly two heteroclinic orbits.*

3.1.3 Bautin bifurcations in the T system

In this section we present the results reported in [126]. Using the linear transformation $(x, y, z) \to (X_1, Y_1, Z_1)$,

$$x = X_1 + x_0, y = Y_1 + x_0, z = Z_1 - 1 + c/a,$$

the T system becomes

$$\begin{array}{rcl} \dot{X}_1 & = & a(Y_1 - X_1) \\ \dot{Y}_1 & = & -ax_0 Z_1 - aX_1 Z_1 \\ \dot{Z}_1 & = & x_0(X_1 + Y_1) - bZ_1 + X_1 Y_1 \end{array} \tag{3.7}$$

when E_1 is translated to O. Its characteristic polynomial at O is

$$P(\lambda) = \lambda^3 + \lambda^2(a + b) + bc\lambda + 2ab(c - a). \tag{3.8}$$

We showed that the T system undergoes a Bautin-type bifurcation at E_1. By symmetry, the same bifurcation occurs at E_2. Consider further $a, b, c \neq 0$, $\frac{b}{a}(c - a) > 0$ and $ac - 2a^2 > 0$. Denote by $b_s = a - 2a^2/c$ for a and c arbitrarily fixed. Therefore, (3.8) has two purely imaginary roots $\pm i\omega$ at $b = b_s$ and because the eigenvalues are continuous with respect to the parameter b, there exist positive values b, with $|b - b_s|$ small enough, such that the complex eigenvalues of (3.8) are

$$\lambda = \alpha(a, b, c) + i\omega(a, b, c)$$

and $\overline{\lambda}$, where $\omega(a, b_s, c) = \sqrt{ac - 2a^2}$ and $\alpha(a, b_s, c) = 0$. The algorithm for detecting the Bautin bifurcation in our system can be described in the following steps.

Step 1. Write the system restricted to the center manifold at $b = b_s$.
Step 2. Find the first Lyapunov coefficient $\ell_1(0)$.
Step 3. Determine the expression of the second Lyapunov coefficient $\ell_2(0)$.
For the first two steps we assume that b is the varying parameter while a and c are arbitrarily fixed. Let us briefly describe the three steps.

Step 1. For $b = b_s$ consider the transformation

$$\begin{pmatrix} X_1 \\ Y_1 \\ Z_1 \end{pmatrix} = \begin{pmatrix} 1 & -\frac{a}{\omega}qx_0 & qx_0 \\ \frac{2a-c}{c} & -\frac{a}{\omega}x_0 & 0 \\ -\frac{2}{c}\sqrt{c - 2a - b} & 0 & 1 \end{pmatrix} \begin{pmatrix} X \\ Y \\ Z \end{pmatrix}.$$

The vectors in the matrix are

$$v_2' = \frac{v_2 + v_3}{2} = \left(-\frac{a}{\omega}qx_0, -\frac{a}{\omega}x_0, 0\right), \; v_3' = \frac{v_2 - v_3}{2i} = (qx_0, 0, 1)$$

and

$$v_1 = \left(1, \frac{2a - c}{c}, -\frac{2}{c}\sqrt{c - 2a - b}\right),$$

where v_1,

$$v_2 = \left(-\frac{a}{\omega}qx_0 + iqx_0, -\frac{a}{\omega}x_0, i\right) \text{ and } v_3 = \left(-\frac{a}{\omega}qx_0 - iqx_0, -\frac{a}{\omega}x_0, -i\right),$$

with $q = \frac{a^2}{\omega^2 + a^2}$, are eigenvectors of the Jacobian matrix of (3.8) at O. After performing the computations, the system (3.8) in complex form with $z = Y + iZ$, $w = Y - iZ$, $v = X$, reads:

$$\begin{aligned} \dot{v} &= 2a\frac{a - c}{c}v + g_1(v, z, w) \\ \dot{z} &= -i\omega z + g_2(v, z, w) + ig_3(v, z, w), \end{aligned} \tag{3.9}$$

where

$$\begin{aligned} g_1(v, z, w) &= a_{200}v^2 + a_{020}z^2 + \bar{a}_{020}w^2 + a_{110}vz + \bar{a}_{110}vw + a_{011}zw, \\ g_2(v, z, w) &= b_{200}v^2 + b_{020}z^2 + \bar{b}_{020}w^2 + b_{110}vz + \bar{b}_{110}vw + b_{011}zw, \\ g_3(v, z, w) &= c_{200}v^2 + c_{020}z^2 + \bar{c}_{020}w^2 + c_{110}vz + \bar{c}_{110}vw + c_{011}zw. \end{aligned}$$

The coefficients of these expressions can be found in [126]. Assume the equation of the central manifold is of the form

$$v = Az^2 + Bzw + Cw^2 + Ez^3 + Fz^2w + Gzw^2 + Hw^3 + ... \tag{3.10}$$

Deriving this equation and using (3.9) we obtain two forms of $\dot{v}$ from which we can determine the coefficients $A, B, ..., H$ (see [126]). Inversing the time $t \to -t$, the system on the central manifold reads

$$\dot{z} = i\omega z - g_2(v, z, w) - ig_3(v, z, w). \tag{3.11}$$

Step 2. Using the first three coefficients A, B, C, the first Lyapunov coefficient $\ell_1(0)$ can be determined from:

$$\ell_1(0) = \frac{1}{2\omega^2}Re(\omega g_{21} + ig_{20}g_{11}). \tag{3.12}$$

In addition, applying the implicit function theorem in (3.8) it follows that

$$Re\left(\frac{d\lambda}{db}\,|_{b=b_s,\lambda=i\sqrt{ac-2a^2}}\right)=\frac{1}{2}c^2\frac{2a-c}{2ac^2-8a^2c+4a^3+c^3}\neq 0.$$

Step 3. Finally, the second Lyapunov coefficient is determined from

$$\begin{aligned}12\ell_2(0)=\frac{1}{\omega}Re\ g_{32}+\frac{1}{\omega^2}Im&\left[g_{20}\overline{g}_{31}-g_{11}(4g_{31}+3\overline{g}_{22})\right.\\&\left.-\frac{1}{3}g_{02}(g_{40}+\overline{g}_{13})-g_{30}g_{12}\right]+\frac{1}{\omega^3}\eta_1+\frac{1}{\omega^4}\eta_2,\end{aligned}\tag{3.13}$$

where,

$$\begin{aligned}\eta_1=Re&\left[g_{20}\left(\overline{g}_{11}(3g_{12}-\overline{g}_{30})+g_{02}(\overline{g}_{12}-\frac{1}{3}g_{30})+\frac{1}{3}\overline{g}_{02}g_{03}\right)\right.\\&\left.+\,g_{11}\left(\overline{g}_{02}\left(\frac{5}{3}\overline{g}_{30}+3g_{12}\right)+\frac{1}{3}g_{02}\overline{g}_{03}-4g_{11}g_{30}\right)\right]+Im(3g_{20}g_{11})Im\ g_{21},\end{aligned}$$

$$\eta_2=Im\left[g_{11}\overline{g}_{02}(\overline{g}_{20}^2-3\overline{g}_{20}g_{11}-4g_{11}^2)\right]+Im(g_{20}g_{11})\left[3Re(g_{20}g_{11})-2|g_{02}|^2\right].$$

More details can be found in [126]. Finally, we obtained the following result:

Theorem 3.1.8. *If $a,b,c\neq 0$, $\frac{b}{a}(c-a)>0$, $ac-2a^2>0$, $2ac^2-8a^2c+4a^3+c^3\neq 0$ and $\ell_1(0)\neq 0$ in (3.12), the T system undergoes a Hopf bifurcation at $b=b_s$. Moreover, if $\ell_1(0)=0$ at $b=b_s$ and the second Lyapunov coefficient $\ell_2(0)\neq 0$ in (3.13), the T system undergoes a Bautin bifurcation leading to the existence of at most two limit cycles in a small neighborhood of the equilibrium E_1.*

3.1.4 Bounded orbits in the Shimizu-Morioka system

In this section we consider the Shimizu-Morioka system [104]

$$\dot{x}=y,\ \dot{y}=(1-z)x-\lambda y,\ \dot{z}=-\alpha(z-x^2)$$

and describe the results we reported in [122]-[123]. The system is related to an asymptotic normal form for bifurcations of triply degenerate equilibrium states and periodic orbits [135, 105]. The system was studied lately in [106, 107, 108, 100, 105]. It has been shown numerically that the system has a Lorenz attractor [3]. The proof was based on a method from [109]. More details can be found in [98] and [110]. In [79] some global dynamical aspects of the Shimizu - Morioka system are given. A study of the local Hopf bifurcations of codimension one and two in the Shimizu - Morioka system has been reported in [74]. The authors obtained results related to the bifurcation diagrams of these kinds of Hopf bifurcation. The diagrams contribute to the understanding of the qualitative behavior of the system's solutions for different values of the parameters.

In [140] it is explored the multifractal, self-similar organization of heteroclinic and homoclinic bifurcations of saddle singularities in the parameter space of the Shimizu - Morioka model. It is pointed out the contribution of the Shilnikov saddle-foci to the complex transformations that underlie the transitions from the Lorenz attractor to wildly chaotic dynamics. The authors *demonstrate how the original computational technique, based on the symbolic description and kneading invariants, can disclose the complexity and universality of parametric structures and their link with nonlocal bifurcations in this representative model.*

In our work [122] we provided an analytic (free of computer assistance) proof of the existence of the homoclinic loops with zero saddle value in this system. The results can be considered as an important step forward towards a fully analytical proof of the existence of the Lorenz attractor in the Shimizu - Morioka system.

The homoclinic butterfly here is a pair of homoclinic loops symmetric to each other by $(x, y, z) \to (-x, -y, z)$. By the symmetry of the system, it is enough to establish the existence of only one of the loops. The loop is an orbit which tends to the saddle equilibrium state $O(0, 0, 0)$ when $t \longrightarrow \pm\infty$. The saddle value σ is the sum of the positive characteristic exponent at O with the nearest to the imaginary axis negative one. In order to apply the criterion from [109], we need $\sigma = 0$, which is equivalent to $\lambda = (1 - \alpha^2)/\alpha$, as one can easily see. From now on we impose this restriction on α and λ. After scaling the time $t \to t/\alpha$ and $y \to \alpha y$, the system takes the form

$$\dot{x} = y,\ \dot{y} = (a + 1)(1 - z)x - ay,\ \dot{z} = -z + x^2, \tag{3.14}$$

where $a = \lambda/\alpha = -1 + 1/\alpha^2$. The main result of this subsection is the next theorem.

Theorem 3.1.9. *There exists a value $a_0 > 0$ such that the system (3.14) at $a = a_0$ has a homoclinic loop to the saddle point $O(0, 0, 0)$.*

We proved the existence of the homoclinic loop by means of a refined version of the *method of systems comparison*, developed in [13, 12]. Roughly speaking, the method consists in finding the traces which the stable and unstable manifolds

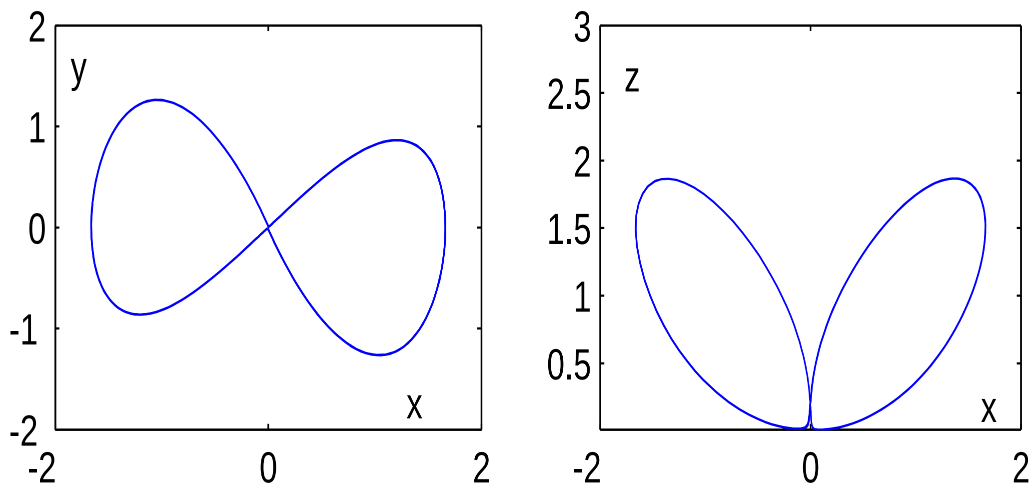

Figure 3.2: Two homoclinic orbits (homoclinic butterfly) at $a \cong 1.718$.

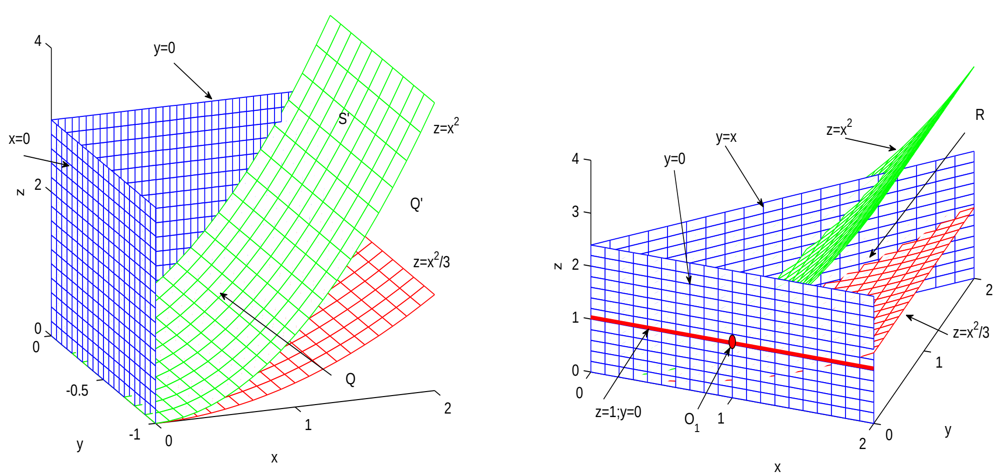

Figure 3.3: Surfaces and regions related to Lemma 3.1.1.

of the saddle point leave on a Poincaré section, the surface $z = x^2$ in our case. Once certain bounds are found for the position of the traces, we show that when the parameter a varies the two traces meet one another and form a homoclinic loop. We illustrated numerically and showed that at $a_0 \simeq 1.718$ the system has a homoclinic orbit (cf. [106, 107, 108]).

We want to describe briefly the main steps we used towards the proof of the theorem. We **first estimated the unstable manifold**. The equilibrium points of system (3.14) are $O(0,0,0)$, $O_1(1,0,1)$ and $O_2(-1,0,1)$. The point $O(0,0,0)$ is a saddle with a one-dimensional unstable manifold W_0^u and a two-dimensional stable manifold W_0^s, and with zero saddle value ($a \geq 0$). The curve W_0^u is divided by O into two branches, the separatrices. Denote by W_+^u the separatrix which leaves O towards $x > 0$. We found that the equation of W_+^u is

$$y = x - \frac{(a+1)}{3(a+4)}x^3 + o(x^3),\ z = \frac{1}{3}x^2 + \frac{2(a+1)}{45(a+4)}x^4 + o(x^4). \tag{3.15}$$

A first result is given in the next lemma.

Lemma 3.1.1. *For every $a \geq 0$, the separatrix W_+^u leaves R at a finite moment of time by intersecting transversely the surface*

$$S := \left\{y = 0,\ z > 1,\ \sqrt{z} < x < \sqrt{3z}\right\}.$$

After crossing S, the separatrix intersects transversely

$$S' := \left\{x > 0,\ y < 0,\ z = x^2\right\}.$$

After crossing S', it either stays in the region

$$Q := \{x > 0, y < 0, z > x^2\}$$

forever, and then it tends to O and forms a homoclinic loop, or it leaves Q by either transversely intersecting the plane $x = 0$, or transversely intersecting the plane $y = 0$ at $x < 1$, Figs.3.3.

Its proof can be found in [122]. This lemma allows us to establish the existence of the sought homoclinic loop at some $a_0 > 0$ in the following way. Let A_1 be the set of parameters $a \geq 0$ for which the separatrix W_+^u leaves the region Q by crossing $x = 0$, and A_2 be the set of parameters $a \geq 0$ for which the separatrix

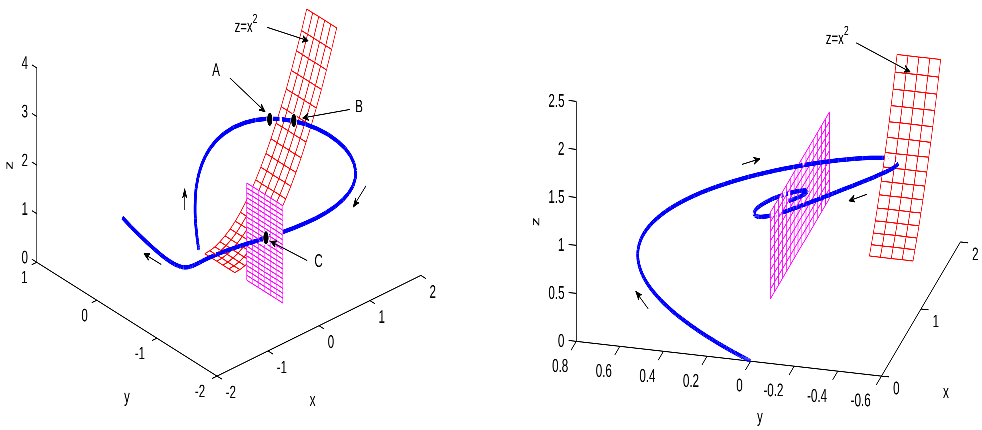

Figure 3.4: The separatrix W_+^u for small and large a. For $a = 1$ (left), W_+^u crosses first $y = 0$ at $A(1.79, 0.00, 1.73)$, enters $Q : x > 0, y < 0, z > x^2$ through $B(1.46, -1.30, 2.14)$ and leaves Q by $x = 0$ at $C(0.00, -1.12, 1.13)$, while for $a = 10$ (right), after crossing $y = 0$ and entering Q, W_+^u leaves Q by $y = 0$ at $(0.97, 0.00, 0.99)$.

W_+^u leaves Q by crossing $y = 0$, Fig.3.4. Because of the transversality of the intersection of W_+^u with either plane, the sets A_1 and A_2 are open (as subsets of $[0, +\infty)$). Thus, if we prove that both these sets are nonempty, i.e. there exist $a_1 \geq 0$ such that W_+^u leaves Q by crossing $x = 0$ and $a_2 \geq 0$ such that W_+^u leaves Q by crossing $y = 0$, we will immediately obtain that there exists $a_0 \in (a_1, a_2)$ which belongs to neither of the two sets. By the lemma, at $a = a_0$, the separatrix W_+^u forms the homoclinic loop.

The **second main step** in proving our theorem was to study the behaviour of the system at small and large a. More details on the proof are described in [122].

In the following we describe briefly the results reported in [123] on the Shimizu-Morioka system. This work contributed to the results presented in [122].

Consider a surface S in $\mathbb{R}^3$ given by

$$S : \; F(x, y, z) = 0,$$

where $F \in C^1(\mathbb{R}^3)$. A normal vector to S at a point $(x, y, z) \in S$ is the gradient vector $grad\ F(x, y, z) = (F'_x, F'_y, F'_z)$. The surface S splits the space in two regions, according to $F > 0$ (the positive region) or $F < 0$ (the negative region). Assume the normal vector $grad\ F(x, y, z)$ lies in the positive region.

If a trajectory (for t increasing) of a differential system

$$\dot{u} = f(u), \tag{3.16}$$

where $\dot{u} = (\dot{x}, \dot{y}, \dot{z})$, $f(u) = (f_1(x, y, z), f_2(x, y, z), f_3(x, y, z))$, hits the surface S at a point $A(x_0, y_0, z_0)$ coming from the positive region $F > 0$, then the vector field f at A makes with the gradient vector $grad\ F$ at A an angle larger than $90°$. As

$$\cos(gradF, f) = \frac{grad\ F \cdot f}{|grad\ F| \cdot |f|},$$

it follows that $grad\ F \cdot f < 0$ at A. On the other hand,

$$\frac{d}{dt}F(x, y, z)|_{F=0} = F_x\dot{x} + F_y\dot{y} + F_z\dot{z}|_{F=0} = grad\ F \cdot f < 0, \text{at } A.$$

Proposition 3.1.2. *If the derivative (for t increasing) along a trajectory of the system (3.16),*

$$\frac{d}{dt}F(x, y, z)|_{F=0} < 0,$$

then the trajectory hits the surface $S : F(x, y, z) = 0$ coming from the positive region $F(x, y, z) > 0$. If

$$\frac{d}{dt}F(x, y, z)|_{F=0} > 0,$$

then it crosses the surface $S : F(x, y, z) = 0$ coming from the negative region $F(x, y, z) < 0$. For t decreasing, the scenario is inversely, i.e. if

$$\frac{d}{dt}F(x, y, z)|_{F=0} < 0,$$

the trajectory hits the surface S coming from the negative region and if

$$\frac{d}{dt}F(x, y, z)|_{F=0} > 0,$$

the trajectory hits the surface S coming from the positive region.

Tracing the unstable manifold W_+^u. Assume $a+1>0$. Consider the equation of W_+^u in the neighborhood of $O(0,0,0)$ given by

$$\begin{aligned} y &= a_1x + a_2x^2 + a_3x^3 + ... \\ z &= b_1x + b_2x^2 + b_3x^3 + b_4x^4 + ... \end{aligned} \tag{3.17}$$

As

$$W_0^u = W_+^u \cup W_-^u$$

is invariant under the action of the flow, after computing the coefficients, W_+^u for x small enough is given by

$$y = x + ...,\ z = \frac{1}{3}x^2 + ... \ . \tag{3.18}$$

Hence, for x small enough W_+^u lies in the region

$$R = \{(x,y,z) : 0 < y < x, \frac{1}{3}x^2 < z < x^2, x > 0\}.$$

We want to estimate now the $x-$coordinate of the point where W_+^u crosses $y=0$. Consider in $\mathbb{R}^3$ the surface in

$$\{y = x - bx^2, 0 < z < x^2, b > 0\}.$$

As $x - bx^2 < x, b > 0$ the surface

$$\{y = x - bx^2\}$$

is below W_+^u for x small enough. We are interested under what conditions, trajectories lying in $\frac{1}{3}x^2 < z < x^2$ can cross this surface.

Proposition 3.1.3. *The surface*

$$\{y = x - bx^2, 0 < z < x^2, b > 0\}$$

is a surface without contact for trajectories of the system (i.e. transversal to the flow). If t increases, the trajectories of the system cross the surface on the side $y < x - bx^2$ for all $0 < x < \frac{b(a+3)}{a+1+2b^2}, b > 0$. In particular, if $b = 1$ we obtain that the trajectories of the system (and implicitly W_+^u) for $0 < z < x^2$ cross $y = 0$ for $x \geq 1$.

Consider now a curve above W_+^u,

$$y = cx - dx^2, c > 1, d > 0.$$

One may notice that for any $d > 0,\ c > 1$ we have $cx - dx^2 > x$ for x small enough, more exactly if $x < (c-1)/d$. So the surface $y = cx - dx^2$ is above W_+^u for x small enough.

Proposition 3.1.4. *There exists $c > 1, d > 0, c/d = \sqrt{3}$ such that the surface in $\mathbb{R}^3$,*

$$y = cx - dx^2, \frac{1}{3}x^2 < z$$

is a surface without contact for trajectories of the system for all $x > 0$. If t increases, trajectories of the system cross the surface for all $a > 2, a^2 - 8a - 8 > 0$ on the side $y > cx - dx^2$. Consequently, for $a > 2, a^2 - 8a - 8 > 0$ the trajectories (and implicitly W_+^u) starting in

$$y < cx - dx^2, \frac{1}{3}x^2 < z$$

cross $y = 0$ for $x \leq \sqrt{3}$.

Remark 3.1.2. *The above Propositions 3.1.3-3.1.4 say that the separatrix W_+^u crosses the plane $y = 0$ at a point $K(x_u, 0, z_u)$ with $1 < x_u < \sqrt{3}$ if a is large enough (in fact for $a^2 - 8a - 8 > 0$ and $a > 2$).*

Tracing the stable W_0^s manifold. As the positive part of the Oz axis, denoted by d^+, belongs to W_0^s, we express W_0^s in a small neighborhood of some parts of d^+ in the form

$$y = -f(t)x,\ z = z_0 e^{-t}, t > 0.$$

Denote by $TW^s\,|_A$ the tangent space to W_0^s at the point A.

Proposition 3.1.5. *a) There exists a sequence $z_0, z_1, ..., z_k, ...$, where $z_{k+1} > z_k$ and $z_0 > 1 + \frac{a^2}{4(a+1)}$ such that the tangent space*

$$TW^s\,|_{A_k} = \{(x, y, z) : y = 0\},$$

where $k = 0, 1, 2, ...$ and $A_k = (0, 0, z_k)$.
b) For $z < z_0$ we express

$$TW^s\,|_A = \{(x, y, z) : y = -f_0(t)x, z = z_0 e^{-t}, t > 0\},$$

where $A = (0,0,z)$ and $f_0(t)$ is a solution of the Riccati equation (generally unsolvable)

$$f'^2(t) - af(t) - (a+1)(1 - z_0 e^{-t}), \tag{3.19}$$

which is bounded for $t > 0, f_0(0) = 0$ and such that

$$\frac{1}{2}(a + \sqrt{(a+2)^2 - 4(a+1)z_0 e^{-t}}) < f_0(t) < a+1, t > t_0 > 0, \tag{3.20}$$

where $t_0 := ln\frac{4(a+1)z_0}{(a+2)^2} > 0$.

This result implies that in the neighborhood of the integral line

$$d^+ : \{x = y = 0, z > 0\},$$

the two-dimensional manifold W^s for $z \leq z_0$ can be expressed as

$$\{y = -f_0(t)x, z = z_0 e^{-t}, t \geq 0\}.$$

So for $0 < \varepsilon \ll 1$ we can find a curve

$$C = W^s \cap \{x^2 + y^2 = \varepsilon^2,\ 0 \leq z \leq z_0\}.$$

Proposition 3.1.6. *Consider the region in $\mathbb{R}^3$,*

$$R_1 = \{-(a+1)x < y < 0\}$$

where $y = 0$ and $y = -(a+1)x$ are seen as surfaces in $\mathbb{R}^3$. Then the curve $C \subset R_1$ for ε small enough. In addition, for decreasing t, each trajectory starting on C up to its intersection with the plane $y = 0$, remains in the region R_1 and will cross this plane only for $z > 1$.

The proofs of these results can be found in [123].

3.2 Non-smooth dynamical systems

3.2.1 A generalization of the Nordmark map

The results on a two-dimensional non-smooth discrete dynamical system (a Poincaré-like map) we obtained in [124] are presented in this section. The map generalizes in some sense the so-called Nordmark map, which is related to one-dimensional impacting oscillators near grazing points, and constitute an intuitive basis for dynamics related to degenerate grazing in such oscillators. More exactly, we studied map $P = (P_i, P_{ni})$ given by

$$P_i : \begin{cases} x_{m+1} = \alpha x_m + y_m + s\sqrt[2k]{x_m} + \mu \\ y_{m+1} = -\lambda_1 \lambda_2 r x_m \end{cases}, x_m > 0, \tag{3.21}$$

respectively,

$$P_{ni} : \begin{cases} x_{m+1} = (\lambda_1 + \lambda_2)\, x_m + y_m + \mu \\ y_{m+1} = -\lambda_1 \lambda_2 x_m \end{cases}, x_m \leq 0, \tag{3.22}$$

with $\alpha, \mu, a, b \in \mathbb{R}$, $0 \leq r \leq 1$, $s = \pm 1$, $\lambda_1 = a + ib$, $\lambda_2 = a - ib$, $|\lambda_1| < 1$, $|\lambda_2| < 1$, respectively, $k \geq 1$ and $m \geq 1$ integers. The first branch P_i of P is called the impacting map while the second branch P_{ni} the non-impacting map. The variable x_m represents the state of the oscillator at time t_m and y_m its velocity; see [26, 81, 85] for more details. The map P is a generalization of the Nordmark map, [26, 85], given by

$$\begin{cases} x_{m+1} = y_m - \sqrt{x_m} + \mu \\ y_{m+1} = -\gamma r_1^2 x_m \end{cases}, \; x_m > 0, \tag{3.23}$$

respectively,

$$\begin{cases} x_{m+1} = \alpha_1 x_m + y_m + \mu \\ y_{m+1} = -\gamma x_m \end{cases}, x_m \leq 0, \tag{3.24}$$

in the sense that for $k = 1$, $\alpha = 0$, $s = -1$ and redenoting the parameters by $r = r_1^2$, $\gamma = \lambda_1 \lambda_2$, $\alpha_1 = \lambda_1 + \lambda_2$, one obtains (3.24) from (3.21)-(3.22).

The Nordmark map is related to a discrete form of a class of two-order non-autonomous differential equations in the form

$$\ddot{x} = A\,(x, \dot{x}, t)\,, \tag{3.25}$$

where $A\,(x, \dot{x}, t)$ is periodic of period $T > 0$ in t, namely $A\,(x, \dot{x}, t + T) = A\,(x, \dot{x}, t)\,$, as a model for one-dimensional impacting oscillators (such as, an oscillator hitting a rigid wall, a particle moving in a magnetic field, a ball bouncing on a vibrating table) and describes the dynamics of an orbit in a neighbourhood of grazing points. Other studies related to these topics can be found, for example, in [7], [25], [35], [80], [86]. When dealing with impact oscillators two assumptions are quite present, namely, the impact time of an orbit with the impact barrier is assumed zero, respectively, the leaving velocity v_s from the impact depends only on the hitting velocity v_i in the form

$$v_s = -r_1 v_i,$$

where $0 \leq r_1 \leq 1$ is called coefficient of restitution. In [81] we meet a generalization of the Nordmark map which uses

$$x_{m+1} = \alpha_2 x_m + y_m \pm \sqrt{x_m} + \mu$$

on $x_m > 0$ in (3.24). In order to understand the subject and results we obtained we give some more details as follows.

The map $P = (P_i, P_{ni})$ is continuous but not differentiable (non-smooth) on $x = 0$. This singularity at $x = 0$ gives rise to unusual bifurcations. The non-impacting branch P_{ni} has a fixed point $E\,(x_0, y_0)$ with

$$x_0 = \frac{\mu}{(1-\lambda_1)(1-\lambda_2)}, y_0 = \frac{-\mu\lambda_1\lambda_2}{(1-\lambda_1)(1-\lambda_2)} \tag{3.26}$$

on $x < 0$ for $\mu < 0$ since $|\lambda_1| < 1$ and $|\lambda_2| < 1$. Since the point $E\,(x_0, y_0)$ lies in the interior of the domain of definition of the function P_{ni}, namely $(x_0, y_0) \in (-\infty, 0) \times \mathbb{R}$, the Jacobian matrix

$$\begin{pmatrix} \lambda_1 + \lambda_2 & 1 \\ -\lambda_1\lambda_2 & 0 \end{pmatrix}$$

of P_{ni} at $E\,(x_0, y_0)$ is well defined and has the eigenvalues λ_1, λ_2 with $|\lambda_1| < 1$ and $|\lambda_2| < 1$. Therefore, the multiplicators of the fixed point $E\,(x_0, y_0)$ are λ_1, λ_2 with $|\lambda_1| < 1$ and $|\lambda_2| < 1$, so that $E\,(x_0, y_0)$ is a stable fixed point. The point $E\,(x_0, y_0)$ corresponds to a stable periodic orbit Γ^* of period T in the differential equation (3.25).

Increasing μ to 0, the fixed point E approaches O and for $\mu = 0$ they coincide. For $\mu > 0$ the point E is not a fixed point anymore on $x < 0$ but there might be another fixed point on the impacting side $x > 0$, $F\,(x^*, y^*)$.

When $s = +1$, the fixed point F indeed exists provided that the equation

$$\sqrt[2k]{x} = \delta x - \mu \tag{3.27}$$

with $\delta = 1 - \alpha + \lambda_1\lambda_2 r$ and $\mu > 0$ has positive real roots. On $\delta < 0$, (3.27) has no real roots on the impacting side $x > 0$ and has exactly one root for $\delta > 0$ on $x > 0$. When $s = -1$, the fixed point F exists if the equation

$$\sqrt[2k]{x} = \mu - \delta x \tag{3.28}$$

has positive real roots.

Denote by Γ_n^p a period orbit of period p of the map $P = (P_i, P_{ni})$ having exactly $n-$points on the impacting side. We focused in our study on detecting Γ_1^p orbits. We may assume that the single impacting point of Γ_n^p is the first point.

Denote by $(x_m, y_m)\,, m \geq 1$ a generic point on an orbit of the map P and by

$$z_m = \begin{pmatrix} x_m \\ y_m \end{pmatrix}, \hat{\mu} = \begin{pmatrix} \mu \\ 0 \end{pmatrix}, J = \begin{pmatrix} \lambda_1 + \lambda_2 & 1 \\ -\lambda_1\lambda_2 & 0 \end{pmatrix} \text{ where } |\lambda_1| < 1 \text{ and } |\lambda_2| < 1. \tag{3.29}$$

With these notations P_{ni} becomes

$$z_{m+1} = Jz_m + \hat{\mu}. \tag{3.30}$$

Hence,

$$\Gamma_1^p = \{z_1, z_2, ..., z_p\}$$

where $x_1 > 0$ and $x_2 < 0, ..., x_p < 0$. Since Γ_n^p has period p, we must have $z_{p+1} = z_1$. On the non-impacting side, Γ_n^p has points of the form

$$z_{m+1} = J^{m-1}z_2 + \left(I + J + ... + J^{m-2}\right)\hat{\mu} \tag{3.31}$$

where $m = 2, 3, ..., p$, $I = \begin{pmatrix} 1 & 0 \\ 0 & 1 \end{pmatrix}$, and

$$z_2 = \begin{pmatrix} x_2 \\ y_2 \end{pmatrix} = \begin{pmatrix} \alpha x_1 + y_1 + s\sqrt[2k]{x_1} + \mu \\ -\lambda_1\lambda_2 r x_1 \end{pmatrix}.$$

More details can be found in [124]. Consider first **the case of the real parameters** λ_1 and λ_2 with $0 < \lambda_2 < \lambda_1 < 1$. Keep also $s = -1$. Skipping here more calculations, we obtain

$$x_{m+1} = \mu A + \frac{1}{\lambda_1 - \lambda_2}\left[(\lambda_1^m - \lambda_2^m)\left(y_1 - x_1^{\frac{1}{2k}}\right) + x_1\beta_1\right] \tag{3.32}$$

and

$$y_{m+1} = \mu B + \frac{1}{\lambda_1 - \lambda_2}\left[(\lambda_1\lambda_2^m - \lambda_1^m\lambda_2)\left(y_1 - x_1^{\frac{1}{2k}}\right) + x_1\beta_2\right] \tag{3.33}$$

where

$\beta_1 = \alpha\lambda_1^m - \alpha\lambda_2^m + r\lambda_1\lambda_2^m - r\lambda_1^m\lambda_2$ and $\beta_2 = \alpha\lambda_1\lambda_2^m - \alpha\lambda_1^m\lambda_2 - r\lambda_1^2\lambda_2^m + r\lambda_1^m\lambda_2^2$, respectively,

$$A = \frac{\lambda_1 - \lambda_2 - \lambda_1^{m+1} + \lambda_2^{m+1} - \lambda_1 \lambda_2^{m+1} + \lambda_1^{m+1} \lambda_2}{(\lambda_1 - 1)(\lambda_2 - 1)(\lambda_1 - \lambda_2)}$$

and

$$B = -\frac{\lambda_1 \lambda_2}{(\lambda_1 - 1)(\lambda_2 - 1)(\lambda_1 - \lambda_2)} (\lambda_1 - \lambda_2 - \lambda_1^m + \lambda_2^m - \lambda_1 \lambda_2^m + \lambda_1^m \lambda_2).$$

But $x_{p+1} = x_1$ and $y_{p+1} = y_1$ lead to

$$F(x_1, \mu) := -x_1^{\frac{1}{2k}} + Cx_1 + \mu D = 0 \tag{3.34}$$

where

$$\begin{aligned} C &= \frac{1}{\lambda_2^p - \lambda_1^p} \lambda_1 - \lambda_2 + \left(\lambda_1^{p-1} - \lambda_2^{p-1}\right) \lambda_1 \lambda_2 \\ &\quad + r \frac{1}{\lambda_2^p - \lambda_1^p} \left(\lambda_1^p \lambda_2 - \lambda_1 \lambda_2^p + \lambda_1^{p+1} \lambda_2^p - \lambda_1^p \lambda_2^{p+1}\right) + \alpha \end{aligned}$$

and

$$D = (\lambda_1 - \lambda_2) \frac{(\lambda_2^p - 1)(\lambda_1^p - 1)}{(\lambda_2 - 1)(\lambda_1 - 1)(\lambda_1^p - \lambda_2^p)}.$$

For x_1 root of (3.34), we find

$$y_1 = -\frac{x_1}{\lambda_1^p - \lambda_2^p} (\lambda_1^p \lambda_2 - \lambda_1 \lambda_2^p + r \lambda_1^p \lambda_2^p (\lambda_1 - \lambda_2)) - \mu K \tag{3.35}$$

where

$$K = \frac{1}{(\lambda_1 - 1)(\lambda_2 - 1)(\lambda_1^p - \lambda_2^p)} \left(\lambda_1^{p+1} \lambda_2 - \lambda_1 \lambda_2^{p+1} + \lambda_1^p \lambda_2^{p+1} - \lambda_1^{p+1} \lambda_2^p + \lambda_1 \lambda_2^p - \lambda_1^p \lambda_2\right).$$

Since $0 < \lambda_2 < \lambda_1 < 1$, one can show that for $p \geq 2$

$$\frac{\lambda_2}{\lambda_2 - 1} < K \leq -\frac{\lambda_1 \lambda_2}{\lambda_1 + \lambda_2} < 0. \tag{3.36}$$

Finally we have the following theorem whose proof can be found in [124].

Theorem 3.2.1. *If the parameters λ_1 and λ_2 satisfy the inequalities $0 < \lambda_2 < \lambda_1 < 1$, then the map $P = (P_i, P_{ni})$ can have up to two one-impacting periodic orbits of period p for any fixed $\mu > 0$ and $k \geq 1$. More exactly,*

a) if $C \leq 0$ the map P may have a unique Γ_1^p orbit;

b) if $C > 0$ the map P has no Γ_1^p orbits if $F(x_1^0, \mu) > 0$; it may have two Γ_1^p orbits if $F(x_1^0, \mu) < 0$ and one orbit if $F(x_1^0, \mu) = 0$;
Moreover, the stability of Γ_1^p is given by the eigenvalues of the matrix

$$M(x_1, y_1) = \begin{pmatrix} \frac{\partial x_{p+1}}{\partial x_1} & \frac{\partial x_{p+1}}{\partial y_1} \\ \frac{\partial y_{p+1}}{\partial x_1} & \frac{\partial y_{p+1}}{\partial y_1} \end{pmatrix} = \begin{pmatrix} \alpha_p^1 & \frac{1}{\lambda_1 - \lambda_2}\left(\lambda_1^p - \lambda_2^p\right) \\ \alpha_p^2 & \frac{\lambda_1 \lambda_2}{\lambda_1 - \lambda_2}\left(\lambda_2^{p-1} - \lambda_1^{p-1}\right) \end{pmatrix} \tag{3.37}$$

where x_1 is a root of (3.34),

$\alpha_p^1 = \frac{1}{\lambda_1 - \lambda_2}\left(-\frac{1}{2k}\left(\lambda_1^p - \lambda_2^p\right)\left(\frac{\mu}{x_1}D + C\right) + \beta_1\right)$ *and*

$\alpha_p^2 = \frac{1}{\lambda_1 - \lambda_2}\left(-\frac{\lambda_1 \lambda_2}{2k}\left(\lambda_2^{p-1} - \lambda_1^{p-1}\right)\left(\frac{\mu}{x_1}D + C\right) + \beta_2\right).$

Secondly we studied **the case of the complex eigenvalues**

$$\lambda_1 = r\left(\cos\varphi + i\sin\varphi\right), \ \lambda_2 = r\left(\cos\varphi - i\sin\varphi\right),$$

where $0 < r < 1$, $\varphi \neq n\pi$, and n is integer. The results we obtained in this case have been presented in [129]. In this case we have

$$\begin{aligned} J^{m-1} &= T\begin{pmatrix} \lambda_1^{m-1} & 0 \\ 0 & \lambda_2^{m-1} \end{pmatrix} T^{-1} = \begin{pmatrix} \frac{\lambda_1^m - \lambda_2^m}{\lambda_1 - \lambda_2} & \frac{\lambda_1^{m-1} - \lambda_2^{m-1}}{\lambda_1 - \lambda_2} \\ -\frac{\lambda_1^{m-1} - \lambda_2^{m-1}}{\lambda_1 - \lambda_2}\lambda_1\lambda_2 & -\frac{\lambda_1^{m-2} - \lambda_2^{m-2}}{\lambda_1 - \lambda_2}\lambda_1\lambda_2 \end{pmatrix} \\ &= \begin{pmatrix} r^{m-1}\frac{\sin m\varphi}{\sin\varphi} & r^{m-2}\frac{\sin\varphi(m-1)}{\sin\varphi} \\ -r^m\frac{\sin\varphi(m-1)}{\sin\varphi} & -r^{m-1}\frac{\sin\varphi(m-2)}{\sin\varphi} \end{pmatrix}, \end{aligned}$$

for all $m \geq 2$, respectively,

$$\begin{aligned} x_{m+1} &= \frac{r^{m-1}\sin m\varphi}{\sin\varphi}\left(y_1 + s x_1^{\frac{1}{2k}}\right) + x_1\frac{r^{m-1}}{\sin\varphi}\left(\alpha\sin m\varphi - rc\sin\varphi\left(m-1\right)\right) + \mu A_m, \\ y_{m+1} &= -\frac{r^m\sin\varphi\left(m-1\right)}{\sin\varphi}\left(y_1 + s x_1^{\frac{1}{2k}}\right) \\ &\quad -x_1\frac{r^m}{\sin\varphi}\left(\alpha\sin\varphi\left(m-1\right) - rc\sin\varphi\left(m-2\right)\right) + \mu B_m, \end{aligned}$$

where

$$A_m = \frac{1}{(r^2 - 2r\cos\varphi + 1)\sin\varphi}\left(\sin\varphi - r^m \sin(m+1)\varphi + r^{m+1}\sin m\varphi\right),$$

and

$$B_m = -\frac{r^2}{(r^2 - 2r\cos\varphi + 1)\sin\varphi}\left(\sin\varphi - r^{m-1}\sin m\varphi + r^m \sin(m-1)\varphi\right).$$

For the case of **large** φ, namely, $\varphi \nrightarrow n\pi$ we obtained the following theorem whose complete form and proof are given in [129].

Theorem 3.2.2. *The map $P = (P_1, P_2)$ has at most one Γ_1^p orbit for any $p \geq 2$ and $k \geq 2$ fixed. More exactly,*

a) if $C_p \geq 0, \mu D_p \geq 0$ or $C_p < 0, \mu D_p < 0$, P has no period–p one-impacting Γ_1^p orbits;

b) if $C_p \geq 0, \mu D_p < 0$, or $C_p < 0, \mu D_p \geq 0$, P has at most one period–p one-impacting Γ_1^p orbit.

When $\varphi \to n\pi$, we meet again two cases. Assume firstly $\varphi \to 2n\pi$ with n integer. Then we obtain

$$A_p = \frac{1}{(r-1)^2}\left(1 - (p+1)r^p + pr^{p+1}\right),\ B_p = -\frac{r^2}{(r-1)^2}\left(1 - pr^{p-1} + (p-1)r^p\right)$$

respectively,

$$C_p = -\frac{s}{p}\left(-p\alpha + r^{1-p} + cr^{p+1} + r(p-1)(c+1)\right) \text{ and } D_p = \frac{s}{p}r^{1-p}\frac{(r^p-1)^2}{(r-1)^2}.$$

These lead to a corollary to the above theorem.

Corollary 3.2.1. *The map $P = (P_1, P_2)$ has at most one Γ_1^p orbit for any $k \geq 2$ fixed and p large enough. More exactly, for $s = \pm 1$, the map P has at most one period–p one-impacting Γ_1^p orbit on $\mu > 0$ while P has no Γ_1^p orbits on $\mu < 0$. The stability of the Γ_1^p orbit is given by the eigenvalues of the matrix $J(x^*)$.*

A similar result one obtains when $\varphi \to (2n+1)\pi$ with n integer.

3.2.2 Studying models for impact oscillators

The dynamics in a neighborhood of a grazing periodic orbit in a piecewise smooth model in the presence of discontinuous jumps is studied in [34]. A method for controlling the persistence of a local attractor is discussed. The model is of the form

$$\dot{x} = f(x) = \begin{pmatrix} x_2 \\ -\frac{1}{\omega^2}x_1 - \frac{2\gamma}{\omega}x_2 + x_4\left[\left(\frac{1}{\omega^2} - 1\right)\cos x_3 - \frac{2\gamma}{\omega}\sin x_3\right] \\ 1 \\ 0 \\ 0 \end{pmatrix},$$

$x = (x_1, x_2, x_3, x_4, x_5)$, provided that $x_1 - x_5 \geq 0$. A discrete, linear feedback method is used to prove the existence of an attractor near the grazing orbit. When the model's parameters approach those corresponding to grazing orbits, the deviation of the attractor from the grazing orbit tends to zero. A discontinuity mappings approach is used for the study of the model's dynamics near the grazing state. A recent paper [134] describes a mechanical experiment related to impact oscillators. A novel dynamics not observed in common impact oscillators is pointed out. The mechanical system is harmonically-excited and has a strong nonlinearity induced by the impacts. A discrete sequence of energy impulses affecting the impact oscillators within the experiments are taken into account. The experiment is related to a classic pinball machine in which a ball striking a bumper experiences a sudden impulse, introducing additional unpredictability to the motion of the ball. A useful tool in studying non-smooth systems is to associate a smooth system to a non-smooth one, that is, smoothing non-smooth systems. Recent results on this topic have been reported in [49]. The authors used methods based on changes of variables and low-pass filter formulations to obtain their results. They briefly describe the state space reconstruction method for recovering a differentiable dynamical system from its time series data.

Applications of non-smooth dynamical systems, and in particular impact oscillators undergoing grazing bifurcations, are met in computational neuroscience as well. The authors in [32] show that many techniques originally developed for the study of impact oscillators are directly relevant to the analysis of spiking models from neuroscience. A planar nonlinear model of type integrate-and-fire with a piecewise linear vector field and a state dependent reset upon spiking is particularly studied, because the model has the potential to generate realistic trains of spikes. Other ideas on how non-smooth dynamical systems may contribute to neuroscience modeling are discussed in the work.

In the following we present the results reported in [125]. A second-order non-autonomous differential equation

$$\ddot{x} = A\left(x, \dot{x}, t\right), \tag{3.38}$$

where the function $A\left(x, \dot{x}, t\right)$ is periodic in t of period $T > 0$, is considered a model for one-dimensional impact oscillators [85]. A fixed rigid barrier is assumed to be placed at $x = x_b$ and the oscillator's motion takes place on $x > x_b$. No other barriers exist on $x > x_b$ and the motion is assumed smooth on this side, that is, the motion is described by the equation (3.38) with A as smooth as needed on $x > x_b$. The equation (3.38) is equivalent to the autonomous 3D system

$$\dot{x} = v,\ \ \dot{v} = A(x, v, \theta),\ \ \dot{\theta} = 1, \tag{3.39}$$

where $\dot{x}(t) = v(t)$ and $\theta(t) = t + \theta_0$ for some $\theta_0 \in \mathbb{R}$ fixed.

The state space where the dynamics of the oscillator takes place (including the impacts) is the set $X = [x_b, +\infty) \times \mathbb{R} \times \mathbb{R}$, while the barrier, denoted by Σ, reads

$$\Sigma = \{x_b\} \times \mathbb{R} \times \mathbb{R}.$$

The functions $x\left(t\right)$ and $v(t)$ are as smooth as needed on $X \setminus \Sigma$. We denote by Σ_0, Σ_+, Σ_-, respectively the disjoint subsets of Σ corresponding to $v = 0$, $v > 0$ and $v < 0$.

The models developed in [85] and [81] assume the existence of a periodic grazing orbit which touches tangent Σ_0 with zero velocity and *positive acceleration*. In [125] we started to study a model which does not satisfies fully these conditions. We considered A of the form

$$A\left(x, \dot{x}, \theta\right) = K + D\cos\theta - \omega^2 x,$$

with some real constants K, D, and $\omega \neq 0, 1$. Denote the flow of the system (3.39) by

$$\Phi\left(t, u_0\right) = \left(x\left(t, u_0\right), v\left(t, u_0\right), \theta\left(t, \theta_0\right)\right)$$

with the initial condition $u_0 = (x_0, v_0, \theta_0)$ where

$$x\left(0, x_0, v_0, \theta_0\right) = x_0, v\left(0, x_0, v_0, \theta_0\right) = v_0, \theta\left(0, \theta_0\right) = \theta_0.$$

Disregarding the barrier we can compute the flow analytically and obtain

$$x\left(t,u_0\right)=C_1\cos\theta\omega+C_2\sin\theta\omega+\frac{1}{\omega^4-\omega^2}\left(K\omega^2-K+\omega^2D\cos\theta\right), \quad (3.40)$$

$$v\left(t,u_0\right)=\frac{dx}{dt}\left(t,u_0\right),$$

and $\theta(t)=t+\theta_0$, where

$$C_1=p\cos\left(\theta_0\omega\right)-q\sin\left(\theta_0\omega\right),\ C_2=p\sin\left(\theta_0\omega\right)+q\cos\left(\theta_0\omega\right),$$

with

$$p=x_0+\frac{1}{\omega^2-\omega^4}\left(K\omega^2-K+\omega^2D\cos\theta_0\right)\ textand\ q=\left(v_0-\frac{D}{1-\omega^2}\sin\theta_0\right)\frac{1}{\omega}.$$

Assume further $x_b=0$. The particular orbit Γ_p through the initial point $O=(0,0,0)$, is given by

$$x_p=\frac{1}{\omega^4-\omega^2}\left(-K+K\omega^2+\omega^2D\cos\theta-\left(K-K\omega^2-\omega^2D\right)\cos\theta\omega\right)$$

and

$$v_p=\frac{1}{\omega^3-\omega}\left(-\omega D\sin\theta+\left(K-K\omega^2-\omega^2D\right)\sin\theta\omega\right).$$

Hence Γ_p is periodic of period $T=2\pi n$ for $\omega=\frac{m}{n}$, m,n integers.

We studied first the case $K+D\cos\theta<0$ for all real θ. The orbit Γ_p is not a proper grazing orbit since the acceleration at the grazing point is negative in this case. We obtained in this case that all orbits impact several times the barrier and then stop.

Secondly we assumed that $K+D\cos\theta>0$, for all real θ. Since $-\omega^2x$ is negative, the acceleration of Γ_p at the grazing point may also be negative. We studied firstly here the case when our model has a proper grazing orbit Γ_p which crosses tangent the barrier at O with positive acceleration A_2. When $\omega>1$, $D<0$ and

$$K-K\omega^2-\omega^2D<0, K+D>0$$

this scenario is possible. Performing some computations (see [125]) we obtain a two-branched Poincaré map $P=\left(P_{ni},P_i\right)$, in the form

$$P_{ni}:\begin{cases} x_{n+1}=x_n \\ \theta_{n+1}=2\theta_n \end{cases},x_n\geq 0 \quad (3.41)$$

respectively,

$$P_i : \begin{cases} x_{n+1} = & r^2 x_n \\ \theta_{n+1} = & 2\theta_n - 2\,(1+r)\sqrt{-\frac{2}{A_2} x_n} \end{cases} , x_n \leq 0. \tag{3.42}$$

We showed in this case that any orbit starting from the non-impacting side will never impact the barrier. In the last case studied here we assumed that Γ_p crosses tangent the barrier at O with positive acceleration A_2 but impacts later the barrier, Fig.3.5. This case is possible in our model since for $|\theta - \pi|$ small enough that we have

$$x(\theta) = \frac{1}{\omega^4 - \omega^2}\left((1-\cos\pi\omega)\left(\omega^2-1\right)K - \omega^2 D\left(\cos\pi\omega + 1\right)\right) + O\left(\theta - \pi\right) \tag{3.43}$$

and $x(\theta) < 0$ for all real $\omega > 1$ and $K < 0$, $K + D > 0$. Hence Γ_p impacts the barrier around $\theta \approx \pi$ and may loose its periodicity due to the impacts.

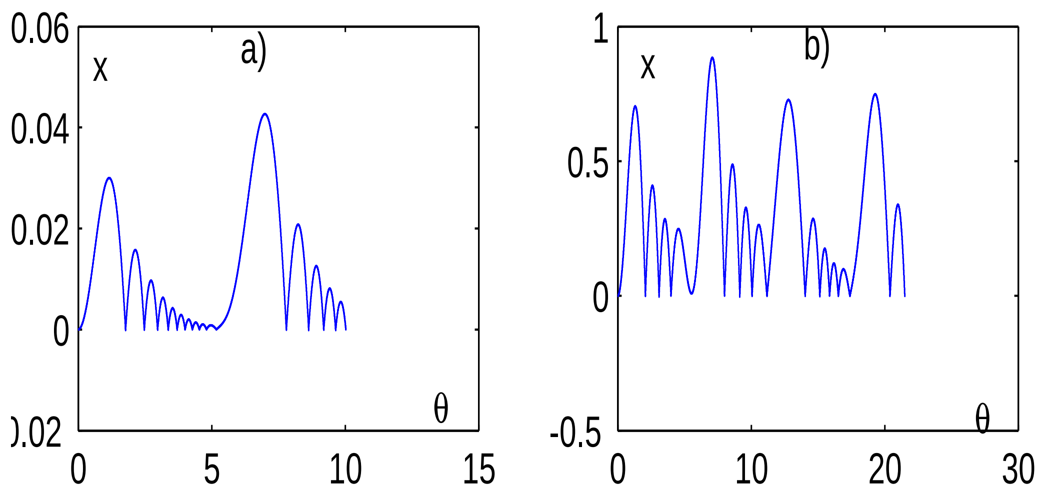

Figure 3.5: Incomplete grazing orbits in the system (3.39) for $r = 0.8, K = -0.1$, $D = 0.2, \omega = 2$, $x_0 = 0, v_0 = 0, \theta_0 = 0$, a), respectively, $K = -0.1$ and $D = 2$, b).

3.3 Perturbed Hamiltonian systems

3.3.1 Bifurcations in a class of perturbed Hamiltonian systems and associated nontwist cubic maps

In this section we describe briefly the results reported in [128]. One-degree-of-freedom Hamiltonian systems subjected to time periodic perturbations (i.e. 3/2 d.o.f) are used in studying various models in astronomy, plasma physics, fluid dynamics and mechanics. Such a Hamiltonian given in action-angle variables (I, θ), has the general form

$$H(\theta, I, t) = H_0(I) + \varepsilon H_p(\theta, I, t), \tag{3.44}$$

where the Hamiltonian H_p is a $2\pi-$periodic function in θ and t. Models for magnetic configurations of hot plasma physics devices such as tokamaks [36], [82] are using such Hamiltonian systems. Other models using Hamiltonians of type (3.44) can be found in [18], [27], [113], [78], [84]. Theoretical studies of reconnection and transport barrier problems met in tokamaks can be found in [1], [50], [19], [6], [93], [29]. An approach based on quadratic non-twist stroboscopic maps has been used for the study of the involved 3/2 d.o.f. Hamiltonian systems. Studies on the creation of magnetic transport barriers in plasma physics are presented in [42], [30] while in [9], [20], [2] the effect of the reconnection on chaotic transport of particles is presented. Quadratic maps were most used to study reconnection phenomena, which assumes the existence of twin periodic orbits with the same rotation number. These phenomena were revealed also in systems generated by cubic non-twist maps [51], [136], [118], [119].

Our purpose in [128] was to study the reconnection processes and their effect on the existence of transport barriers for systems generated by Hamiltonians with quartic unperturbed part of the form

$$H_{a,b,\varepsilon}(\theta, I, t) = I^2/2 - aI^3/3 + bI^4/4 + \varepsilon H_p(\theta, I, t), \tag{3.45}$$

when $a > 0$, $b > 0$ are fixed and the perturbation parameter ε varies in the interval $(0, \infty)$. Since $H_p(\theta, I, t)$ is $2\pi-$periodic in θ and t, it can be expanded in a Fourier series

$$H_p(\theta, I, t) = \sum_{m,n \in \mathbb{Z}} H_{mn}(I) \cos(n\theta - mt + c_{mn}). \tag{3.46}$$

Our study aims to bring contributions to the understanding of the dynamics of systems having many transport barriers [48], [41], [102], [97]. We started with a Hamiltonian of the form

$$H_{int}(\theta, I) = I^2/2 - aI^3/3 + bI^4/4 + \varepsilon \cos n\theta, \tag{3.47}$$

because it is related to the analysis of local and global bifurcations of discrete systems generated by stroboscopic maps [112], as *approximate interpolating* systems associated to the maps. We showed that the non-integrable system corresponding to (3.45) and the integrable one corresponding to (3.47) have similar dynamics for relatively small values of ε.

The approximate interpolating system. The Hamiltonian (3.47) is obtained from $H_{a,b,\varepsilon}(\theta, I, t)$ and leads to the system

$$\begin{cases} \dot{\theta} = & I - aI^2 + bI^3 \\ \dot{I} = & \varepsilon n \sin n\theta \end{cases} . \tag{3.48}$$

For the unperturbed system ($\varepsilon = 0$ in (3.48)) we have the following result. The proof can be found in [128].

Proposition 3.3.1. *Let consider the unperturbed system*

$$\dot{\theta} = I - aI^2 + bI^3; \;\; \dot{I} = 0.$$

a) For $a^2 < 4b$ all the points situated on the circle $I = 0$ are equilibrium points. The points situated on the circle $I = I_0$ rotate in inverse trigonometric sense if $I_0 < 0$, respectively in the trigonometric sense if $I_0 > 0$.

b) For $a^2 = 4b$ there are two circles formed by equilibrium points: $I = 0$ and $I = 1/\sqrt{b}$. The points situated on the circle $I = I_0$ rotate in inverse trigonometric sense if $I_0 < 0$, respectively in the trigonometric sense if $I_0 > 0$ (and $I_0 \neq 1/\sqrt{b}$). A local maximum speed of rotation is obtained on the circle $I = 0.5/\sqrt{b}$.

c) For $a^2 > 4b$ all points situated on the circles $I = 0$, $I = I_1 := \frac{a-\sqrt{a^2-4b}}{2b}$ and $I = I_2 := \frac{a+\sqrt{a^2-4b}}{2b}$ are equilibria (fixed points which do not rotate). The points on the circle $I = I_0$ rotate in the inverse trigonometric sense if $I_0 \in (-\infty, 0) \cup (I_1, I_2)$, respectively in the trigonometric sense if $I_0 \in (0, I_1) \cup (I_2, +\infty)$. Local maximum speed of rotation is obtained on the circles $I = I_{\max} = \frac{a-\sqrt{a^2-3b}}{3b}$ (for the rotation in the trigonometric sense), respectively $I = I_{\min} = \frac{a+\sqrt{a^2-3b}}{3b}$ for the rotation in the inverse trigonometric sense.

Figure 3.6a depicts the phase portrait of the unperturbed interpolating system corresponding to $a = 1.5$, $b = 0.4$, $n = 3$. The dynamics of the unperturbed interpolating system is closely related to the winding function

$$W(I) = \frac{dH_0}{dI} = I - aI^2 + bI^3$$

which is not monotonous for $a^2 > 3b$ (Figure 3.6b).

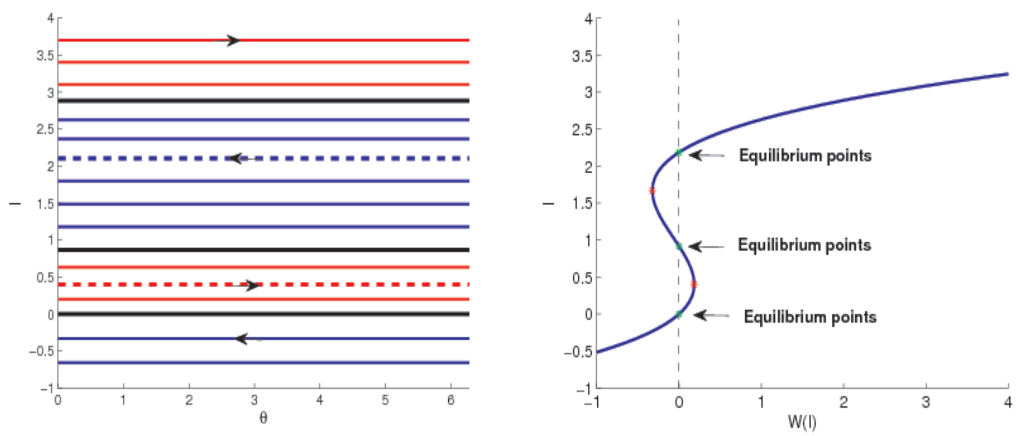

Figure 3.6: a) The phase portrait of the unperturbed interpolating system (left); b) The winding function corresponding to the interpolating Hamiltonian for $a = 1.5$, $b = 0.4$, $n = 3$ (right).

The following proposition describes the equilibrium points of the approximate interpolating Hamiltonian $H_{int}(\theta, I)$. A proof can be found in [128].

Proposition 3.3.2. *For $a^2 > 4b$ the system (3.48) has $6n$ equilibria.*

$$\begin{aligned} P_0 &= (0,0), \quad P_1 = (\pi/n, 0), \quad ... \quad P_{2n-1} = ((2n-1)\pi/n, 0) \\ Q_0 &= (0, I_1), \quad Q_1 = (\pi/n, I_1), \quad ... \quad Q_{2n-1} = ((2n-1)\pi/n, I_1) \\ R_0 &= (0, I_2), \quad R_1 = (\pi/n, I_2), \quad ... \quad R_{2n-1} = ((2n-1)\pi/n, I_2) \end{aligned}$$

where $I_1 = \frac{a-\sqrt{a^2-4b}}{2b}$ and $I_2 = \frac{a+\sqrt{a^2-4b}}{2b}$ are the solutions of the equation $bI^2 - aI + 1 = 0$. The equilibria P_{2k}, Q_{2k+1}, R_{2k}, are hyperbolic while P_{2k+1}, Q_{2k}, R_{2k+1}, are elliptic for all $k \in \{0, 1, ..., n-1\}$.

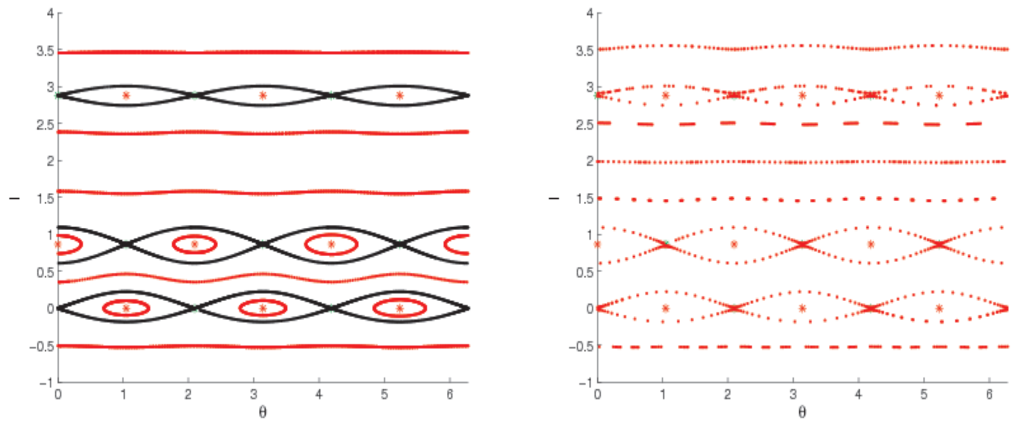

Figure 3.7: Phase portrait in systems with small perturbations: a) in the interpolating Hamiltonian system (left); b) in the discrete system (3.52) corresponding to the non-autonomous Hamiltonian system for $a = 1.5$, $b = 0.4$, $n = 3, \varepsilon = 0.01$ (right).

The route to reconnection of the $H_{int}(\theta, I)$ chains. We assumed a and b fixed with $a^2 - 4b > 0$ and let the perturbation's amplitude ε to vary. Denote by L_P, L_Q and L_R the three chains containing the equilibrium points P_{2k}, Q_{2k+1}, respectively R_{2k}, $k \in \{0, 1, ..., n-1\}$. For small enough ε (for instance $0 < \varepsilon < 0.01$), the Hamiltonian system displays three distinct Poincaré–Birkhoff chains (Figure 3.7a). At a critical value, called threshold of reconnection, the hyperbolic points of two chains get connected by common branches of their invariant manifolds, Figure 3.8a. The threshold of reconnection are given in the following proposition.

Proposition 3.3.3. *The reconnection threshold of the Poincaré–Birkhoff chains L_P and L_Q in the system (3.48) is:*

$$\varepsilon_{P,Q} = \frac{I_1^2}{24}(3 - aI_1). \tag{3.49}$$

The threshold of reconnection of the chains L_Q and L_R in the system (3.48) is:

$$\varepsilon_{Q,R} = \varepsilon_{P,Q} - \frac{I_2^2}{24}(3 - aI_2). \tag{3.50}$$

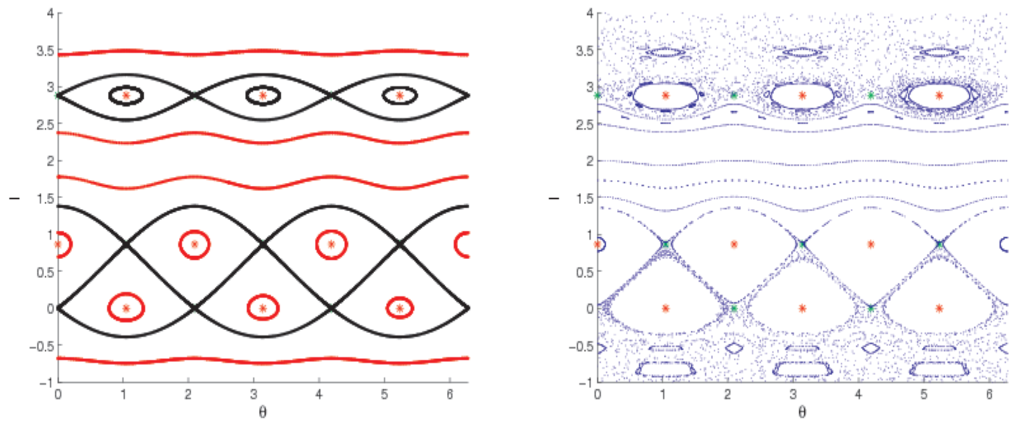

Figure 3.8: Phase portraits at the threshold of reconnection of L_P and L_Q: a) in the interpolating Hamiltonian system (left); b) in the discrete system (3.52) corresponding to the non-autonomous Hamiltonian system ($a = 1.5$, $b = 0.4$, $n = 3, \varepsilon = 0.0532$).

Remark 3.3.1. *If $3 - aI_2 = 0$, i.e. $a^2 = 4.5b$ we have $\varepsilon_{P,Q} = \varepsilon_{Q,R}$, so the chains L_P, L_Q and L_R reconnect at the same threshold (triple reconnection).*

If $3 - aI_2 < 0$, i.e. $4b < a^2 < 4.5b$ we have $\varepsilon_{Q,R} < \varepsilon_{P,Q}$ so the chains L_P and L_Q reconnect first.

If $3 - aI_2 > 0$, i.e. $a^2 > 4.5b$ we have $\varepsilon_{Q,R} > \varepsilon_{P,Q}$ so the chains L_Q and L_R reconnect first.

Since the analysis of the last two cases is similar, we will present only one of them: $\varepsilon_{Q,R} < \varepsilon_{P,Q}$.

Increasing ε from $\varepsilon_{P,Q}$, two dimerized chains L_{PQ} and L_{QP}, containing the hyperbolic points of L_P respectively the hyperbolic points of L_Q are formed, Figure 3.9a. The dimerized chain L_{PQ} surrounds the elliptic points of L_Q and the dimerized chain L_{QP} surrounds the elliptic points of L_P. The dimerized chains L_{PQ} and L_{QP} are separated by meanders, because their equilibrium points situated on the same symmetry line have different types (one is hyperbolic, the other is elliptic).

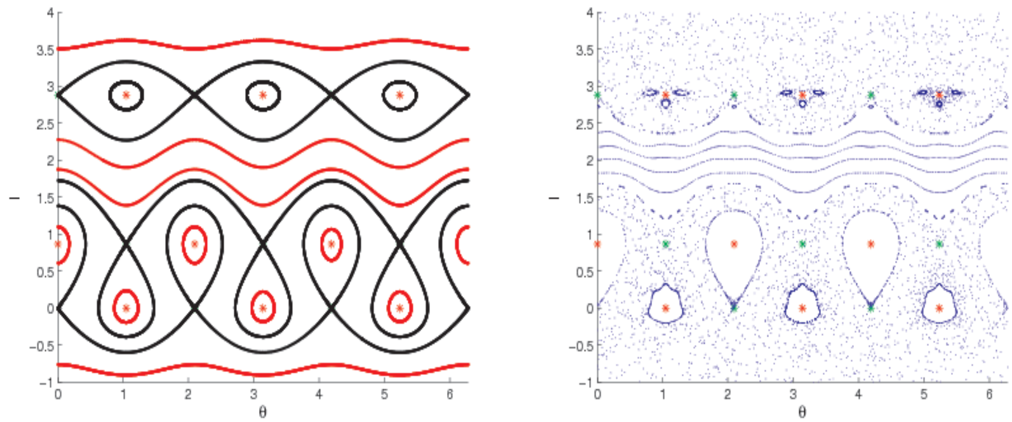

Figure 3.9: Phase portrait with dimerized islands: a) in the interpolating Hamiltonian system b) in the discrete system (3.52) corresponding to the non-autonomous Hamiltonian system ($a = 1.5$, $b = 0.4$, $n = 3, \varepsilon = 0.15$).

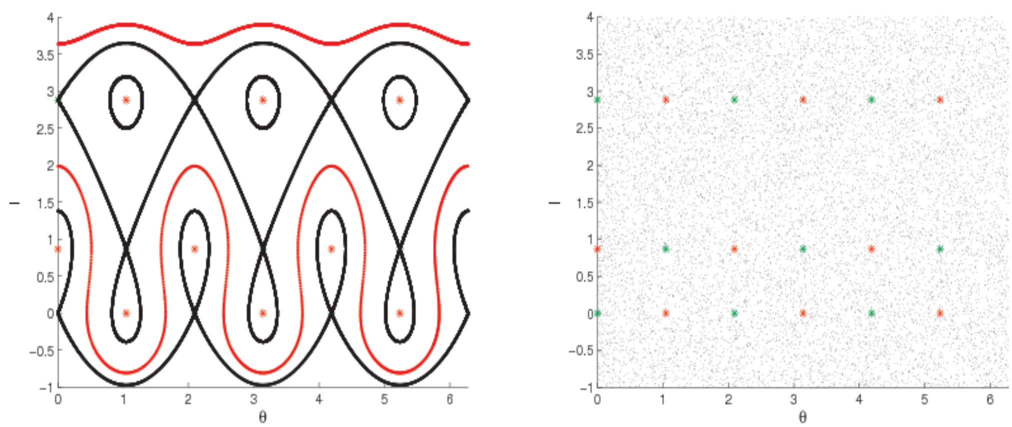

Figure 3.10: Phase portraits at the threshold of reconnection of L_R and L_{QP}; a) in the interpolating Hamiltonian system b) in the discrete system (3.52) corresponding to the non-autonomous Hamiltonian system ($a = 1.5$, $b = 0.4$, $n = 3, \varepsilon = 0.5117$).

When ε increases, the Poincaré–Birkhoff chain L_R approaches the dimerized chain L_{QP}. At the threshold of reconnection $\varepsilon_{Q,R}$ the hyperbolic points of the chains L_{QP} and L_R get connected by common branches of their invariant manifolds, Figure 3.10a.

A discrete approach for studying the 3/2 d.o.f. Hamiltonian system. The non-autonomous system corresponding to the Hamiltonian (3.45) is

$$\begin{cases} \dot{\theta} = & I - aI^2 + bI^3 + \varepsilon \frac{\partial H_p}{\partial I} \\ \dot{I} = & -\varepsilon \frac{\partial H_p}{\partial \theta} \end{cases} . \tag{3.51}$$

The system is not integrable and we used a technique described in [1] for its study. To this end, we constructed a map of the form (see [128])

$$\begin{cases} \theta_{k+1} = & \left(\theta_k + (I_k + \frac{\varepsilon}{2} n \sin n\theta_k) - a(I_k + \frac{\varepsilon}{2} n \sin n\theta_k)^2 + b(I_k + \frac{\varepsilon}{2} n \sin n\theta_k)^3\right) (mod\ 2\pi) \\ I_{k+1} = & I_k + \frac{\varepsilon}{2} n \sin n\theta_k + \frac{\varepsilon}{2} n \sin n\theta_{k+1} \end{cases} . \tag{3.52}$$

This discrete system (3.52) fits the basic properties of the interpolating system (3.48).

Proposition 3.3.4. *For $a^2 > 4b$ the fixed points of the map (3.52) coincide with the equilibrium points of the interpolate Hamiltonian system (3.48) and have the same type.*

Remark 3.3.2. *The coincidence of the equilibrium points shows the close relation between the dynamics of the system (3.52) and of the integrable system generated by (3.47), for small enough amplitude of the perturbation parameter ε.*

Remark 3.3.3. *It is interesting to remark that the involutions I_0 and I_1 were considered in many papers ([92], [139]) in order to describe the reversing symmetry group of the standard non-twist maps [92]. However R_0 and R_1 are not involutions and the system (3.52) has not a reversing symmetry group.*

Numerical illustrations, discussions and conclusions can be further read in [128].

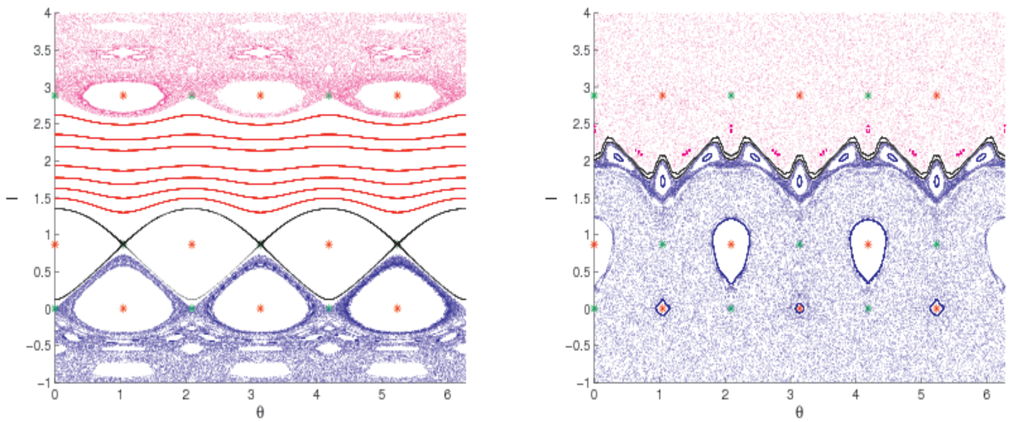

Figure 3.11: Phase portrait of the discrete system (3.52) for $a = 1.5$, $b = 0.4$, $n = 3$ and a) $\varepsilon = \varepsilon_{PQ} - 0.02$; the barrier T_{PQ} still exists between L_P and the chaotized L_Q, and b) $\varepsilon = \varepsilon_{PQ} + 0.18$; the barrier T_{RQ} is drawn in black.

3.3.2 Limit cycles in a class of perturbed Hamiltonian systems

The 16th Hilbert's problem is concerned with the maximal number and relative position of limit cycles in differential polynomial systems of the form

$$\frac{dx}{dt} = P_n(x,y), \frac{dy}{dt} = Q_n(x,y), \tag{3.53}$$

where P_n and Q_n are polynomials of degree n. When dealing with limit cycles, the following two classical theorems are important.

Theorem 3.3.1. *(Poincaré, [24]) A continuous autonomous system* $\dot{x} = P(x,y)$, $\dot{y} = Q(x,y)$, *has no periodic solutions in a region* $D \subset \mathbb{R}^2$ *if there exists a continuously differentiable function* $f : D \to \mathbb{R}$ *such that*

$$\dot{f} = P(x,y)\frac{\partial f}{\partial x} + Q(x,y)\frac{\partial f}{\partial y}$$

is of constant sign in D *and the equality* $\dot{f} = 0$ *cannot be satisfied on a whole orbit of the system.*

Theorem 3.3.2. *(Bendixon–Dulac Theorem, [24]). A dynamical system $\dot{x} = P(x,y)$, $\dot{y} = Q(x,y)$, with P, Q functions of class C^1 defined in $\Omega \subset \mathbb{R}^2$ has no periodic solutions in a simply connected region $D \subset \Omega$ if there exists a C^1 function $F : D \to \mathbb{R}$ such that the divergence*

$$\frac{\partial(FP)}{\partial x} + \frac{\partial(FQ)}{\partial y}$$

is of constant sign in D and is not identically zero in any open subset in D.

The 16th Hilbert's problem is still not solved. A crucial result of this research field is the following: any polynomial vector field has finitely many limit cycles, [39], [56]. In terms of the configurations of limit cycles in planar vector fields, an important result is presented in [71]. For quadratic planar systems, it is known that only the distribution (3 : 1) has four limit cycles but, to our knowledge, it does not exist a rigorous proof of this result. This is the reason why many researchers still study the maximal number of limit cycles in quadratic polynomial vector fields.

Our results presented in [130] contribute to this effort. We investigated a class of quadratic Hamiltonian systems of the form

$$\begin{array}{rl} \dot{x} = & \frac{\partial H}{\partial y} + \varepsilon f(x,y,\varepsilon) \\ \dot{y} = & -\frac{\partial H}{\partial x} + \varepsilon g(x,y,\varepsilon) \end{array}, \tag{3.54}$$

where $f(x,y,\varepsilon)$ and $g(x,y,\varepsilon)$ are two polynomials of order n which depend analytically on a small parameter ε. The system (3.54) at $\varepsilon = 0$ is called unperturbed.

We describe in the following the approach we used in studying the limit cycles of the system (3.54). If the unperturbed system (3.54) has a center and a period annulus A, that is, for each $h \in (\alpha, \beta)$, the set

$$\{(x,y) \in \mathbb{R}^2 : H(x,y) = h\}$$

contains a closed smooth curve Γ_h free of critical points, which depends continuously on $h \in (\alpha, \beta)$. Denote by $P(h,\varepsilon)$ the Poincaré map defined on a transversal segment to the flow of system (3.54). Then, the displacement function $d(h,\varepsilon)$ can be approximated by (see [11], [55])

$$d(h,\varepsilon) := P(h,\varepsilon) - h = \varepsilon M_1(h) + \varepsilon^2 M_2(h) + ... + \varepsilon^k M_k(h) + ... \tag{3.55}$$

where $M_k(h)$, $k \geq 1$, are called the Melnikov functions. They can be calculated for some particular classes of systems, see [55, 68, 141, 142], but $M_k(h)$ are not known in general. Using a method presented in [44] (see also [54]) the Melnikov functions $M_k(h)$ can be calculated in the following conditions. Assume (f, g) is a perturbation in (3.54) and denote by

$$\omega = g(x, y, \varepsilon)dx - f(x, y, \varepsilon)dy.$$

Thus, using a Taylor series on ε, we can write

$$\omega = \omega_0 + \varepsilon\omega_1 + \varepsilon^2\omega_2 + ... \tag{3.56}$$

with

$$\omega_0 = g(x, y, 0)dx - f(x, y, 0)dy, \ \omega_1 = g'_\varepsilon(x, y, 0)dx - f'_\varepsilon(x, y, 0)dy,$$

$$\omega_2 = g''_{\varepsilon^2}(x, y, 0)dx - f''_{\varepsilon^2}(x, y, 0)dy$$

and so on. The system (3.54) can be rewritten in a *Pfaffian* form $dH - \varepsilon\omega = 0$. In this notation, $M_1(h)$ is simply

$$M_1(h) = \oint_{\Gamma_h} \omega_0, \ \Gamma_h \in A.$$

The following results are reported in [54].

Proposition 3.3.5. *Assume that the first Melnikov function $M_1(h) \equiv 0$ is identically zero. Then there exists in the period annulus A of the unperturbed system (3.54) a continuous function $q_0(x, y)$ and a locally Lipschitz continuous function $Q_0(x, y)$ such that the form ω_0 can be expressed as*

$$\omega_0 = q_0 dH + dQ_0.$$

Theorem 3.3.3. *Assume that $M_1(h) \equiv 0$. Then $M_2(h)$ is given by*

$$M_2(h) = \oint_{\Gamma_h} (q_0\omega_0 + \omega_1), \ \Gamma_h \in A. \tag{3.57}$$

Remark 3.3.4. *The above procedure can be extended to the case in which $M_k(h) \equiv 0$ for all $1 \le k \le m$. In this case, one defines successively the one-forms $\Omega_0, \Omega_1, ..., \Omega_m$ by*

$$\Omega_0 = \omega_0,\ \ \Omega_k = \omega_k + \sum_{i+j=k-1} q_i\omega_j,$$

$k = 1, 2, ..., m$, where the one-form Ω_k can be expressed as $\Omega_k = q_k dH + dQ_k$ with q_k, Q_k as in the Proposition 3.3.5. Then, by induction, one obtains

$$M_{m+1}(h) = \oint_{\Gamma_h} \Omega_m.$$

It is known that, if $M_1(h)$ is not identically zero then each simple zero $h_0 \in (\alpha, \beta)$ of $M_1(h)$ gives birth for ε small enough to a limit cycle $\Gamma^{\varepsilon}_{h_0}$ in the perturbed system (3.54) that depends smoothly on ε and tends to Γ_{h_0} as $\varepsilon \to 0$. On the other hand, there exist perturbations (f, g) such that $M_1(h)$ is identically zero, $M_1(h) \equiv 0$. In this case, the next term $M_2(h)$ in the series $d(h, \varepsilon)$ is used for studying the limit cycles. If $M_2(h)$ is also zero we have to investigate $M_3(h)$ and the procedure may continue endless.

In [130] we considered a class of quadratic perturbed Hamiltonian systems in the form:

$$\begin{array}{rl} \dot{x} = & y(1+y) - \varepsilon P(x,y) \\ \\ \dot{y} = & -x(1+y) + \varepsilon Q(x,y) \end{array}, \tag{3.58}$$

where $\varepsilon > 0$ is a small parameter and P, Q are two polynomials of order two

$$P(x,y) = a_{00} + a_{10}x + a_{01}y + a_{20}x^2 + a_{11}xy + a_{02}y^2$$

and

$$Q(x,y) = b_{00} + b_{10}x + b_{01}y + b_{20}x^2 + b_{11}xy + b_{02}y^2.$$

The main result reported in [130] is given by the next theorem.

Theorem 3.3.4. *Let $M_k(h), k \ge 1$, be the Melnikov functions associated to the system (3.58). Then $M_1(h) = 0$ has at most 3 roots, taking into account their multiplicities, and the number of roots is reached. If $M_1(h) \equiv 0$ then $M_2(h) = 0$ has at most 3 roots, taking into account their multiplicities. If $M_1(h) \equiv 0$ and $M_2(h) \equiv 0$ then $M_3(h) = 0$ has at most 2 roots, taking into account their multiplicities. If*

$$M_1(h) = M_2(h) = M_3(h) \equiv 0$$

then $M_k(h) = 0$ has no real roots or $M_k(h) \equiv 0$ for all $k \geq 4$. Therefore, taking into account the expansion of the displacement map (3.55) of ***any order*** *in ε, the system (3.58) has at most three limit cycles which bifurcate from the period annulus of the unperturbed system and this upper bound is reached.*

We describe here the first step we used in the proof of this theorem. More details can be found in [130]. The unperturbed system (3.58), i.e. for $\varepsilon = 0$, has a center at the origin $(0, 0)$ and a first integral

$$H(x, y) = (x^2 + y^2)/2,$$

that is $dH = 0$. Consider further the restriction of H on the unit disc $x^2 + y^2 < 1$. The solutions of the unperturbed system lie on the circles $x^2 + y^2 = 2h$ with $0 < 2h < 1$. The displacement function $d(h, \varepsilon) = P(h, \varepsilon) - h$ associated to the system (3.58) can be expressed as a Taylor series in ε by

$$d(h, \varepsilon) = \varepsilon M_1(h) + \varepsilon^2 M_2(h) + ... + \varepsilon^k M_k(h) + ... \tag{3.59}$$

which is convergent for small ε. The Melnikov functions $M_k(h)$ are defined for $h \in (0, 1/2)$.

Transform in the following the system (3.58) in a Pfaffian form $dH = \varepsilon\omega$. Since $H = (x^2 + y^2)/2$ we can write

$$\begin{aligned} dH &= xdx + ydy \\ &= \frac{\varepsilon Q(x, y) - dy}{1 + y} dx + \frac{dx + \varepsilon P(x, y)}{1 + y} dy = \varepsilon\omega, \end{aligned}$$

where ω is the $1-$form

$$\omega = \frac{Q(x, y)}{1 + y} dx + \frac{P(x, y)}{1 + y} dy. \tag{3.60}$$

As ω does not depend on ε, from (3.56) we have $\omega = \omega_0, \omega_1 = \omega_2 = ... = 0$ and

$$M_1(h) = \oint_{H=h} \omega. \tag{3.61}$$

Now we want to express ω in the form $\omega = q_0 dH + dQ_0 + N_0$.

Denote by

$$\alpha_{00} = \frac{dx}{1 + y}, \;\; \beta_{10} = \frac{x}{1 + y} dy, \;\; \beta_{11} = \frac{xy}{1 + y} dy. \tag{3.62}$$

From the term $\frac{Q(x,y)}{1+y}dx$ we get

$$\alpha_{10}=\frac{xdx}{1+y}=\frac{dx^2}{2(1+y)}=\frac{d(2H-y^2)}{2(1+y)}=\frac{dH}{1+y}-d(y-\ln(1+y))$$

and similarly

$$\begin{aligned}
&\alpha_{01}=\tfrac{y}{1+y}dx=dx-\alpha_{00},\ \alpha_{20}=\tfrac{x^2}{1+y}dx=\tfrac{x}{1+y}dH-\beta_{11},\\
&\alpha_{11}=\tfrac{xy}{1+y}dx=\tfrac{y}{1+y}dH-d(y^2/2-y+\ln(y+1)),\\
&\alpha_{02}=\tfrac{y^2}{1+y}dx=2H\alpha_{00}-\tfrac{x}{1+y}dH+\beta_{11},
\end{aligned}$$

and from $\frac{P(x,y)}{1+y}dy$ we obtain

$$\begin{aligned}
&\beta_{00}=\tfrac{dy}{1+y}=d(\ln(1+y)),\ \beta_{01}=\tfrac{ydy}{1+y}=d(y-\ln(1+y)),\\
&\beta_{02}=\tfrac{y^2dy}{1+y}=d(y^2/2-y+\ln(1+y)),\\
&\beta_{20}=\tfrac{x^2dy}{1+y}=2d(H\ln(1+y))-2\ln(1+y)dH-d(y^2/2-y+\ln(1+y)).
\end{aligned}$$

With these computations, we get:

$$q_0=\frac{1}{1+y}\left(b_{10}+\left(b_{20}-b_{02}\right)x+b_{11}y\right)-2a_{20}\ln(1+y),$$

$$dQ_0=b_{01}dx+f\left(y\right)dy+2a_{20}d(H\ln(1+y)),$$

$$N_0=\left(b_{00}-b_{01}\right)\alpha_{00}+2b_{02}H\alpha_{00}+a_{10}\beta_{10}+c_1\beta_{11},$$

where $f\left(y\right)=\frac{a_{00}}{1+y}+\left(a_{01}-b_{10}\right)\frac{y}{1+y}+c_2\frac{y^2}{1+y}$, respectively, $c_1=b_{02}-b_{20}+a_{11}$ and $c_2=a_{02}-a_{20}-b_{11}$.

Since

$$\oint_{H=h}q_0dH=\oint_{H=h}dQ_0=0,$$

it follows

$$M_1\left(h\right)=\left(b_{00}-b_{01}\right)I_1+2b_{02}hI_1+a_{10}I_2+c_1I_3,$$

where the three integrals are

$$I_1:=\oint_{H=h}\alpha_{00}=\frac{2\pi(1-\sqrt{1-2h})}{\sqrt{1-2h}},$$

$$I_2 := \oint_{H=h} \beta_{10} = 2\pi \left(1 + \sqrt{1-2h}\right),$$

and

$$I_3 := \oint_{H=h} \beta_{11} = 2\pi \left(h - 1 - \sqrt{1-2h}\right),\ h \in (0, 1/2).$$

Denoting by $m = \sqrt{1-2h},\ m \in (0,1)$, we have:

$$M_1(m) = \left(m^3 (2b_{02} - c_1) + 2m^2 (a_{10} - c_1 - b_{02}) + mk_1 + 2b_{00} - 2b_{01} + 2b_{02}\right) m^{-1}\pi$$

with $k_1 = 2a_{10} - 2b_{00} + 2b_{01} - 2b_{02} - c_1$.

Assuming $b_{00} - b_{01} \neq 0, b_{02}, a_{10}, c_1 \neq 0$, equation $M_1(m) = 0$ can have at most three real roots for $m \in (0,1)$. Therefore, the system (3.58) can have at most three limit cycles. In addition, this upper bond is attained. Indeed, choosing $b_{01} = 0$, $b_{20} = 0$, $b_{02} = -1$, $a_{10} = -13/29$, $b_{00} = 30/29$, $a_{11} = 19/29$ we find $m \in \{\frac{1}{4}, \frac{1}{3}, \frac{1}{2}\}$.

As the integrals I_1, hI_1, I_2, I_3 are linearly independent, in order to have $M_1(h) \equiv 0$ we impose $b_{00} - b_{01} = 0$ and $b_{02} = a_{10} = c_1 = 0$, which lead to $N_0 \equiv 0$. The second step is to investigate further this case. For the third step we have $M_2(h) \equiv 0$ and study the roots of $M_3(h) \equiv 0$ and so one. More details can be found in [130].

3.4 Degenerate fold-Hopf bifurcations

3.4.1 Degenerate with respect to parameters fold-Hopf bifurcations

We present in this section the results we obtained on a class of degenerate fold-Hopf bifurcations as are they reported in [131]. In order to present briefly the results, we omit the proofs of the theorems in this presentation; they can be found in [131]. Fold-Hopf bifurcations (zero-pair or zero-Hopf) appear in dynamical systems of dimension at least three with two independent parameters. A fold-Hopf bifurcation arises when the Jacobian matrix at an equilibrium point has eigenvalues of the form 0 and $\pm i\omega_0$, $\omega_0 > 0$, for some values of the parameters. More exactly, we studied differential systems of the form

$$\dot{x} = f(x, \alpha) \tag{3.63}$$

$x \in \mathbb{R}^3, \alpha = (\alpha_1, \alpha_2) \in \mathbb{R}^2$, f smooth of class C^r, $r \geq 3$, which has an equilibrium $x = 0$ at $\alpha = 0$. Its Jacobian matrix $J(0)$ has the simple eigenvalues 0 and $\pm i\omega_0$. Using a Taylor decomposition of $f(x,\alpha)$ at $x = 0$, the system (3.63) becomes

$$\dot{x} = a(\alpha) + J(\alpha)x + F(x,\alpha) \tag{3.64}$$

where $a(0) = 0$ and $F(x,\alpha) = O(||x||^2)$. Since the eigenvalues of $J(0)$ are simple and continuous with respect to α, the eigenvalues of $J(\alpha)$ are

$$\nu(\alpha), \ \lambda = \mu(\alpha) + i\omega(\alpha) \text{ and } \bar{\lambda} = \mu(\alpha) - i\omega(\alpha)$$

for all $||\alpha|| = \sqrt{\alpha_1^2 + \alpha_2^2}$ small enough, such that $\nu(0) = \mu(0) = 0$ and $\omega(0) = \omega_0 > 0$; $\nu(\alpha)$ is the real eigenvalue. We used the notations $x = 0$ and $\alpha = 0$ instead of $x = (0,0,0)$ and $\alpha = (0,0)$.

The system (3.64) has been intensively studied in [59] for the case when $a(\alpha) \neq 0$ for all $||\alpha|| = \sqrt{\alpha_1^2 + \alpha_2^2}$ small enough, $\alpha \neq 0$, and a normal form based on five generic conditions has been obtained and studied. The results reported in [59] are highly based on the five generic conditions. We aimed in our work to study the behavior of the system (3.64) in a more general framework, namely, when one or more of the five generic conditions are removed. We approached this research problem by considering that $a(\alpha) \equiv 0$ for all $\alpha \in \mathbb{R}^2$, and showed that this condition leads to a degeneracy in one of the five generic conditions. The results reported in [59] are highly based on the condition $a(\alpha) \neq 0$. We showed in our study that breaking the condition, that is assuming $a(\alpha) \equiv 0$, the system (3.64) may have a different behavior which cannot be obtained from the non-degenerate case. Fold-Hopf bifurcations are met in various models and contexts [95], [91], [61], [58], [47], [33] and [138]. A problem related to the 3-dimensional center at the zero-Hopf singularity has been recently studied in [45] while a result on arbitrary generic unfoldings of a zero-Hopf singularity is reported in [37]. Other models that may lead to degenerate fold-Hopf bifurcations can be found in [77], [23], [115], [62], [63], [118], [119], [52].

In order to help the reader to understand degenerate fold-Hopf bifurcations we will describe briefly in the following the framework of the non-degenerate cases according to the theory presented in [59]. The system (3.64) is equivalent to

$$\begin{aligned} \dot{u} &= \Gamma(\alpha) + \nu(\alpha)u + g(u,z,\bar{z},\alpha) \\ \dot{z} &= \Omega(\alpha) + \lambda(\alpha)z + h(u,z,\bar{z},\alpha) \end{aligned} \tag{3.65}$$

where

$$u = \langle p_0(\alpha), x\rangle, z = \langle p_1(\alpha), x\rangle$$

and $p_0(\alpha) \in \mathbb{R}^3, p_1(\alpha) \in \mathbb{C}^3$ are two adjoint eigenvectors given by

$$J^T(\alpha)p_0(\alpha) = \nu(\alpha)\, p_0(\alpha) \quad \text{and} \quad J^T(\alpha)p_1(\alpha) = \bar{\lambda}(\alpha)p_1(\alpha) \tag{3.66}$$

such that

$$\langle p_0(\alpha), q_0(\alpha)\rangle = \langle p_1(\alpha), q_1(\alpha)\rangle = 1 \quad \text{and} \quad \langle p_1(\alpha), q_0(\alpha)\rangle = \langle p_0(\alpha), q_1(\alpha)\rangle = 0 \tag{3.67}$$

for all $||\alpha||$ small enough. The vectors $q_0(\alpha)$ and $q_1(\alpha)$ are two eigenvectors corresponding to the eigenvalues $\nu(\alpha)$ and $\lambda = \mu(\alpha) + i\omega(\alpha)$, i.e.

$$J(\alpha)q_0(\alpha) = \nu(\alpha)\, q_0(\alpha)$$

and

$$J(\alpha)q_1(\alpha) = \lambda(\alpha)q_1(\alpha).$$

We can write

$$x = uq_0(\alpha) + zq_1(\alpha) + \bar{z}\bar{q}_1(\alpha).$$

Here

$$\Gamma(\alpha) = \langle p_0(\alpha), a(\alpha)\rangle, \Omega(\alpha) = \langle p_1(\alpha), a(\alpha)\rangle \tag{3.68}$$

are smooth functions of α with $\Gamma(0) = \Omega(0) = 0$ and

$$\begin{aligned} g(u, z, \bar{z}, \alpha) &= \langle p_0(\alpha), F(uq_0(\alpha) + zq_1(\alpha) + \bar{z}\bar{q}_1(\alpha), \alpha)\rangle \\ h(u, z, \bar{z}, \alpha) &= \langle p_1(\alpha), F(uq_0(\alpha) + zq_1(\alpha) + \bar{z}\bar{q}_1(\alpha), \alpha)\rangle \end{aligned}$$

are smooth functions of their variables whose Taylor expansions in $u, z, \bar{z}$ start with quadratic terms:

$$\begin{aligned} g(u, z, \bar{z}, \alpha) &= \textstyle\sum_{j+k+l\geq 2} \frac{1}{j!k!l!} g_{jkl}(\alpha)u^j z^k \bar{z}^l \\ h(u, z, \bar{z}, \alpha) &= \textstyle\sum_{j+k+l\geq 2} \frac{1}{j!k!l!} h_{jkl}(\alpha)u^j z^k \bar{z}^l. \end{aligned}$$

Using the changes

$$\begin{aligned} v &= u + \delta_0 + \delta_1 u + \delta_2 z + \delta_3 \bar{z} + \frac{1}{2}V_{020}z^2 + \frac{1}{2}V_{002}\bar{z}^2 + V_{110}uz + V_{101}u\bar{z} \\ w &= z + \Delta_0 + \Delta_1 u + \Delta_2 z + \Delta_3 \bar{z} + \frac{1}{2}W_{200}u^2 + \frac{1}{2}W_{020}z^2 \\ &\quad + \frac{1}{2}W_{002}\bar{z}^2 + W_{101}u\bar{z} + W_{011}z\bar{z} \end{aligned} \tag{3.69}$$

where $\delta_i(\alpha), \Delta_i(\alpha)$ are smooth functions, $\delta_i(0) = \Delta_i(0) = 0, i = 0, 1, 2, 3$, the system (3.65) can be further brought to the so-called Poincaré normal form. More exactly, the following theorem is reported in [59].

Theorem 3.4.1. *If (G.1) $g_{200}(0) \neq 0$, then there exists a locally defined smooth, invertible variable transformation of the form* (3.69)*, smoothly depending on the parameters, that for $||\alpha||$ small enough brings the system* (3.65) *in the form*

$$\begin{aligned} \dot{v} &= \gamma(\alpha) + \frac{1}{2}G_{200}(\alpha)v^2 + G_{011}(\alpha)|w|^2 + \frac{1}{6}G_{300}(\alpha)v^3 \\ &\quad + G_{111}(\alpha)v|w|^2 + O\left(||(v,w,\bar{w})||^4\right) \\ \dot{w} &= R(\alpha)\, w + H_{110}(\alpha)vw + \frac{1}{2}H_{210}(\alpha)v^2w + \frac{1}{2}H_{021}(\alpha)w|w|^2 + O\left(||(v,w,\bar{w})||^4\right) \end{aligned} \tag{3.70}$$

where $v \in \mathbb{R}, w \in \mathbb{C}$ and $\gamma(\alpha), G_{jkl}(\alpha)$ are real-valued smooth functions while $R(\alpha), H_{jkl}(\alpha)$ are complex-valued smooth functions such that $\gamma(0) = 0, R(0) = i\omega_0$. Their expressions at $\alpha = 0$ are given in the paper's Appendix.

If in addition (G.2) $G_{011}(0) \neq 0$, the Poincaré form (3.70) *can be further reduced to* (3.73) *by means of time reparametrization*

$$dt = \left(1 + e_1(\alpha)\, v + e_2(\alpha)\, |w|^2\right) d\tau \tag{3.71}$$

and transformations

$$u = v + e_4(\alpha)\, v + \frac{1}{2}e_3(\alpha)\, v^2 \text{ and } z = w + K(\alpha)\, vw \tag{3.72}$$

where $e_i \in \mathbb{R}, K \in \mathbb{C}$ are smooth functions and $e_4(0) = 0$. More exactly, the system (3.70) *is locally smoothly orbitally equivalent near the origin to the system*

$$\begin{aligned} \dot{u} &= \delta(\alpha) + B(\alpha)u^2 + C(\alpha)|z|^2 + O(||u,z,\bar{z}||^4) \\ \dot{z} &= \Sigma(\alpha)z + D(\alpha)uz + E(\alpha)u^2z + O(||u,z,\bar{z}||^4) \end{aligned} \tag{3.73}$$

where $u \in \mathbb{R}, z \in \mathbb{C}$ and $\delta(\alpha), B(\alpha), C(\alpha), E(\alpha)$ are real-valued smooth functions while $\Sigma(\alpha), D(\alpha)$ are complex-valued smooth functions (given in the Appendix for $\alpha = 0$) such that $\delta(0) = 0, \Sigma(0) = i\omega_0$.

Finally, if (G.3) $E(0) \neq 0$ is satisfied, using the linear scaling

$$\begin{aligned} u &= \frac{B(\alpha)}{E(\alpha)}\xi, \\ z &= \frac{B^3(\alpha)}{C(\alpha)\, E^2(\alpha)}\zeta \end{aligned}$$

and the time-reparametrization, $t = \frac{E(\alpha)}{B^2(\alpha)}\tau$, *the system* (3.73) *leads to the normal form:*

$$\begin{array}{rcl} \dot{\xi} & = & \beta_1(\alpha) + \xi^2 + s|\zeta|^2 + O(|| \left(\xi, \zeta, \bar{\zeta}\right) ||^4) \\ \dot{\zeta} & = & (\beta_2(\alpha) + i\omega_1(\alpha))\zeta + (\theta(\alpha) + i\omega_2(\alpha))\xi\zeta + \xi^2\zeta + O(|| \left(\xi, \zeta, \bar{\zeta}\right) ||^4) \end{array} \quad (3.74)$$

where $s = sign\,[B(0)C(0)] = \pm 1$ *and*

$$\begin{array}{rcl} \beta_1(\alpha) & = & \dfrac{E^2(\alpha)}{B^3(\alpha)}\delta(\alpha), \quad \beta_2(\alpha) = \dfrac{E(\alpha)}{B^2(\alpha)} Re(\Sigma(\alpha)), \\ \theta(\alpha) + i\omega_2(\alpha) & = & \dfrac{D(\alpha)}{B(\alpha)}, \quad \omega_1(\alpha) = \dfrac{E(\alpha)}{B^2(\alpha)} Im(\Sigma(\alpha)), \end{array} \quad (3.75)$$

with $|| \left(\xi, \zeta, \bar{\zeta}\right) ||^4 = \left(\xi^2 + |\zeta|^2\right)^2$. *Given two more generic conditions (G.4) "*$\theta_0 = \theta(0) \neq 0$*" and (G.5) "the map* $\alpha \longmapsto (\beta_1(\alpha), \beta_2(\alpha))$ *is regular at* $\alpha = 0$*," the form* (3.74) *leads to the truncated normal form*

$$\begin{array}{rcl} \dot{\xi} & = & \beta_1 + \xi^2 + sr^2 \\ \dot{r} & = & r\left(\beta_2 + \theta(\alpha)\xi + \xi^2\right) \\ \dot{\varphi} & = & \omega_1 + \omega_2\xi \end{array}. \quad (3.76)$$

In [131] we studied mainly the dynamics of the system (3.74) when $a(\alpha) \equiv 0$ for all $\alpha \in \mathbb{R}^2$.

Dealing with normal forms. The regularity of the maps

$$\alpha \longmapsto (\beta_1(\alpha), \beta_2(\alpha)) \text{ and } \alpha \longmapsto (\gamma(\alpha), \mu(\alpha))$$

at $\alpha = 0$ is equivalent (see [59]). However, to check the regularity of either of the maps in particular models is not a simple exercise as we can see from the next example.

Example 1. Consider the 3D differential system

$$\dot{x} = \alpha_1 - x - y - z, \ \dot{y} = x + ny + bxy, \quad \dot{z} = \alpha_2 + bx - cz, \quad (3.77)$$

where $b = -\frac{1}{n}\left(\alpha_1 + \alpha_2 - n\alpha_1 + (n-1)^2\right)$ and $c = n - 1 - \alpha_1$, with $n \neq 0$ and $b \neq 0$. When $\alpha_1 = \alpha_2 = 0$, $O(0,0,0)$ is the unique equilibrium point of the system and has the eigenvalues 0 and $\pm i\omega_0$, $\omega_0 > 0$, where

$$\omega_0 = \sqrt{\frac{1-n}{n}\left(n^2 + n - 1\right)}$$

for all $n \in I = \left(-\frac{1}{2}\sqrt{5} - \frac{1}{2}, 0\right) \cup \left(\frac{1}{2}\sqrt{5} - \frac{1}{2}, 1\right)$. Hence, if $n \in I$ the system (3.77) undergoes fold-Hopf bifurcations, degenerate or not. The expressions of $\beta_1(\alpha)$, $\beta_2(\alpha)$ and $\gamma(\alpha)$ in terms of the parameters of the system (3.77) cannot be obtained directly from some known formulas. Hence, (G5) for the system (3.77) (and other similar models) cannot be easily verified. In [131] we filled firstly this gap and obtained a result concerning this problem which is given in the next theorem. We do not write its proof here.

Theorem 3.4.2. *The terms $\gamma(\alpha)$ and $R(\alpha)$ in* (3.70) *are given by*

$$\begin{aligned} \gamma &= \Gamma + \Omega\delta_2 + \bar{\Omega}\delta_3 + \Gamma\delta_1 - \frac{1}{6}G_{300}\delta_0^3 - \frac{1}{2}G_{200}\delta_0^2 - G_{111}\Delta_0\bar{\Delta}_0\delta_0 - G_{011}\Delta_0\bar{\Delta}_0 \\ &= \frac{\partial\Gamma(0)}{\partial\alpha_1}\alpha_1 + \frac{\partial\Gamma(0)}{\partial\alpha_2}\alpha_2 + O(\alpha_1,\alpha_2)^2, \end{aligned} \tag{3.78}$$

respectively,

$$\begin{aligned} R &= \lambda - H_{110}\frac{\delta_0}{\Delta_2+1} + \frac{1}{\Delta_2+1}\left(\Omega W_{020} + \bar{\Omega}W_{011}\right) - H_{110}\frac{\Delta_0\delta_2 + \delta_0\Delta_2}{\Delta_2+1} \\ &\quad -\frac{1}{2}H_{021}\frac{\Delta_0\left(\bar{\Delta}_3\Delta_0 + 2\bar{\Delta}_0(\Delta_2+1)\right)}{\Delta_2+1} - \frac{1}{2}H_{210}\frac{\delta_0\left((\Delta_2+1)\delta_0 + 2\Delta_0\delta_2\right)}{\Delta_2+1}, \end{aligned} \tag{3.79}$$

where all terms are evaluated at α.

The expressions of $\delta(\alpha)$ and $\Sigma(\alpha)$ in (3.73) *are given by*

$$\begin{aligned} \delta(\alpha) &= \gamma(\alpha)(1 + e_4(\alpha)) \\ &= \frac{\partial\Gamma(0)}{\partial\alpha_1}\alpha_1 + \frac{\partial\Gamma(0)}{\partial\alpha_2}\alpha_2 + O(\alpha_1,\alpha_2)^2, \end{aligned} \tag{3.80}$$

respectively,

$$\begin{aligned} \Sigma(\alpha) &= R(\alpha) + \gamma(\alpha)K(\alpha) \\ &= a_1^1\alpha_1 + a_2^1\alpha_2 + O(\alpha_1,\alpha_2)^2, \end{aligned} \tag{3.81}$$

where, for $i = 1, 2$,

$$\begin{aligned} a_i^1 &= \frac{\partial\lambda(0)}{\partial\alpha_i} - H_{110}(0)c_i + \frac{\partial\Omega(0)}{\partial\alpha_i}W_{020}(0) + \frac{\partial\bar{\Omega}(0)}{\partial\alpha_i}W_{011}(0) + \frac{\partial\Gamma(0)}{\partial\alpha_i}K(0), \\ c_i &= \frac{\partial\Omega(0)}{\partial\alpha_i}\frac{V_{110}(0)}{G_{200}(0)} + \frac{\partial\bar{\Omega}(0)}{\partial\alpha_i}\frac{V_{101}(0)}{G_{200}(0)} + \frac{\partial\nu(0)}{\partial\alpha_i}\frac{1}{G_{200}(0)}. \end{aligned} \tag{3.82}$$

By $O(\alpha_1,\alpha_2)^2$ we denote all terms in a Taylor expansion starting with quadratic terms, namely

$$O\left(\alpha_1,\alpha_2\right)^2 = c_{20}\alpha_1^2 + c_{11}\alpha_1\alpha_2 + c_{02}\alpha_2^2 + ...$$

Corollary 3.4.1. *Denote by $a(\alpha) = (a_1(\alpha), a_2(\alpha), a_3(\alpha))$. If*

$$\frac{\partial a_i}{\partial \alpha_j}(0) = 0$$

for all $i = 1,2,3$ and $j = 1,2$, that is, the linear part of $a(\alpha)$ is zero, then the system (3.63) undergoes degenerate fold-Hopf bifurcations with respect to (G5).

We apply now the result of the theorem in the above example.

Remark 3.4.1. *(Example 1, continuation) Based on the result of Theorem 3.4.2, we can now study easier the regularity of the map*

$$\alpha \longrightarrow (\gamma(\alpha), \mu(\alpha))$$

for which we need only to determine the linear terms of $\Gamma(\alpha)$ and $\mu(\alpha)$. Consider the above Example 1. The Jacobian matrix $J(\alpha)$ has the characteristic polynomial

$$P(\lambda) = \lambda^3 - \lambda^2\alpha_1 - \lambda\frac{1}{n}\left(n^3 - 2n + 1 - \alpha_1 n^2 + \alpha_1 + \alpha_2\right) + \alpha_2. \tag{3.83}$$

For $n \in I$ the eigenvalues of $J(\alpha)$ at $\alpha = 0$ are 0 and $\pm i\omega_0$, respectively, when α lies in a sufficiently small neighborhood V_0 of $\alpha = (0,0)$ they are of the form

$$\lambda_1 = \nu(\alpha), \lambda = \mu(\alpha) + i\omega(\alpha), \bar{\lambda} = \mu(\alpha) - i\omega(\alpha)$$

for all $\alpha \in V_0$, such that $\nu(0) = \mu(0) = 0$ and $\omega(0) = \omega_0 > 0$. Using the implicit function theorem we can find the linear approximations of these eigenvalues. Indeed, from (3.83) we get $\nu = \nu(\alpha_1,\alpha_2)$, respectively, $\lambda = \lambda(\alpha_1,\alpha_2)$ for all $\alpha = (\alpha_1,\alpha_2) \in V_0$, given by

$$\nu(\alpha) = -\frac{1}{\omega_0^2}\alpha_2 + O_1\left(\alpha_1,\alpha_2\right)^2, \tag{3.84}$$

respectively,

$$\lambda = \frac{1}{2}\alpha_1 + \frac{1}{2\omega_0^2}\alpha_2 + i\frac{\left(n^2-1\right)\alpha_1 - \alpha_2}{2n\omega_0} + O_1\left(\alpha_1,\alpha_2\right)^2 + iO_2\left(\alpha_1,\alpha_2\right)^2. \tag{3.85}$$

Two eigenvectors $q_0(0)$ *and* $q_1(0)$ *corresponding to the eigenvalues* $\nu(\alpha)$ *and* $\mu(\alpha)+i\omega(\alpha)$ *at* $\alpha=0$*, respectively, two adjoint eigenvectors* $p_0(0)$ *and* $p_1(0)$ *satisfying* (3.66) *and* (3.67) *are:*

$$q_0(0)=\begin{pmatrix}-n\\1\\n-1\end{pmatrix},\quad q_1(0)=\begin{pmatrix}n(2n-1)\\-n^3-i\omega_0 n^2\\n(n-1)^2-in\omega_0(n-1)\end{pmatrix},$$

respectively,

$$p_0(0)=\frac{-1}{n^2+n-1}\begin{pmatrix}n\\1\\\frac{-n}{n-1}\end{pmatrix},\ p_1(0)=\frac{n-1-i\omega_0}{2n(2n-1)\omega_0^2}\begin{pmatrix}n+i\omega_0\\1\\n+i\frac{n\omega_0}{n-1}+1\end{pmatrix}.$$

Since $a(\alpha)$ *corresponding to the system* (3.77) *is* $a(\alpha)=(\alpha_1,0,\alpha_2)$*, we need only* $p_0(0)$ *in order to calculate the linear term of* $\Gamma(\alpha)=\langle p_0(\alpha),a(\alpha)\rangle$ *because we know* $a(0)=(0,0,0)$*. Hence, we have*

$$\Gamma(\alpha)=\frac{-n}{n^2+n-1}\alpha_1+\frac{n}{(n^2+n-1)(n-1)}\alpha_2+O(\alpha_1,\alpha_2)^2. \tag{3.86}$$

Since $\mu(\alpha)=\frac{1}{2}\alpha_1+\frac{1}{2\omega_0^2}\alpha_2+O(\alpha_1,\alpha_2)^2$ *we can calculate now the determinant*

$$\begin{vmatrix}\frac{\partial\Gamma(0)}{\partial\alpha_1}&\frac{\partial\Gamma(0)}{\partial\alpha_2}\\\frac{\partial\mu(0)}{\partial\alpha_1}&\frac{\partial\mu(0)}{\partial\alpha_2}\end{vmatrix}=-\frac{n(n+1)}{2(n^2+n-1)^2}\neq0,$$

for all $n\in I$*,* $n\neq-1$*. It follows that the maps* $\alpha\longmapsto(\beta_1(\alpha),\beta_2(\alpha))$ *and* $\alpha\longmapsto(\gamma(\alpha),\mu(\alpha))$ *are regular at* $\alpha=0$ *for all* $n\in I$*,* $n\neq-1$*, and non-regular at* $n=-1$*, which, in turn, imply that the generic condition (G5) is non-degenerate for the system* (3.77) *when* $n\in I$*,* $n\neq-1$*, and degenerate when* $n=-1$*. Hence,* $n=-1$ *is a bifurcation value and we expect the system to have different behaviors when* n *crosses* -1*.*

The next proposition we obtained is useful to understand the results to follow.

Proposition 3.4.1. *Consider an expression of the form*

$$F(\alpha_1,\alpha_2)=c_1\alpha_1^2(1+O(\alpha_1,\alpha_2))+c_2\alpha_1\alpha_2(1+O(\alpha_1,\alpha_2))+c_3\alpha_2^2(1+O(\alpha_1,\alpha_2)) \tag{3.87}$$

where $c_1^2 + c_2^2 + c_3^2 \neq 0$ *and* $O(\alpha_1, \alpha_2) \to 0$ *as* $(\alpha_1, \alpha_2) \to (0,0)$. *Then*

$$F(\alpha_1, \alpha_2) > 0 \text{ if } c_1\alpha_1^2 + c_2\alpha_1\alpha_2 + c_3\alpha_2^2 > 0,$$

respectively,

$$F(\alpha_1, \alpha_2) < 0 \text{ if } c_1\alpha_1^2 + c_2\alpha_1\alpha_2 + c_3\alpha_2^2 < 0$$

for all $||\alpha||$ *small enough.* $O(\alpha_1, \alpha_2)$ *denotes all terms in a Taylor series starting with the linear terms.*

Assume in the following $a(\alpha) \equiv 0$ at all $\alpha \in \mathbb{R}^2$. The following results will show that the system's dynamics in the two cases (i.e. when $a(\alpha) \neq 0$ and $a(\alpha) \equiv 0$) are independent on each other and must be treated separately. The next theorem is the first proof of this statement. Denote by $b_i = \frac{\partial \nu(0)}{\partial \alpha_i}$, $i = 1, 2$, the coefficients of the linear part of the real eigenvalue

$$\nu(\alpha) = b_1\alpha_1 + b_2\alpha_2 + O(\alpha_1, \alpha_2)^2.$$

Assume further that $b_1^2 + b_2^2 \neq 0$.

Theorem 3.4.3. *If* $a(\alpha) \equiv 0$ *for all* $\alpha \in \mathbb{R}^2$ *in* (3.64) *then the normal form* (3.76) *has at least two equilibrium points for all* $||\alpha||$ *small enough, excepting eventual on the line* $b_1\alpha_1 + b_2\alpha_2 = 0$, *and undergoes a degenerate fold-Hopf bifurcation with respect to the parameters. Moreover,*

$$\beta_1(\alpha) = -\frac{4E^2(0)}{G_{200}^4(0)}(b_1\alpha_1 + b_2\alpha_2)^2 + O(\alpha_1, \alpha_2)^3 \tag{3.88}$$

and

$$\beta_2(\alpha) = \frac{4E(0)}{G_{200}^2(0)} Re(a_1^1\alpha_1 + a_2^1\alpha_2) + O(\alpha_1, \alpha_2)^2 \tag{3.89}$$

where

$$a_i^1 = \frac{\partial \mu(0)}{\partial \alpha_i} - \frac{\partial \nu(0)}{\partial \alpha_i}\frac{H_{110}(0)}{G_{200}(0)}, i = 1, 2.$$

Remark 3.4.2. *Based on Proposition 3.4.1 we notice that* $\beta_1(\alpha) < 0$ *for all* $||\alpha|| = \sqrt{\alpha_1^2 + \alpha_2^2}$ *small enough and* $b_1\alpha_1 + b_2\alpha_2 \neq 0$. *This is a new property which does not exist in the non-degenerate framework and will have an important role in the system's behavior. It arises from* $a(\alpha) \equiv 0$. *Because of this property, the system under study* (3.76) *has always at least* ***two equilibria*** *for all* $\|\alpha\| \neq 0$ *small enough (excepting eventual on the line* $b_1\alpha_1 + b_2\alpha_2 = 0$ *) which is not the case in the non-degenerate framework, when the system can have* ***zero, one, two or three equilibria*** *for* $\|\alpha\|$ *small enough.*

Remark 3.4.3. *a) The cases* $b_1^2 + b_2^2 = 0$ *and/or* $a_1^2 + a_2^2 = 0$ *are more involved and we do not treat them here.*

b) From Proposition 3.4.1, we have that $\beta_2(\alpha) > 0$ *if* $E(0)(a_1\alpha_1 + a_2\alpha_2) > 0$, *respectively,* $\beta_2(\alpha) < 0$ *if* $E(0)(a_1\alpha_1 + a_2\alpha_2) < 0$.

Two bifurcation curves in the parametric space α_1, α_2 arise from the Theorem 3.4.3, namely:

$$d : b_1\alpha_1 + b_2\alpha_2 = 0 \ \text{ and } \ D : a_1\alpha_1 + a_2\alpha_2 = 0$$

for $\|\alpha\|$ small, where $a_1 = Re\left(a_1^1\right)$ and $a_2 = Re\left(a_2^1\right)$, provided that $a_1^2 + a_2^2 \neq 0$ and $b_1^2 + b_2^2 \neq 0$.

Disregarding the higher order terms in (3.88) and (3.89) we write shortly

$$d : \beta_1(\alpha) = 0 \ \text{ and } \ D : \beta_2(\alpha) = 0,$$

that is, the curve d is obtained from $\beta_1(\alpha) = 0$ and D from $\beta_2(\alpha) = 0$.

We will proceed now to the analysis of the 3D system (3.76) in which $\beta_1 = \beta_1(\alpha)$ and $\beta_2 = \beta_2(\alpha)$ are two functions depending on α. The first two equations in (3.76) are independent on the third one, which describes a rotation around the ξ-axis. For $||\xi||$ small enough $\dot{\varphi} \approx \omega_1(\alpha)$. As explained in [59], we can reduce the study of the 3D system (3.76) to the study of a 2D system using the first two equations from (3.76):

$$\begin{array}{rcl} \dot{\xi} & = & \beta_1(\alpha) + \xi^2 + sr^2 \\ \dot{r} & = & r\left(\beta_2(\alpha) + \theta(\alpha)\,\xi + \xi^2\right) \end{array} \tag{3.90}$$

Let us give now some results of this 2D system. Since $\beta_1(\alpha) \leq 0$ the system (3.90) can have up to four equilibria:

$$A_1\left(\sqrt{-\beta_1(\alpha)}, 0\right) \ \text{ and } \ A_2\left(-\sqrt{-\beta_1(\alpha)}, 0\right)$$

lying on the $\xi-$axis and corresponding to $r = 0$, respectively,

$$A_3 = \left(\xi_3(\alpha), r_3(\alpha)\right) \ \text{ and } \ A_4 = \left(\xi_4(\alpha), r_4(\alpha)\right),$$

where

$$\xi_3(\alpha) = -\frac{1}{2}\theta(\alpha) - \frac{1}{2}\sqrt{\theta^2(\alpha) - 4\beta_2(\alpha)}, \ \xi_4(\alpha) = -\frac{1}{2}\theta(\alpha) + \frac{1}{2}\sqrt{\theta^2(\alpha) - 4\beta_2(\alpha)}$$

and $r_{3,4}(\alpha) = \sqrt{-s\left(\beta_1(\alpha) + \xi_{3,4}^2(\alpha)\right)} > 0$ whenever $-s\left(\beta_1(\alpha) + \xi_{3,4}^2(\alpha)\right) > 0$, corresponding to $r \neq 0$. The Taylor expansions of ξ_3 and ξ_4 for $\theta_0 = \theta(0) < 0$ lead to:

$$\xi_3 = g_1\alpha_1 + g_2\alpha_2 + O(\alpha_1, \alpha_2)^2 \text{ and } \xi_4 = -\theta_0 + O(\alpha_1, \alpha_2), \tag{3.91}$$

respectively, for $\theta_0 = \theta(0) > 0$,

$$\xi_3 = -\theta_0 + O(\alpha_1, \alpha_2) \text{ and } \xi_4 = g_1\alpha_1 + g_2\alpha_2 + O(\alpha_1, \alpha_2)^2$$

where

$$g_i = -\frac{1}{\theta_0}\frac{\partial\beta_2(0)}{\partial\alpha_1} = -\frac{1}{\theta_0}\frac{E(0)}{B^2(0)}a_i,\ i = 1, 2.$$

Hence, only A_3 or A_4 lies in a small neighborhood of the origin for $||\alpha||$ small enough and only this one will be studied further. Call the one to be studied *the third equilibrium point of the system* and denote it generically by $A_3 = (\xi_3, r_3)$. It is clear that $\xi_3(0) = r_3(0) = 0$.

Proposition 3.4.2. *A new bifurcation curve h in the parametric space arises from the expression of $\beta_1 + \xi_3^2$, which reduces to two lines $h = h^1 \cup h^2$, given for $||\alpha||$ small enough by*

$$h^1 : \alpha_2 = h_0\alpha_1 \text{ and } h^2 : \alpha_2 = h_0'\alpha_1$$

where $h_0 = -\frac{2a_1+\theta_0 b_1}{2a_2+\theta_0 b_2}$ and $h_0' = -\frac{2a_1-\theta_0 b_1}{2a_2-\theta_0 b_2}$. The lines h^1 and h^2 coincide when $h_0 = h_0'$. The third equilibrium A_3 is born or dies when α crosses the lines h^1, h^2. The expression of $\beta_1 + \xi_3^2$ is given by

$$\beta_1 + \xi_3^2 = h_2\alpha_2^2 + 2h_3\alpha_1\alpha_2 + h_1\alpha_1^2 + O(\alpha_1, \alpha_2)^3, \tag{3.92}$$

where

$$h_i = \frac{4}{\theta_0^2}\frac{E^2(0)}{G_{200}^4(0)}\left(4a_i^2 - \theta_0^2 b_i^2\right), i = 1, 2 \text{ and } h_3 = \frac{4}{\theta_0^2}\frac{E^2(0)}{G_{200}^4(0)}\left(4a_1a_2 - \theta_0^2 b_1 b_2\right).$$

We assume $h_1^2 + h_2^2 + h_3^2 \neq 0$.

The proof of this Proposition is based on the expression of $\beta_1 + \xi_3^2$, which, from (3.88) and (3.91), can be put in the form (3.92). Since the quadratic terms of this expression lead to a quadratic equation which always has real roots, the two lines h^1 and h^2 follow from the two factors of the equation. Disregarding the tailing terms in (3.92), we can say the curve h has the form

$$h : \beta_1 + \xi_3^2 = 0.$$

The following theorem classifies the equilibria $A_{1,2}$. We use the short notation $\{\beta_1 + \xi_3^2 < 0\}$ in place of

$$\left\{(\alpha_1, \alpha_2) \in \mathbb{R}^2; \beta_1(\alpha) + \xi_3^2(\alpha) < 0\right\}.$$

Theorem 3.4.4. *Suppose A_1 and A_2 are the equilibria of* (3.90) *lying on the $\xi-$axis. Then:*

a) A_1, A_2 are (unstable, stable) nodes if $\theta_0 > 0$ and $(\alpha_1, \alpha_2) \in \{\beta_1 + \xi_3^2 < 0\}$;

b) A_1, A_2 are both saddles if $\theta_0 < 0$ and $(\alpha_1, \alpha_2) \in \{\beta_1 + \xi_3^2 < 0\}$;

c) A_1 is an unstable node and A_2 a saddle if $\theta_0 \neq 0$ and $(\alpha_1, \alpha_2) \in \{\beta_1 + \xi_3^2 > 0\} \cap \{\beta_2 > 0\}$;

d) A_1 is a saddle and A_2 a stable node if $\theta_0 \neq 0$ and $(\alpha_1, \alpha_2) \in \{\beta_1 + \xi_3^2 > 0\} \cap \{\beta_2 < 0\}$.

Its proof can be found in [131]. Concerning the **third equilibrium** A_3 we have the following results. The matrix $J(\alpha)$ at A_3 has the eigenvalues

$$\lambda_{1,2} = \xi_3 \pm \sqrt{\Delta},$$

where

$$\Delta = \xi_3^2 + 2s\left(2\xi_3 + \theta(\alpha)\right) r_3^2. \tag{3.93}$$

In its lowest terms, Δ expresses

$$\Delta = k_2\alpha_2^2 + 2k_3\alpha_1\alpha_2 + k_1\alpha_1^2 + O\left(\alpha_1, \alpha_2\right)^3 \tag{3.94}$$

where

$$k_i = \frac{8}{\theta_0^2}\frac{E^2(0)}{G_{200}^4(0)}\left(\theta_0^3 b_i^2 + 2\left(1 - 2\theta_0\right) a_i^2\right),\ i = 1, 2,$$

respectively,

$$k_3 = \frac{8}{\theta_0^2}\frac{E^2(0)}{G_{200}^4(0)}\left(b_1 b_2 \theta_0^3 + 2a_1 a_2\left(1 - 2\theta_0\right)\right);$$

assume $k_1^2 + k_2^2 + k_3^2 \neq 0$. The algebraic expression of Δ gives rise to a bifurcation curve in the parametric α_1, α_2 space for $\|\alpha\|$ small enough and denote it by k. More exactly, using the lowest terms in (3.94), we define a curve k by

$$k : k_2\alpha_2^2 + 2k_3\alpha_1\alpha_2 + k_1\alpha_1^2 = 0.$$

Δ may change its sign when (α_1, α_2) crosses k. On k its sign is positive or negative depending on higher order terms and typically $\Delta = 0$ only at $\alpha = 0$; k does not coincide typically to the curve $\xi_3 = 0$. We also use the notation

$$k : \Delta = 0.$$

Remark 3.4.4. *The third equilibrium A_3 is born when $\alpha = (\alpha_1, \alpha_2)$ crosses the bifurcation curve h and its stability is determined when α crosses the curve k.*

The following theorem characterizes the third equilibrium point.

Theorem 3.4.5. *If A_3 is the third equilibrium point of* (3.90)*, then:*
a) if $s\theta_0 > 0$, A_3 is a saddle;
b) if $s\theta_0 < 0$, A_3 is a focus on $\{\Delta < 0\}$ and a node on $\{\Delta \geq 0\}$;
c) Both as a node and a focus, A_3 is stable on $(\theta_0 > 0, s = -1, \beta_2 > 0)$ and $(\theta_0 < 0, s = +1, \beta_2 < 0)$, respectively, unstable on $(\theta_0 > 0, s = -1, \beta_2 < 0)$ and $(\theta_0 < 0, s = +1, \beta_2 > 0)$.

More details can be found in [131]. We will proceed in the following to present five **bifurcation diagrams.** In these diagrams we use the generic phase portraits displayed in Figs.3.12-3.13 with the following meanings: "nn" and "ss" mean A_1, A_2 are (unstable/stable) nodes, respectively, saddles and are the single equilibria, "sn" means A_1 is a node, A_2 a saddle and A_3 does not exist, "sns" stands for A_1 a saddle, A_2 a node and A_3 a saddle, "snuf" is when A_1 is a saddle, A_2 a node and A_3 an unstable focus, "ssc", respectively, "ssh", correspond to A_1, A_2 saddles and the existence of the **circle** emerging from the Hopf bifurcation of the 2D system, respectively, the **heteroclinic cycle** emerging from the heteroclinic connections in the 2D system, and so on. In these notations, the first letter is for A_1, the second for A_2 and the last one or two letters (if appear) for A_3, excepting "ssc" and "ssh". Notice that A_1 and A_2 exist for all $\|\alpha\|$ small and when A_1 is a node it is unstable, respectively, when A_2 is a node it is stable.

The bifurcation diagrams has been obtained for $E(0) > 0$, $a_2, b_2 > 0$, $a_1, b_1 < 0$, $a_1 b_2 - a_2 b_1 < 0$, $b_1\alpha_1 + b_2\alpha_2 \neq 0$ and $2a_2 \pm \theta_0 b_2 > 0$. Other conditions lead to similar diagrams. A_1, A_2 exist for all $\|\alpha\|$ small enough in all these cases.

Case 1. $\theta_0 > 0$, $s = +1$. Then one can check that

$$0 < -\frac{b_1}{b_2} < h_0 < -\frac{a_1}{a_2} < h_0'. \tag{3.95}$$

Since $s\theta_0 > 0$, A_3 is a saddle whenever it exists, namely on $\beta_1 + \xi_3^2 < 0$, and it coexists with the nodes $A_{1,2}$. The lines h^1, h^2 cross the quadrants 1 and 3 and

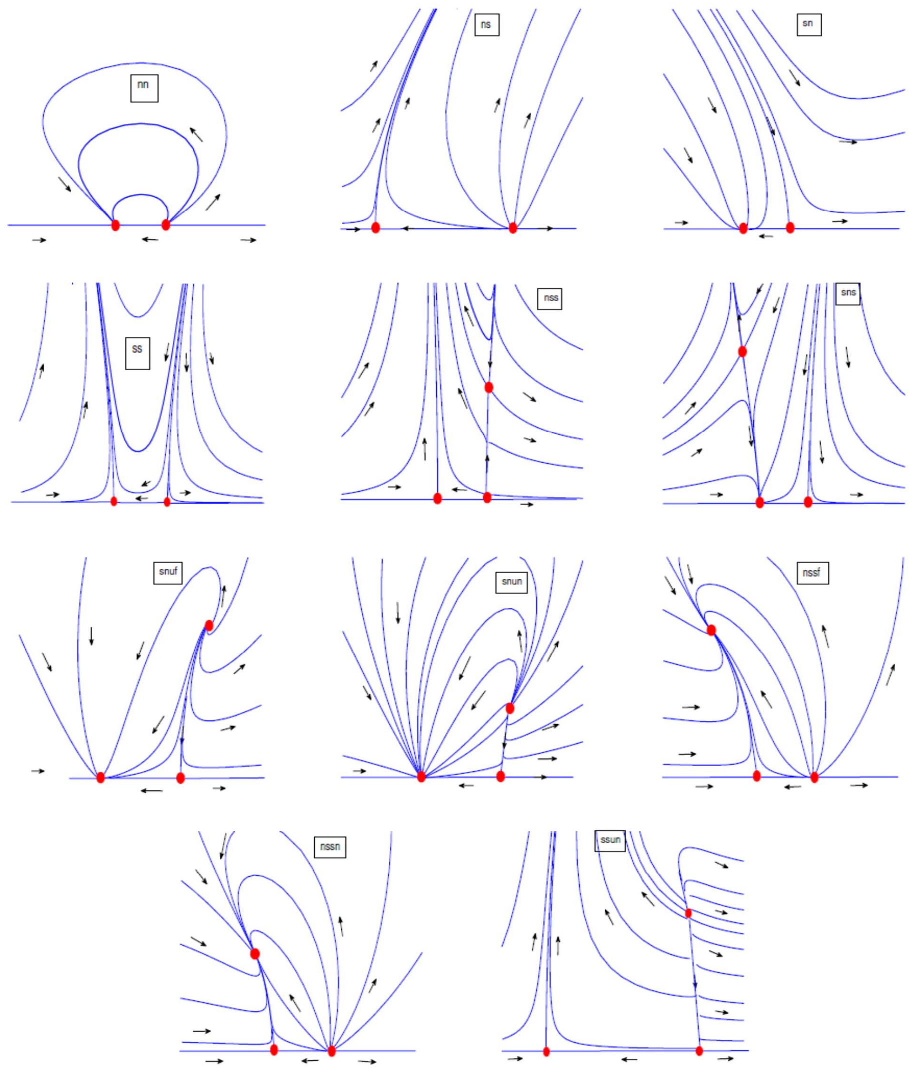

Figure 3.12: Generic phase portraits of the $2D$ system (3.90).

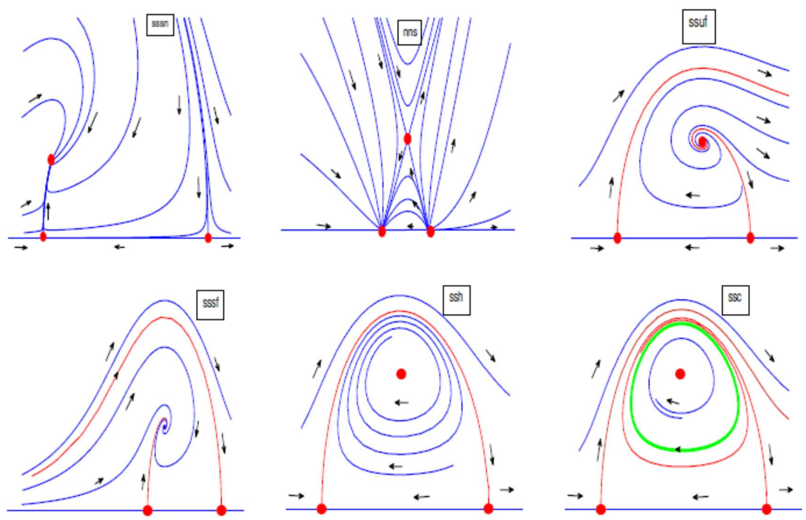

Figure 3.13: Generic phase portraits of the $2D$ system (3.90).

the curve $D : \beta_2 = 0$ lies between them. The bifurcation diagram is given in Fig. 3.14 a).

Case 2. $\theta_0 < 0$, $s = -1$. In this case

$$0 < -\frac{b_1}{b_2} < h_0' < -\frac{a_1}{a_2} < h_0. \tag{3.96}$$

A_3 is a saddle and coexists on $\beta_1 + \xi_3^2 > 0$ with the node A_1 and the saddle A_2 on $\alpha_2 > 0$ or $\alpha_1 < 0$, respectively, with the saddle A_1 and the node A_2 on $\alpha_2 < 0$ or $\alpha_1 > 0$. Fig. 3.14 b) shows the bifurcation diagram.

Case 3. $0 < \theta_0 \leq \frac{1}{2}$, $s = -1$. A_3 exists on $\beta_1 + \xi_3^2 > 0$ as a node because $\Delta \geq 0$ for all $\|\alpha\|$ small, being stable on $\beta_2 > 0$ respectively, unstable on $\beta_2 < 0$. A_3 coexists with A_1 and A_2 as in the Case 2. The inequalities in (3.95) are valid in this case. The bifurcation diagram is depicted in Fig. 3.15 a).

Case 4. $\theta_0 > \frac{1}{2}$, $s = -1$. A_3 exists on $\beta_1 + \xi_3^2 > 0$ as a node if $\Delta \geq 0$ or a focus if $\Delta < 0$, being stable on $\beta_2 > 0$, respectively, unstable on $\beta_2 < 0$. A_3 coexists with A_1 and A_2 as in the Case 2. Assume further $\theta_0^3 b_2^2 - 4\theta_0 a_2^2 + 2a_2^2 > 0$ and $\theta_0^3 b_1^2 - 4\theta_0 a_1^2 + 2a_1^2 < 0$. Then one can show that

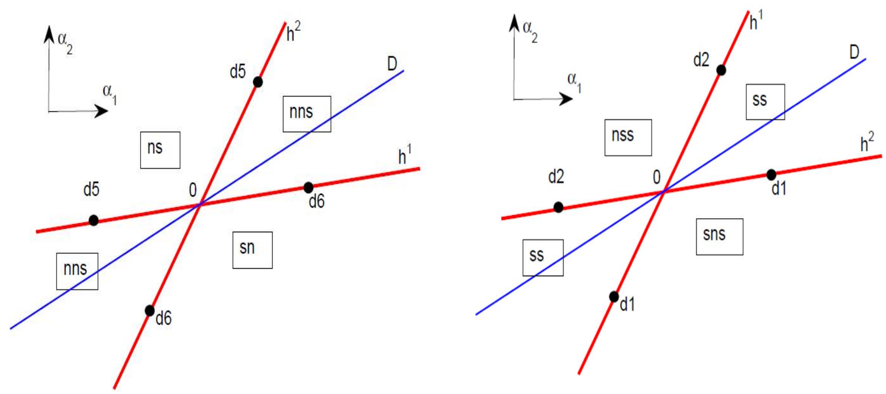

Figure 3.14: Bifurcation diagrams for: a) $\theta_0 > 0$ and $s = +1$, (left); b) $\theta_0 < 0$ and $s = -1$ (right).

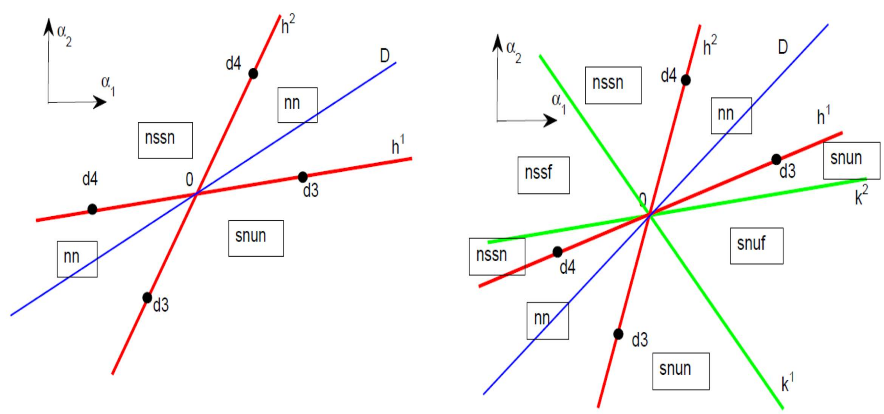

Figure 3.15: Bifurcation diagrams for: a) $0 < \theta_0 \leq \frac{1}{2}$ and $s = -1$, (left); b) $\theta_0 > \frac{1}{2}$ and $s = -1$ (right). The generic portraits on the lines k^1, k^2 are the same as in their neighborhood corresponding to A_3 a node, namely "nssn" for $\alpha_1 < 0$, respectively, "snun" for $\alpha_1 > 0$.

$$k_0 < 0 < -\frac{b_1}{b_2} < k_0' < h_0 < -\frac{a_1}{a_2} < h_0',$$

since

$$k_0' + \frac{b_1}{b_2} = -\frac{1}{b_2}\frac{2\left(2\theta_0 - 1\right)\left(a_1 b_2 - a_2 b_1\right)}{\theta_0^2 b_2 \sqrt{\frac{2}{\theta_0}\left(2\theta_0 - 1\right)} + 2a_2\left(2\theta_0 - 1\right)} > 0$$

and

$$k_0 k_0' = \frac{\theta_0^3 b_1^2 - 4\theta_0 a_1^2 + 2a_1^2}{\theta_0^3 b_2^2 - 4\theta_0 a_2^2 + 2a_2^2} < 0.$$

Since $\theta_0\beta_1 < 0$ the curve H does not exist. More curves than in the previous cases appear in the bifurcation diagram, Fig. 3.15 b).

Case 5. $\theta_0 < 0$, $s = +1$. A_3 exists on $\beta_1 + \xi_3^2 < 0$ as a node if $\Delta \geq 0$ or a focus if $\Delta < 0$, along with the saddles $A_{1,2}$. Assume now $\theta_0^3 b_i^2 - 4\theta_0 a_i^2 + 2a_i^2 > 0$, $i = 1, 2$, and get

$$0 < -\frac{b_1}{b_2} < h_0' < k_0 < -\frac{a_1}{a_2} < k_0' < h_0.$$

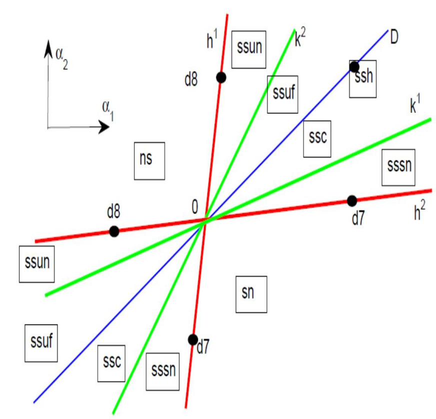

Figure 3.16: Bifurcation diagram for $\theta_0 < 0$ and $s = +1$. The generic portraits on the lines k^1, k^2 are the same as in their neighborhood corresponding to A_3 a node, namely ”ssun” or ”sssn”.

Both as a node and a focus A_3 is stable on $\beta_2 < 0$, respectively, unstable on $\beta_2 > 0$. The Hopf bifurcation curve H arises in this case and because $\theta_0\beta_1 > 0$

for all $\|\alpha\|$ small, H coincides to $D : \{\beta_2 = 0\}$. An unstable limit cycle T is born through the Hopf bifurcation and T coexists with the stable focus A_3 on $\beta_2 < 0$. Varying the parameter α the cycle T approaches the heteroclinic cycle on D when its period tends to infinity and then disappears. The bifurcation diagram is depicted in Fig.3.16.

Bifurcations in the 3D system. We want to describe now the corresponding results for the 3D system. The method is described in [59]. The two equilibria A_1 and A_2 in (3.90) are also equilibria in (3.76). Indeed, the 3D system (3.76) in cartesian coordinates reads

$$\begin{array}{rcl} \dot{x} & = & x\left(\beta_2 + \theta z + z^2\right) - y\left(\omega_1 + \omega_2 z\right) \\ \dot{y} & = & x\left(\omega_1 + \omega_2 z\right) + y\left(\beta_2 + \theta z + z^2\right) \\ \dot{z} & = & \beta_1 + z^2 + s\left(x^2 + y^2\right). \end{array} \tag{3.97}$$

It has two equilibria lying on the $z-$axis,

$$A_1 = \left(0, 0, \sqrt{-\beta_1(\alpha)}\right) \text{ and } A_2 = \left(0, 0, -\sqrt{-\beta_1(\alpha)}\right)$$

for $\beta_1(\alpha) \leq 0$. The eigenvalues of the Jacobian matrix

$$\begin{pmatrix} \beta_2 + \theta z + z^2 & -\left(\omega_1 + \omega_2 z\right) & x\left(\theta + 2z\right) - y\omega_2 \\ \omega_1 + \omega_2 z & \beta_2 + \theta z + z^2 & y\left(\theta + 2z\right) + x\omega_2 \\ 2sx & 2sy & 2z \end{pmatrix}$$

are

$$2\sqrt{-\beta_1} \text{ and } p_2^+ = \beta_2 + \theta\sqrt{-\beta_1} - \beta_1 \pm i\left(\omega_1 + \sqrt{-\beta_1}\omega_2\right) \text{ at } A_1,$$

respectively,

$$-2\sqrt{-\beta_1} \text{ and } p_2^- = \beta_2 - \theta\sqrt{-\beta_1} - \beta_1 \pm i\left(\omega_1 - \sqrt{-\beta_1}\omega_2\right) \text{ at } A_2.$$

Remark 3.4.5. *Since the real part of p_2^+ coincides to λ_2^+, respectively, p_2^- coincides to λ_2^-, the stability of A_1 and A_2 in the 3D system is adequately described by their counterparts equilibria in the 2D system.*

If one assumes in (3.97) $\beta_2 + \theta z + z^2 = 0$, which has the roots

$$z_{1,2} = -\frac{1}{2}\theta \pm \frac{1}{2}\sqrt{\theta^2 - 4\beta_2},$$

then from the first two equations of (3.97) one gets

$$x\dot{x} + y\dot{y} = 0$$

which leads to $x^2 + y^2 = r_0^2$, for some $r_0 \in \mathbb{R}$. If in addition

$$\beta_1 + z^2 + s\left(x^2 + y^2\right) = 0,$$

i.e. $\dot{z} = 0$, we can find $r_{1,2} = \sqrt{-s\left(\beta_1 + z_{1,2}^2\right)}$, whenever $-s\left(\beta_1 + z_{1,2}^2\right) \geq 0$; $s^2 = 1$. These give rise to two limit cycles

$$x^2 + y^2 = r_{1,2}^2$$

lying in the planes $z = z_{1,2}$ of the phase space of the 3D system. Hence, as expected, these two limit cycles in the 3D system correspond to the equilibria A_3 and A_4 in the 2D system, where $z_1 = \xi_3$, respectively, $z_2 = \xi_4$. Only one of them lies in a sufficiently small neighbourhood of the origin and this is denoted further by C. The circle C has the same stability as the point A_3 of the 2D system.

On the other hand, the unstable limit cycle T born through Hopf bifurcation around A_3 in the 2D system gives rise to an invariant torus in the 3D system of the same type as T, while the heteroclinic orbit linking A_1 to A_2 in the 2D system and obtained when α crosses the bifurcation curve D corresponds a sphere in the 3D system.

Figs. 3.17-3.18 show the main phase portraits of the 3D system corresponding to Figs. 3.12-3.13 of the 2D system. We obtained these pictures by integrating the 3D system (3.97) for various initial conditions and values of the parameters. In all these pictures we used $\omega_1 = 0.1$ and $\omega_2 = -0.1$. We kept the same notations as for the 2D system: "nn", "ss", "sns", "snuf" and others; "ssc", respectively, "ssh", correspond to A_1, A_2 saddles and the existence of the **torus** emerging from the Hopf bifurcation of the 2D system, respectively, the **sphere** emerging from the heteroclinic connection in the 2D system.

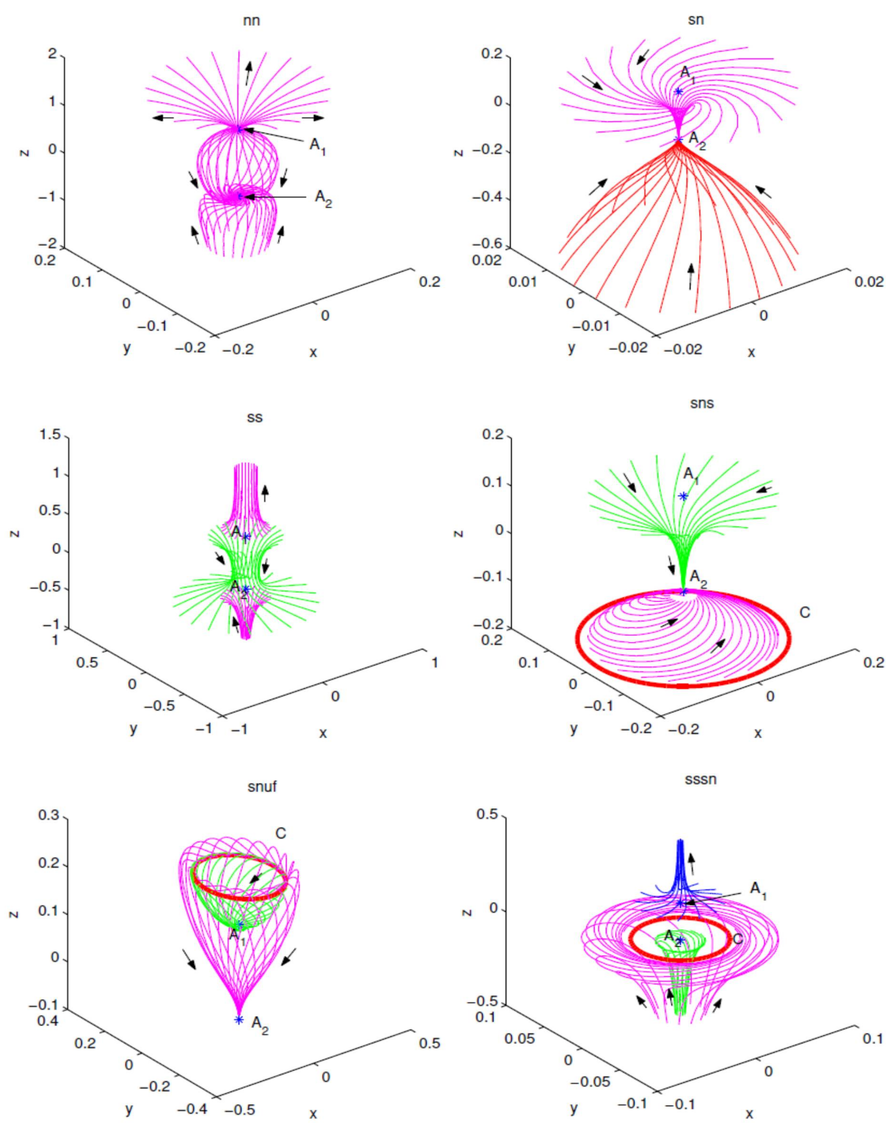

Figure 3.17: Generic phase portraits of the 3D system. In all cases $\omega_1 = 0.1$ and $\omega_2 = -0.1$ The other numeric values are as follows: "nn" $\beta_1 = -0.5, \beta_2 = -0.001$, $s = -1$, $\theta_0 = 1$; "sn" $\beta_1 = -0.01, \beta_2 = -0.2$, $s = 1$, $\theta_0 = 1$; "ss" $\beta_1 = -0.12, \beta_2 = -0.14$, $s = -1$, $\theta_0 = -1$; "sns" $\beta_1 = -0.01, \beta_2 = -0.24$, $s = -1$, $\theta_0 = -1$, "snuf" $\beta_1 = -0.01, \beta_2 = -0.24$, $s = -1$, $\theta_0 = 1$; "sssn" $\beta_1 = -0.01, \beta_2 = -0.1$, $s = 1$, $\theta_0 = -1$.

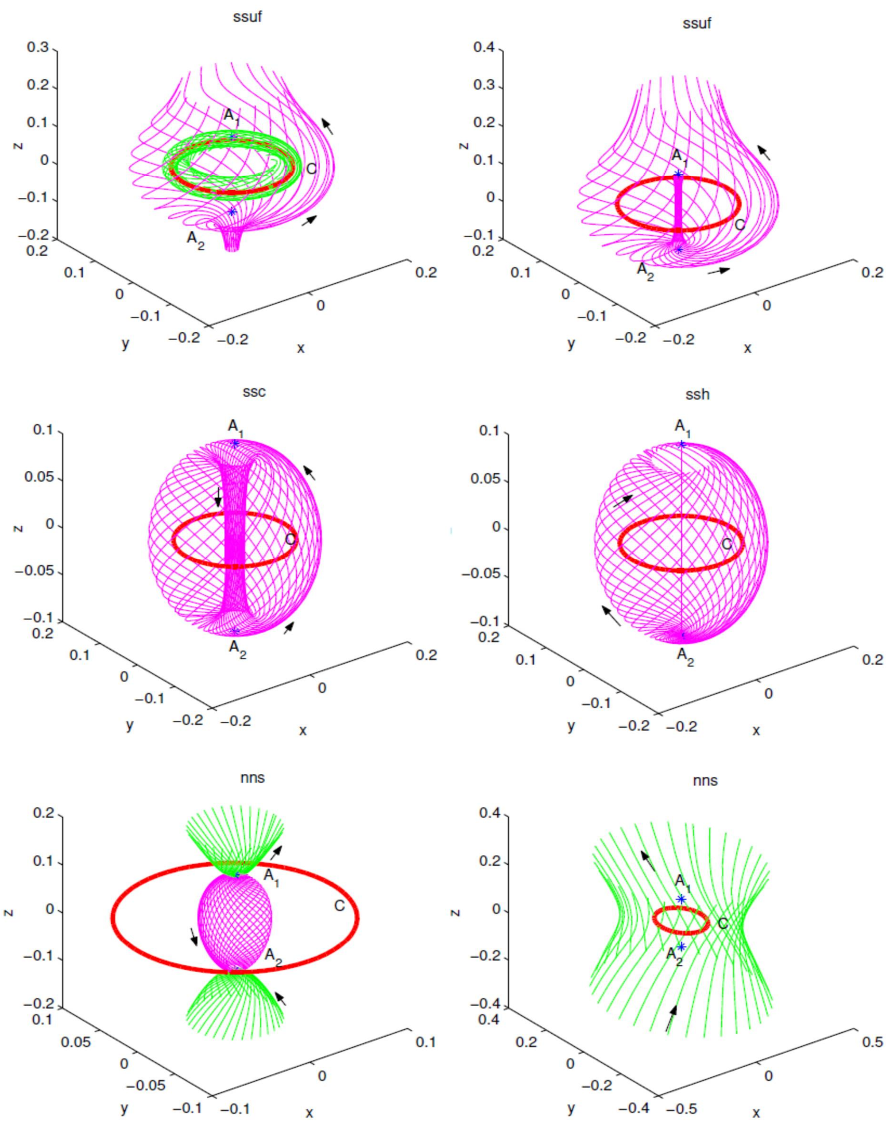

Figure 3.18: Generic phase portraits of the 3D system. In all cases $\omega_1 = 0.1$ and $\omega_2 = -0.1$ The other numeric values are as follows: "ssuf" $\beta_1 = -0.01, \beta_2 = 0.02$, $s = 1$, $\theta_0 = -1$; "ssc" $\beta_1 = -0.01, \beta_2 = -0.002$, $s = 1$, $\theta_0 = -1$; "ssh" $\beta_1 = -0.01, \beta_2 = -0.0028$, $s = 1$, $\theta_0 = -1$ and "nns" $\beta_1 = -0.01, \beta_2 = -0.011$, $s = 1$, $\theta_0 = 1$.

Chapter 4

Future plans for career development

My future plans for career development have two main directions: teaching and research. I want to build further upon my experience of about 20 years in teaching and research in academic environments both in Romania and in other worldwide prestigious universities.

4.1 Plans for teaching

For **teaching**, I plan to:
1. continue my teaching activities in Mathematics to university students, especially from the Politehnica University Timisoara; the students may be undergraduate, master or doctoral students;
2. publish textbooks and other teaching materials for students to support them with more materials for their learning process;
3. support the students in their learning process with additional teaching hours (office time);
4. participate in symposiums, workshops and other actions designed to exchange experience in teaching with other colleagues from Romania or worldwide;
5. invite other professors from abroad in exchange programs such as Erasmus to teach courses to our students;
6. participate in exchange programs and teach courses to students from other universities, from Romania or other countries;
7. contribute to the organization of various competitions for students at local

and national level;
8. participate to various committees related to teaching and students;
9. participate to committees formed for employing new professors in the university;
10. supervise master and doctoral students;
11. involvement in actions establishing the curricula in Mathematics for students;
12. involvement in the organization of master and doctoral studies in the university;
13. elaborate research proposals for master and doctoral thesis;
14. participate in other teaching-related activities in the university;
15. contribute to the university library with my published textbooks and other materials from my field of research as fully free resources for students and other readers.

4.2 Plans for scientific research

In terms of **scientific research** I have the following plans:
1. continue exploring research themes in Mathematics, especially related to Dynamical Systems Theory;
2. maintain the present collaborations I have with other national and international researchers and extend my scientific interactions to other new collaborators working in my research-related fields;
3. participation to research stages at other international universities, research institutes or companies;
4. publish research articles in international journals;
5. participation in conferences, workshops and seminars for disseminating my research results or as a listener;
6. elaborate research projects and submit them to various national or international competitions for funding, such as Horizon 2020, Structural Funds and the Romanian Ministry of Research funds;
7. organize consortia for participation in competitions of projects;
8. coordinate research teams for performing research activities on specific topics from my field of research;
9. collaborate with private companies for developing innovative products;
10. supporting the doctoral school in Mathematics from the university;
11. continue the activity as a scientific referent to various journals related to my

field of research;
12. extend my fields of research to applications of dynamical systems in Biology, Medicine (especially in Neuroscience) and Engineering;
13. organization of conferences, workshops, seminars, summer schools and other similar actions in my field of research.

In the following I want to describe briefly three directions of research I plan to develop in the following years.

4.2.1 Contributions to understanding degenerate fold-Hopf bifurcations

I started to study degenerate fold-Hopf bifurcations in differential systems of the form

$$\dot{x} = f(x, \alpha), \tag{4.1}$$

with f smooth, $x \in \mathbb{R}^3$, $\alpha \in \mathbb{R}^2$, and the first results I obtained on this topic have been recently published in [131]. There is still a lot of work in this field of research and many open problems wait for to be explored. For example, in [131] I studied the fold-Hopf bifurcation in (4.1) and showed that when $f(0, \alpha)$ has its linear part identically zero for all α lying in a small neighborhood V_0 of 0 in the parametric space, the bifurcation becomes degenerate with respect to G5. This implies that the qualitative behavior of the system (4.1) when $\alpha \in V_0$ is not known in general and no results exist in the literature to tell us how the system behaves in this case, for example, how many period orbits may appear when α varies in V_0. To my knowledge, no general results are known concerning the behavior of a dynamical system of type (4.1) when this undergoes a degenerate fold-Hopf bifurcation. The degeneracy arises when one or more of the five known generic conditions G1–G5 (described above in section 3.4) are not satisfied anymore. The generic conditions arise from the constraints which must be imposed in order to obtain a normal form to the initial system (4.1). A normal form has been obtained in the following way. When G1–G3 are satisfied, (4.1) leads to the system

$$\begin{array}{rcl} \dot{\xi} & = & \beta_1(\alpha) + \xi^2 + s|\zeta|^2 + O(\|\left(\xi, \zeta, \bar{\zeta}\right)\|^4) \\ \dot{\zeta} & = & (\beta_2(\alpha) + i\omega_1(\alpha))\zeta + (\theta(\alpha) + i\omega_2(\alpha))\xi\zeta + \xi^2\zeta + O(\|\left(\xi, \zeta, \bar{\zeta}\right)\|^4) \end{array} \tag{4.2}$$

where $s = sign\,[B(0)C(0)] = \pm 1$ and

$$\begin{aligned} \beta_1(\alpha) &= \frac{E^2(\alpha)}{B^3(\alpha)}\delta(\alpha), \quad \beta_2(\alpha) = \frac{E(\alpha)}{B^2(\alpha)}Re(\Sigma(\alpha)), \\ \theta(\alpha) + i\omega_2(\alpha) &= \frac{D(\alpha)}{B(\alpha)}, \quad \omega_1(\alpha) = \frac{E(\alpha)}{B^2(\alpha)}Im(\Sigma(\alpha)). \end{aligned} \tag{4.3}$$

If two more generic conditions are satisfied, namely (G.4) "$\theta_0 = \theta(0) \neq 0$" and (G.5) "the map $\alpha \longmapsto (\beta_1(\alpha), \beta_2(\alpha))$ is regular at $\alpha = 0$," from (4.2) the following normal form can be obtained

$$\begin{array}{rcl} \dot{\xi} &=& \beta_1 + \xi^2 + sr^2 \\ \dot{r} &=& r\left(\beta_2 + \theta(\alpha)\xi + \xi^2\right) \\ \dot{\varphi} &=& \omega_1 + \omega_2\xi \end{array}. \tag{4.4}$$

When any of the five generic conditions G1–G5 is not satisfied, the normal form (4.4) ceases to exist. The behavior of differential systems of dimension three or more is not known when the parameters of the systems lie in a small neighborhood of the degenerate fold-Hopf bifurcation value. The problem studied here is of local type, that is, we are interested in the behavior of the system only when the parameter varies in a sufficiently small neighborhood of the bifurcation value. Each non-valid generic condition of the five G1–G5, increases the initial codimension of this bifurcation by at least 1. For example, if G1 is not satisfied anymore but the other four G2–G5 remain valid, the emerging degenerate fold-Hopf bifurcation is of codimension 3, while if both G1 and G2 are not valid (but the other three are valid), the codimension becomes 4. It is widely known that the analysis of a bifurcation becomes more and more complicate as the codimension increases beyond 2. Even codimension 3 bifurcations are not known in general and their study require a complex analysis and often laborious computations. I want to continue exploring the behavior of the differential system (4.1) in a degenerate framework. Firstly, I aim to remove the generic conditions G1–G5 one by one at once and study the consequences induced by these removals on the existence of the normal forms. In general, the existing normal forms cease to exist in the new degenerate frameworks and new normal forms should be obtained. Determining a new normal form in the new degenerate frameworks is a hard challenge. Secondly, I want to remove two by two at once generic conditions and so one. The new degenerate frameworks require new approaches to determine new normal forms. Hence, here is a lot of work and a large scientific field waits for to be explored. Several doctoral thesis could be written on this field of research.

I started also to study degenerate fold-Hopf bifurcations in a particular Rössler–type system of the form

$$\dot{x} = -y - z, \quad \dot{y} = x + ay, \quad \dot{z} = -cz + byz, \tag{4.5}$$

where a, b, c are real parameters and $b \neq 0$ by using the averaging theory. Other applications of the averaging theory can be found in [16, 40, 70, 137]. I briefly present in the following the results I obtained so far on this system. I intend to continue the study of this system in the future. The proofs of the theorems are omitted here. The equilibria of (4.5) are $O(0,0,0)$ and $A(-ac/b, c/b, -c/b)$ because $b \neq 0$. The points O and A coincide at $c = 0$ when their eigenvalues are 0 and $a/2 \pm i\omega$, where $\omega = \sqrt{4-a^2}/2$ whenever $-2 < a < 2$. Hence, the system (4.5) may undergo a fold–Hopf bifurcation at $a = 0$, when the eigenvalues are $0, \pm i$.

Denote further by $\alpha = (a, c)$. Writing (4.5) in form (3.64), one can determine the eigenvectors of the Jacobian matrix $J(\alpha)$ of system (4.5) at O for all α. Indeed, the eigenvalues of $J(\alpha)$ are $\lambda_1 = -c$, respectively $\lambda_\pm = a/2 \pm i\omega$, with the corresponding eigenvectors

$$q_0 = \begin{pmatrix} \dfrac{a+c}{c^2+ac+1} \\ -\dfrac{1}{c^2+ac+1} \\ 1 \end{pmatrix}, \quad q_\pm = \begin{pmatrix} -\dfrac{1}{2}a \pm i\omega \\ 1 \\ 0 \end{pmatrix}.$$

The adjoint eigenvectors $p_0(\alpha)$ and $p_\pm(\alpha)$ are

$$p_0 = \begin{pmatrix} 0 \\ 0 \\ 1 \end{pmatrix}, \quad p_\pm = -\frac{1}{4\omega^2 \mp 2ia\omega} \begin{pmatrix} -a \mp 2i\omega \\ -2 \\ 2\dfrac{a \pm 2i\omega}{a + 2c \mp 2i\omega} \end{pmatrix}.$$

Using the transformation

$$u = \langle p_0(\alpha), X \rangle, \; v = \langle p_1(\alpha), X \rangle,$$

where $X = \begin{pmatrix} x & y & z \end{pmatrix}^T$, the system (4.5) becomes

$$\begin{aligned} \dot{u} = {} & -cu - \frac{b}{1+ac+c^2}u^2 + buv + bu\bar{v}, \\ \dot{v} = {} & \left(\frac{1}{2}a + i\omega\right) v + \frac{b}{4}\frac{2\omega + (a+2c)\,i}{\omega\,(1+ac+c^2)} \left(-\frac{1}{1+ac+c^2}u^2 + uv + u\bar{v}\right). \end{aligned} \tag{4.6}$$

At $\alpha = (0,0)$ I obtained the coefficients $B(0) = -b \neq 0$, $D(0) = b/2$ and $G_{011}(0) = 0$. Hence, the fold–Hopf bifurcation of system the (4.5) is degenerate with respect to (G.2) $G_{011}(0) \neq 0$ which implies that the classical theory for studying the fold-Hopf bifurcation is useless. At this point we tried to apply the averaging theory as in [69] and this proved to be successfully. To our needs, we used the following theorem [133].

Consider the differential system

$$\dot{x} = \varepsilon F(t,x) + \varepsilon^2 G(t,x,\varepsilon), \tag{4.7}$$

with $x \in D$, where D is an open subset of $\mathbf{R}^n$, $t \geq 0$. We suppose that both $F(t,x)$ and $G(t,x,\varepsilon)$ are $T-$periodic in t. We define the averaged function

$$f(x) = \frac{1}{T}\int_0^T F(t,x)dt. \tag{4.8}$$

Theorem 4.2.1. *Assume that*

(i) F, its Jacobian $\partial F/\partial x$, its Hessian $\partial^2 F/\partial x^2$, G and its Jacobian $\partial G/\partial x$ are defined, continuous and bounded by a constant independent of ε in $[0,\infty)\times D$ and $\varepsilon \in (0,\varepsilon_0]$.

(ii) F and G are $T-$periodic in t (T independent of ε).

Then the following statements hold.

(a) If p is a zero of the averaged function $f(x)$ and

$$\det\left(\frac{\partial f}{\partial x}\right)\bigg|_{x=p} \neq 0, \tag{4.9}$$

then there exists a $T-$periodic solution $x(t,\varepsilon)$ of equation (4.7) such that $x(0,\varepsilon) \to p$ as $\varepsilon \to 0$.

(b) If all the eigenvalues of the Jacobian matrix $(\partial f/\partial x)$ have negative real part, then the periodic solution $x(t,\varepsilon)$ is asymptotically stable. If some of these eigenvalues have positive real parts, this periodic orbit is unstable.

The results we obtained so far are the following two theorems.

Theorem 4.2.2. *Let $(a, c) = (\varepsilon\alpha, \varepsilon\gamma)$, $b \neq 0$ and ε a sufficiently small parameter. If $(\alpha - \gamma)\gamma \neq 0$, then the Rössler–type system (4.5) has a fold–Hopf bifurcation at the equilibrium point localized at the origin of coordinates when $\varepsilon = 0$, and a periodic orbit $(x(t, \varepsilon), y(t, \varepsilon), z(t, \varepsilon))$ borns at this equilibrium for $\varepsilon > 0$ sufficiently small satisfying*

$$(x(0, \varepsilon), y(0, \varepsilon), z(0, \varepsilon)) = \left(0, \frac{\varepsilon\gamma}{b}, \frac{\varepsilon\gamma}{b}\right) + O(\varepsilon^2).$$

Moreover, this periodic solution is asymptotically stable if $\alpha - \gamma < 0$ and $\gamma < 0$, otherwise it is unstable.

Theorem 4.2.3. *Let $c = a < 0$ and $b \neq 0$, then the Rössler–type system (4.5) has a Hopf bifurcation at the equilibrium point $(-ac/b, c/b, -c/b)$, and a stable periodic orbit borns at this equilibrium for $a - c > 0$ sufficiently small, which in the normalized system to (4.5) is near a circle of radius $\sqrt{\frac{1}{2(a^2+1)}(a - c)}$.*

Remark 4.2.1. *Our system undergoes a Hopf bifurcation at $c = a \leq 0$, which, at $c = a = 0$ becomes a degenerate fold–Hopf bifurcation.*

4.2.2 The contributions of non-smooth dynamical systems to impact oscillators

Impact oscillators introduce in their study non-smooth dynamical systems due to the existing barriers needed for impacts. The impacts may be plastic or elastic but the motion is assumed not to cross the barriers. Outside the barriers the motion is described by a smooth differential dynamical system of the form

$$\ddot{x} = A(x, \dot{x}, t), \tag{4.10}$$

where A is smooth on $x > x_0$ and periodic in t. On an impact barrier the impacts are assumed instantaneously, that is, no motion exists on the barrier surface. The governing law on the barrier is assumed of the form

$$v_s = -rv_i, \tag{4.11}$$

which says that the leaving velocity v_s of an orbit after an impact with the barrier depends only on the hitting velocity of the orbit and the material the barrier is made of (the coefficient r). The relation (4.11) describes in fact the loss of energy due to impacts with the barrier. Applications of impact oscillators can be found in many practical domains such as automotive industry (all kind of tools, cars and machineries that produce vibrations in their use), particle accelerators and even tokamaks (experimental devices for producing clean energy). A barrier changes drastically the smooth motion of a model of form (4.10) and introduces a variety of bifurcations in the model's behavior. For example, particles in a tokamak are accelerated at very high speeds and kept inside by strong magnetic fields but a major problem appears when many particles hit the walls of the container. This leads to cooling of the very hot plasma which, in turn, makes the energy production inefficient. A problem started by Nordmark in [85] deals with impact oscillators that have initially a periodic orbit which touches (grazes) the unique barrier of the model with zero velocity and positive acceleration. Several results have been reported on this topic but more open problems still wait for to be approached. In particular, I am interested to explore a new topic here namely, the case when the grazing periodic orbit becomes degenerate, in the sense that, its acceleration at the grazing point is zero. Moreover, we may consider the degeneracy of higher orders, in the sense that

$$\frac{d^n A}{dt^n}|_{x=x_0} = 0$$

for some $n \geq 2$. The degeneracies introduce new bifurcations which encode up to some extent the behavior of the model. A method often used for studying such problems is based on a Poincaré–like approach, namely, one tracks the successive intersections of a generic orbit to a surface from the phase space. Various surfaces have been proposed in this regard including the surface on the barrier. As it can be observed from [85] the barrier surface method leads to quite complicated transformations needed to determine a normal form of the map. A more successful approach used by several authors is based on the virtual points method. This is the method that might be useful for our planned studies on topics from this field of research.

4.2.3 Applications of dynamical systems in understanding neuronal activities

Dynamical systems theory is actively involved in various bio-mathematical models which try to explain the motion of the ionic electrical currents in neuronal complex networks. A combination of the dynamical systems theory with practical experiments on real biological neurons in laboratories led in the early 60's to the discovery of *action potentials* (electrical impulses), which explain how the electrical ionic current is formed in the neuron's soma and transmitted further through axon to dendrites which communicate further with other neurons. The description of the formation of action potentials is based on a dynamical system formed by four differential equations and is known in the literature as the famous Hodgkin–Huxley model. A Nobel prize in Physiology or Medicine has been shared in 1963 by three scientists, two of them being A. L. Hodgkin and A. F. Huxley. Since then many other bio-mathematical models have been proposed to bring new insights on the behavior of electrical impulses in neurons and neuronal circuitry. Many neurological diseases such as autism, epilepsy, plague sclerosis and others could be better understood and finally cured by understanding better how neurons work.

I started to study several topics in this field of research and one of them is to obtain an improved model for the transmission of neuronal signals. Some of the ideas outlined so far are as follow. Denote by $R(x, y, t)$ the internal variable electrical resistance function of a neuron segment P (R is smooth and positive), by $i(x, t)$ the longitudinal current passing through a transversal section S_x at time t and by $U(x, t)$ the electrical potential at point x and time t.

The longitudinal current $i(x, t)$ on a small segment $P = [x, x + h) \times S,\ h > 0,\ h \to 0$, faces the internal resistance $R(x, x + h, t)$ and can be expressed by Ohm's law

$$i(x, t) = \lim_{h \to 0} \frac{U(x, t) - U(x + h, t)}{R(x, x + h, t)} = -\frac{U'_x(x, t)}{R'_y(x, x, t)}, \tag{4.12}$$

since the transversal currents (the currents entering or leaving the neuron through the membrane) on P are disregarded at this step. On the other hand, the transversal currents face membrane's electrical resistance (not the internal resistance R) and are obtained from other considerations. Denote further by $j(x, t)$ the current injected from exterior through the membrane at position x and time t. This current can be seen as the current injected by synapses or apparatus and assume it faces no electrical resistance to enter the interior of P; we call it the synaptic current. The total synaptic current injected on the whole length of $P = [x, x + h) \times S$ becomes in this case

$$I(x, x + h, t) = \int_x^{x+h} j(z, t)\, dz. \tag{4.13}$$

Denote by $i_m(x, t)$ the current escaping through the membrane at the point x

and time t, namely through the membrane's pores of the section S_x. This current consists of two currents: a capacitive one $i_c(x,t)$ and a resistive one $i_r(x,t)$.

I want to study further this research problem in the future and to obtain in the end an improved model for signal transmission in neurons. Also, I aim to study several phenomenological existing neuronal models (based on discrete or differential dynamical systems) and to propose new others in order to produce new insights of neuronal activity.

Bibliography

[1] S.S. Abdullaev, Construction of Mappings for Hamiltonian Systems and their Applications, Springer (2006).

[2] S.S. Abdullaev, Magnetic Stochasticity in Magnetically Confined Fusion Plasma, Springer (2014).

[3] V. S. Afraimovich, V. V. Bykov, L. P. Shilnikov, On structurally unstable attracting limit sets of Lorenz attractor type, Trans. Mosc. Math. Soc. 2 (1983), 153–216.

[4] Albert C. J. Luo, Prediction of quasi-periodic and chaotic motions in nonlinear Hamiltonian systems, Chaos, Solitons and Fractals 28 (2006), 627–649.

[5] A. Algaba et al., Hypernormal Form for the Hopf-Zero Bifurcation, International Journal of Bifurcation and Chaos 08(10), 1998, 1857–1887.

[6] A. Apte, A. Wurm, P.J. Morrison, Renormalization and destruction of $1/\gamma^2$ tori in the standard nontwist map, Chaos 13 (2003).

[7] A. Bahrami, A. H. Nayfeh, On the dynamics of tapping mode atomic force microscope probes, Nonlinear Dynamics, 2012, 70(2), 1605–1617.

[8] M.C. Baishya and C.G. Chakrabarti, Non-equilibrium fluctuation in Lotka–Volterra system, Bull. Math. Biol. 49:125–31, 1987.

[9] R. Balescu, M. Vlad, F. Spineanu, Tokamap: A Hamiltonian twist map for magnetic field lines in a toroidal geometry, Physical Review E 58 (1998), 951–964.

[10] N. N. Bautin, On the number of limit cycles which appear with the variation of coefficients from an equilibrium position of focus or center type, Transl. Amer. Math. Soc. 100 (1) (1954) 397–413.

[11] A. Buica, A. Gasull, J. Yang, The third order Melnikov function of a quadratic center under quadratic perturbations, J. Math. Anal. Appl. 331(1) (2007) 443–454.

[12] V. N. Belykh, Homoclinic and heteroclinic linkages in concrete systems: Nonlocal analysis and model maps, Amer. Math. Soc. Transl. 200 (2000) 51–62.

[13] V. N. Belykh, Bifurcations of separatrices of a saddle point of the Lorenz system, Differential Equations, 20(10), 1184–1191, 1984.

[14] E. Beretta, V.B. Kolmanowskii and L. Shaikhet, Stability of epidemic model with time delays influenced by stochastic perturbations, Math. Comput. Simul. 45:269–77, 1998.

[15] Y. Cao, K. Chung, J. Xu, A novel construction of homoclinic and heteroclinic orbits in nonlinear oscillators by a perturbation-incremental method, Nonlinear Dynamics, 64(3), 221–236, 2011.

[16] V. Castellanos, J. Llibre, I. Quilantán, Simultaneous periodic orbits bifurcating from two zero-Hopf equilibria in a tritrophic food chain model, J. Applied Mathematics and Physics 1, 2013, 31–38.

[17] B. Castillo-Toledo, J. Jalomo and E. N. Sanchez, Fuzzy robust tracking for the Chen's chaotic attractor, 15th Triennial World Congress, Barcelona, Spain, 2012.

[18] D. del Castillo-Negrete, P. J. Morrison, Chaotic transport created by Rossby waves in shear flow, Phys. Fluid A 5 (1993), 948–965.

[19] D. del-Castillo-Negrete, J.M. Greene, P.J. Morrison, Area preserving nontwist maps: periodic orbits and transition to chaos, Physica D91 (1996) 1–23.

[20] D. del-Castillo-Negrete, J.J. Martinell, Gyroaverage effects on nontwist Hamiltonians: Separatrix reconnection and chaos suppression, Communication in Nonlinear Science and Numerical Simulation 17 (2012), 2031–2044.

[21] S. Celikovski, G. Chen, On the generalized Lorenz canonical form, Chaos, Solitons and Fractals, 2005, 26:1271–1276.

[22] Y. Chang, G. Chen, Complex dynamics in Chen's system, Chaos, Solitons and Fractals, 27, 75–86, 2006.

[23] G. Chen, T. Ueta, Yet another chaotic attractor, Int. J. of Bif. and Chaos, 1999, 9:1465–1466.

[24] C. Chicone, On bifurcation of limit cycles form centers, Lecture Notes in Mathematics, 1455 (1990), 20–43.

[25] D. Chillingworth, Dynamics of an impact oscillator near a degenerate graze, Nonlinearity, 23, (2010), 2723–2748.

[26] W. Chin, E. Ott, H.E. Nusse, C. Grebogi, Grazing bifurcations in impact oscillators, Physical Review E, vol. 50(6), 1994.

[27] R. Cimpoiasu, R. Constantinescu, Nonlinear self-adjointness and invariant solutions in a 2D Rosby wave equation, Central European Journal of Physics 12 (2014), 81–89.

[28] J.W. Connor, T. Fukuda, X. Garbet, C. Gormezano, V. Mukhovatov, M. Wakatani, A review of internal transport barrier physics for steady-state operation of tokamaks, Nuclear Fusion, 44(4), 1–49 (2004).

[29] D.Constantinescu, R. Constantinescu, Transport barriers and diffusion phenomena for the magnetic field lines in Tokamak, Physica Scripta, T118 (2005), 244–250.

[30] D. Constantinescu, M-C. Firpo, Modifying locally the safety profile to improve the confinement of magnetic field lines in tokamak plasmas, Nucl. Fusion 52 (2012), 054006.

[31] D. Constantinescu, M-C. Firpo, Localizing transport barriers in degenerate 3/2 d.o.f. Hamiltonian systems with applicattions to magnetic confinement fusion, IJBC 23 (2013), 1350034.

[32] S. Coombes, R. Thul, K.C.A. Wedgwood, Nonsmooth dynamics in spiking neuron models, Physica D 241 (2012) 2042–2057.

[33] J.D. Crawford and E. Knobloch, Classification and unfolding of degenerate Hopf bifurcations with O(2) symmetry: No distinguished parameter, Physica D: Nonlinear Phenomena, 31(1988), 1–48.

[34] H. Dankowicz, J. Jerrelind, Control of near-grazing dynamics in impact oscillators, Proc. R. Soc. A (2005) 461, 3365–3380.

[35] H. Dankowicz, X. Zhao, S. Misra, Near-grazing dynamics in tapping-mode atomic-force microscopy, International Journal of Non-Linear Mechanics 42 (2007) 697–709.

[36] E. J. Doyle, R. J. Groebner, K. H. Burrell, P. Gohil, T. Lehecka, N. C. Luhmann Jr. et al., Modifications in turbulence and edge electric fields at the L–H transition in the DIII-D tokamak, Physics of Fluids B Vol.3(8), (1991), 2300–2307.

[37] F. Dumortier, S. Ibanez, H. Kokubu and C. Simo, About the unfolding of a Hopf-zero singularity, Discrete and Continuous Dynamical Systems - Series A, 33(2013), 4435–4471.

[38] F. Dumortier, J. Llibre, J.C. Artés, Qualitative theory of planar differential systems, UniversiText, Springer–Verlag, New York, 2006.

[39] J. Écalle, Introduction aux fonctions analysables et preuve constructive de la conjecture de Dulac, Hermann Press, 1992.

[40] R.D. Euzébio, J. Llibre, C. Vidal, Zero–Hopf bifurcation in the FitzHugh-Nagumo system, Mathematical Methods in the Applied Sciences 38, 2015, 4289–4299.

[41] G. L. Eyink, A. Lazarian, E. T. Vishniac, Fast magnetic reconnection and spontaneous stochasticity, The Astrophysical Journal 743:51 (2011), 1–28.

[42] M-C. Firpo, D. Constantinescu, Study of the interplay between magnetic shear and resonances using Hamiltonian models for the magnetic field lines, Physics of Plamas 18, 2011, 032506.

[43] S. Foale, S. R. Bishop, Bifurcations in impact oscillations, Nonlinear Dynamics, 1994, 6(3), 285–299.

[44] J-P. Francoise, Successive derivatives of a first return map, application to the study of quadratic vector fields, Ergodic Theory Dynam. Systems 16 (1996) 87–96.

[45] I. Garcia and C. Valls, The three-dimensional center problem for the zero-Hopf singularity, Discrete and Continuous Dynamical Systems - Series A, 36(2016), 2027–2046.

[46] R.Z. Hasminskij, Stochastic Stability of Differential Equations, Sijthoof and Noordhoof, Alphen aan den Rijn, The Nederlands, 1980.

[47] X. He, C. Li and Y. Shu, Triple-zero bifurcation in van der Pol's oscillator with delayed feedback, Communications in Nonlinear Science and Numerical Simulation, 17(2012), 5229–5239.

[48] M. J. Hole, R. Mills, S. R. Hudson, R.L. Dewar, Relaxed MHD states of a multiple region plasma, Nuclear Fusion 49 (2009), 065019.

[49] J. Hook, Smoothing non-smooth systems with low-pass filters, Physica D 269 (2014) 76–85.

[50] J. E. Howard and S. M. Hohs, Stochasticity and Reconnection in Hamiltonian Systems, Phys. Rev. A 29 (1984), 418–421.

[51] J. E. Howard, J. Humpherys, Nonmonotonic twist maps, Physica D80 (1995) 256–276.

[52] J. Huang and Y. Zhao, Bifurcation of isolated closed orbits from degenerated singularity, Discrete and Continuous Dynamical Systems - Series A, 33(2013), 2861–2883.

[53] R.A. Ibrahim, X. Zhao et al., Vibro-Impact Dynamics of Ocean Systems, LNACM 44, 275–285, Springer-Verlag Berlin Heidelberg 2009.

[54] I. D. Iliev, On second order bifurcations of limit cycles, J. London Maths. Soc. 58 (2) (1998) 353–366.

[55] I. D. Iliev, Higher order Melnikov functions for degenerate cubic Hamiltonians, Ad. Dif. Eq. 1 (1996) 689–708.

[56] Y. Ilyashenko, Finiteness Theorems for Limit Cycles, in: Translations of Mathematical Monographs, Amer. Math. Soc. 94 (1991).

[57] B. Jiang, X. Han, Q. Bi, Hopf bifurcation analysis in the image system, Nonlinear Analysis: Real World Applications, 11(1), (2010), 522–527.

[58] W. Jiang and B. Niu, On the coexistence of periodic or quasi-periodic oscillations near a Hopf-pitchfork bifurcation in NFDE, Communications in Nonlinear Science and Numerical Simulation, 18(2013), 464–477.

[59] Y.A. Kuznetsov, Elements of Applied Bifurcation Theory, Springer-Verlag, 1995.

[60] J. Lamb, J. Roberts, Time-reversal symmetry in dynamical systems: A survey, Physica D 112 (1998), 1–39.

[61] J.S.W. Lamb, M-A Teixeira and K.N. Webster, Heteroclinic bifurcations near Hopf-zero bifurcation in reversible vector fields in $\mathbb{R}^3$, Journal of Differential Equations, 219(2005), 78–115.

[62] C. Lazureanu and T. Binzar, On the symmetries of a Rikitake type system, C. R. Acad. Sci. Paris, Ser. I, 350(2012), 529–533.

[63] C. Lazureanu and T. Binzar, On a new chaotic system, Mathematical Methods in the Applied Sciences, 38(2015), 1631–1641.

[64] G.A. Leonov, N.V. Kuznetsov, On differences and similarities in the analysis of Lorenz, Chen, and Lu systems, Applied Mathematics and Computation 256 (2015) 334–343.

[65] D. Li, Z. Yin, Connecting the Lorenz and Chen systems via nonlinear control, Communications in Nonlinear Science and Numerical Simulation, 14(3), (2009) 655–667.

[66] X. Li, P. Wang, Hopf bifurcation and heteroclinic orbit in a 3D autonomous chaotic system, Nonlinear Dynamics, 73(1-2), 621–632, 2013.

[67] X–F. Li et al., Nonlinear dynamics and circuit realization of a new chaotic flow: A variant of Lorenz, Chen and Lu, Nonlinear Analysis: Real World Applications, 10(4), 2357–2368, 2009.

[68] B-Y Li, Z-F. Zhang, A note on a result of G. S. Petrov about the weakened 16th Hilbert problem, J. Math. Anal. Appl. 190 (1995) 489–516.

[69] J. Llibre, Periodic orbits in the zero-Hopf bifurcation of the Rössler system, Romanian Astron. J. 24, 2014, 49–60.

[70] J. Llibre, E. Pérez-Chavela, Zero-Hopf bifurcation for a class of Lorenz-type systems, Discrete and Continuous Dynamical Systems, Series B, 19, 2014, 1731–1736.

[71] J. Llibre, G. Rodriguez, Configurations of limit cycles and planar polynomial vector fields, J. Differential Equations 198 (2004) 374–380.

[72] J. Llibre, M. Messias, P.R. da Silva, Global dynamics in the Poincaré ball of the Chen system having invariant algebraic surfaces, IJBC, 22 (06), 2012.

[73] J. Llibre, A. Rodrigues, On the Dynamics of the Unified Chaotic System Between Lorenz and Chen Systems, IJBC, 25 (09), 2015.

[74] J. Llibre, C. Pessoa, The Hopf bifurcation in the Shimizu - Morioka system, Nonlinear Dynamics 79(3), (2015), 2197–2205.

[75] E.N. Lorenz, Deterministic nonperiodic flow, J.Atmos. Sci., 20, 130–141, 1963.

[76] T. Lu, X. Zhang, Darboux polynomials and algebraic integrability of the Chen system, IJBC, 17(08), 2739–2748, 2007.

[77] J. Lu, G. Chen, A new chaotic attractor coined, Int. J. of Bif. and Chaos, 2002, 12(3), 659–661.

[78] A. Makarov, S. Prandz, A. Virovlyanski, Ray and wave chaos in underwater acoustics, Physics: Uspekhi 55 (2012), 18–46.

[79] M. Messias, M. R. Alves Gouveia, C. Pessoa, Dynamics at infinity and other global dynamical aspects of Shimizu - Morioka equations, Nonlinear Dynamics, 69(1), (2012), 577–587.

[80] S. Misra, H. Dankowicz, M. Paul, Degenerate discontinuity-induced bifurcations in tapping-mode atomic-force microscopy, Physica D 239 (2010) 33–43.

[81] J. Molenar, J. G de Weger and W. van de Water, Mappings of grazing-impact oscillators, Nonlinearity 14 (2001) 301–321.

[82] P. J. Morrison, Magnetic field lines, hamiltonian dynamics, and nontwist systems, Physics of Plasmas 7 (2000), 2279–2289.

[83] C. Mu, F. Zhang, Y. Shu, S. Zhou, On the boundedness of solutions to the Lorenz-like family of chaotic systems, Nonlinear Dynamics 67(2), (2012), 987–996.

[84] A. Munteanu, E. Petrisor, E. Garcia-Berro, J. Jose, Creation of twistless circles in a model of stellar pulsations, Communications in Nonlinear Science and Numerical Simulation 8 (2003), 355–373.

[85] A.B. Nordmark, Non-periodic motion caused by grazing incidence in an impact oscillator, Journal of Sound and Vibration, 1991, 145(2), 279–297.

[86] A. Okninski, B. Radziszewski, Simple model of bouncing ball dynamics: displacement of the table assumed as quadratic function of time, Nonlinear Dynamics, 2012, 67(2), 1115–1122.

[87] L.F. Olsen and W.M. Schaffer, Chaos versus noisy periodicity: Alternative hypotheses for childhood epidemic, Science, 249:499–504, 1990.

[88] I.I. Ovsyannikov, D.V. Turaev, Analytic proof of the existence of the Lorenz attractor in the extended Lorenz model, http://arxiv.org/abs/1508.07565.

[89] J. Peng, S. Jin, Y. Liu, Design and Analysis of an Image Encryption Scheme Based on Chaotic Maps, International Conference on Intelligent Computation Technology and Automation (ICICTA), 2010, 1115–1118.

[90] L. Perko, Differential Equations and Dynamical Systems, Springer-Verlag, 2001.

[91] M. Perez-Molina and M. F. Perez-Polo, Fold-Hopf bifurcation, steady state, self-oscillating and chaotic behavior in an electromechanical transducer with nonlinear control, Communications in Nonlinear Science and Numerical Simulation, 17(2012), 5172–5188.

[92] E. Petrisor, Nontwist area preserving maps with reversing symmetry group, Int. J. Bif. Chaos, 11 (2001) 497–511.

[93] E. Petrisor, J. Misguich, D. Constantinescu, Reconnection in a global model of Poincaré map describing the magnetic field lines in a reversed shear tokamak, Chaos, Solitons and Fractals 18(2003), 1085–1099.

[94] W-X. Qin, G. Chen, On the boundedness of solutions of the Chen system, J. Math. Anal. Appl. 329 (2007) 445–451.

[95] R. Qesmi, M. Ait Babram and M.L. Hbid, Center manifolds and normal forms for a class of retarded functional differential equations with parameter associated with Fold-Hopf singularity, Applied Mathematics and Computation, 181(2006), 220–246.

[96] K. A. Razumova, V. V. Alikaev, I. S. Bondarenko, A. A. Borschegovskii, V. A. Vershkov, A. V. Gorshkov, Yu. V. Gott et al., Formation of Electron Transport Barriers under ECR Control of the q(r) Profile in the T-10 Tokamak, Plasma Physics Reports, 27(4), 2001, 273–277.

[97] M. Roberto, E.C. da Silva, I.L. Caldas, R.L. Viana, Transport barrier created by dimerized islands, Physica A 342 (2004), 363–369.

[98] C. Robinson, Homoclinic bifurcation to a transitive attractor of Lorenz type, Nonlinearity 2 (1989), 495–518.

[99] O.E. Rössler, An equation for continuous chaos, Physics Letters 57A, 1976, 397–398.

[100] A. Rucklidge, Chaos in a low-order model of magnetoconvection, Physica D 62 (1993) 323–337.

[101] P.L. Sachdev, R. Sarathy, Periodic and chaotic solutions for a nonlinear system arising from a nuclear spin generator, Chaos, Solitons and Fractals, Vol.11, 1994.

[102] R. Santos-Lima, E. M. de Gouveia Dal Pino, A. Lazarian, The role of turbulent magnetic reconnection in the formation of rotationally supported protostellar disks, The Astrophysical Journal 747:21 (2012), 1–8.

[103] S. Shi, A concrete example of the existence of four limit cycles for plane quadratic systems, Sci. Sinica 23 (1980) 153–158.

[104] T. Shimizu, N. Morioka, On the bifurcation of a symmetric limit cycle to an asymmetric one in a simple model, Phys. Lett. A76 (1980), 201–204.

[105] A.L. Shilnikov, L.P. Shilnikov, D.V. Turaev. Normal forms and Lorenz attractors. International Journal of Bifurcation and Chaos 3 (1993), 1123–1139.

[106] A. L. Shilnikov, Bifurcations and chaos in the Morioka-Shimizu model, in Methods of Qualitative Theory and Theory of Bifurcations (Gorky St. Univ., 1986); English translation: Sel. Math. Sov. 10 (1991), 105–117.

[107] A. L. Shilnikov, Bifurcations and chaos in the Morioka-Shimizu model: II, in Methods of Qualitative Theory and Theory of Bifurcations (Gorky St. Univ., 1989), 130–138.

[108] A. L. Shilnikov, On bifurcations of the Lorenz attractor in the Shimizu-Morioka model, Physica D62 (1993), 338–346.

[109] L. P. Shilnikov, The bifurcation theory and quasihyperbolic attractors, Uspehi Mat. Nauk 36:4 (1981), 240–241.

[110] L. Shilnikov, A. Shilnikov, D. Turaev, L. Chua, Methods of Qualitative Theory in Nonlinear Dynamics. Part 2. (World Scientific, 2001).

[111] C.P. Silva, Shilnikov theorem – a tutorial, IEEE transactions. Circuits Syst. I, 1993, 40:675–682.

[112] C. Simó, Invariant curves of analytic perturbed nontwist area preserving maps, Regular and Chaotic Dynamics, 3 (1998) 180–195.

[113] I. P. Smirnov, A. L Virovlyansky, G. M. Zaslavsky, Theory and applications of ray chaos to underwater acoustics, Phys. Rev. E 64 (2001), 036221.

[114] S. M. Soskin, R. Mannella, P.V.E. McClintock, Zero-dispersion phenomena in oscillatory systems, Physics Reports 373 (2003) 247–408.

[115] J.C. Sprott, Some simple chaotic flows, Physical Review E, 50(1994), 647–650.

[116] A. Stefanski, T. Kapitaniak, J. Brindley, Dynamics of coupled Lorenz systems and its geophysical implications, Physica D98, 594–598, 1996.

[117] A. Stefanski, T. Kapitaniak, J. Brindley, V. Astakhov, Torus on-off intermittency in coupled Lorenz systems, Phys. Rev. E57(1), 1175–1177, 1998.

[118] G. Tigan, Analysis of a dynamical system derived from the Lorenz system, Scientific Bulletin of the Politehnica University of Timisoara, Tomul 50(64), Fascicola 1, 2005, 61–72.

[119] G. Tigan, D. Opris, Analysis of a $3D$ chaotic system, Chaos, Solitons and Fractals 36 (2008) 1315–1319.

[120] G. Tigan, D. Constantinescu, Heteroclinic orbits in the T and the Lu systems, Chaos, Solitons and Fractals, 42(1), 20–23, 2009.

[121] G. Tigan, J. Llibre, Heteroclinic, homoclinic and closed orbits in the Chen system, IJBC, 26(4), 1–6, 2016.

[122] G. Tigan, D. Turaev, Analytical search for homoclinic bifurcations in the Shimizu-Morioka model, Physica D 240, 985–989, 2011.

[123] G. Tigan, On a Method of Finding Homoclinic and Heteroclinic Orbits in Multidimensional Dynamical Systems, AMIS, 4(3), 383–394, 2010.

[124] G. Tigan, Analysis of a two-dimensional nonsmooth Poincaré-like map, Nonlinear Dynamics, 2014, 75(4), 643–651.

[125] G. Tigan, A case-study model for impact oscillators, Proceedings of the International Conference on Mathematics and its Applications (ICMA), Timisoara, 2012, pages 185–190.

[126] G. Tigan, Bautin bifurcations in the T system, Proceedings of the International Conference on Mathematics and its Applications (ICMA), Timisoara, 2015, pages 1–6.

[127] G. Tigan, Stochastic stability of a perturbed Lorenz system, Scientific Bulletin of the Politehnica University of Timisoara, Transactions on Mathematics and Physics, Tome 53(67), 2, 1–11, 2008.

[128] G. Tigan, D. Constantinescu, Bifurcations in a family of Hamiltonian systems and associated nontwist cubic maps, Chaos, Solitons and Fractals 91, 128–135, 2016.

[129] G. Tigan, Periodic orbits in a non-smooth discrete map, The 15th International Conference on Applied Mathematics and Computer Science, 5–7 July, 2016, Cluj.

[130] G. Tigan, Using Melnikov functions of any order for studying limit cycles, Journal of Mathematical Analysis and Applications 448, 409–420, 2017.

[131] G. Tigan, Degenerate with respect to parameters fold-Hopf bifurcations, Discrete and Continuous Dynamical Systems - Series A, 37(4), 2115–2140, 2017.

[132] E. Tornatore, S. M. Buccellato, P. Vetro, Stability of a stochastic SIR system, Physica A, 354, 2005:111–126.

[133] F. Verhulst, Nonlinear Differential Equations and Dynamical Systems, Universitext, Springer, 1991.

[134] L. N. Virgin, C. George, A. Kini, Experiments on a non-smoothly-forced oscillator, Physica D: Nonlinear Phenomena, 313(1), (2015), 1–10.

[135] A. G. Vladimirov, D. Yu. Volkov, Low-intensity chaotic operations of a laser with a saturable absorber, Optics Communications 100 (1993), 351-360.

[136] G. Voyatzis, S. Ichtiaroglou, Degenerate bifurcations of resonant tori in Hamiltonian systems, Int. J. Bif. Chaos 9 (1999), 849–863.

[137] Z. Wei et al., Dynamics at Infinity, Degenerate Hopf and Zero-Hopf Bifurcation for Kingni–Jafari System with Hidden Attractors, International Journal of Bifurcation and Chaos 26, 2016, 1650125.

[138] P.D Woods and A.R Champneys, Heteroclinic tangles and homoclinic snaking in the unfolding of a degenerate reversible Hamiltonian-Hopf bifurcation, Physica D: Nonlinear Phenomena, 129(1999), 147–170.

[139] A. Wurm, A. Apte, K. Fuchss, P. J. Morrison, Meanders and reconnection–collision sequences in the standard nontwist map, Chaos: An Interdisciplinary Journal of Nonlinear Science 15 (2005), 023108.

[140] T. Xing, R. Barrio, A. Shilnikov, Symbolic Quest into Homoclinic Chaos, International Journal of Bifurcation and Chaos, 24, 1440004 (2014).

[141] S. Yakovenko, A geometric proof of the Bautin theorem, Concerning the Hilbert 16th problem, AMS Translations-Series 2 165 (American Mathematical Society, Providence, RI), (1995) 203–219.

[142] Z-F. Zhang, B. Y. Li, High order Melnikov functions and the problem of uniformity in global bifurcations, Ann. Mat. Pura Appl., CLXI (1992) 181–212.

[143] F. Zhang, X. Liao, G. Zhang, On the global boundedness of the Lu system, Applied Mathematics and Computation 284 (2016) 332–339.

[144] X. Zhao et al., Modeling and Simulation Methodology for Impact Microactuators, Journal of Micromechanics and Microengineering 14, 775–784 (2004).

[145] T. Zhou, Y. Tang, G. Chen, Chen's attractor exists, IJBC, 14 (9), 3167–3177, 2004.